2000

The Townsite Formation: An Aborted Rift Setting in the Yellowknife Greenstone Belt, N.W.T.

Craig S. Finnigan

THE TOWNSITE FORMATION: AN ABORTED RIFT SETTING IN THE YELLOWKNIFE GREENSTONE BELT, N.W.T.

Craig S. Finnigan
Department of Earth Sciences

Graduate Program In Geology

Submitted in partial fulfillment
of the requirements for the degree of
Master of Science

Faculty of Graduate Studies
The University of Western Ontario
London, Ontario
May, 2000

Abstract

The Townsite Formation is a felsic unit separating the Crestaurum and Yellowknife Bay Formations of the mafic dominated Kam Group. Previous workers have divided the Townsite Formation into the Niven Lake, Brock, and Vee Lake lenticles, separated by Proterozoic faults. While substantiating the general similarity of the lithologies present in these lenticles, the mapping carried out in the present study identifies felsic porphyry phases contemporaneous with gabbro sills. This is indicated by "back veining" of the gabbro by porphyry and the absence of chill margins. In both the Niven Lake and Brock lenticles, injection of quartz feldspar porphyry has produced marginal hydrothermal breccias. These breccias give way northward into vented pyroclastic rocks in the Brock and Vee Lake lenticles. Vent proximal pyroclastic facies of the Vee Lake Lenticle grade laterally into more distal facies.

The pillowed dacites identified by previous workers have basaltic to andesitic composition. The intrusive quartz feldspar porphyry bodies are dacitic in composition, while associated feldspar porphyries have more intermediate composition. Breccias, formed by quartz feldspar porphyry injecting older volcanic flows have andesitic to dacitic bulk composition. Trace element patterns of the feldspar porphyry and quartz feldspar porphyry intrusive phases indicate they were formed by melting of hydrated Kam Group volcanic flows. Partial melting is consistent with experimental results on the melting of hydrous greenstones and amphibolites. Similar patterns are shown by rocks formed by wet melting of juvenile crust both in modern and ancient rifting environments. Combining detailed mapping and analytical results of this study with

previous geochronological data the Townsite Formation is reinterpreted as having formed an aborted rift some twenty million years after cessation of Kam volcanism.

Since the Townsite Formation is spatially related to mineralized segments of both the Campbell and Giant shear systems, it is likely that the intrusion of quartz feldspar porphyries played a role in the genesis of these deposits: there is a "quartz-feldspar porphyry /Au" association in the Yellowknife camp.

TABLE OF CONTENTS

LIST OF FIGURES

LIST OF PHOTOGRAPHIC PLATES

LIST OF APPEDICIES

Chapter 1

Introduction

1.1 General Statement and Purpose of Study

Gold mining began in the Yellowknife Camp in the early 1930's when Johnny Baker and partner Hugh Muir found a gold rich quartz vein in the Burwash sedimentary rocks on the east shore of Yellowknife Bay. This vein yielded 16 tons of ore grading at 13.6 ounces per ton. A shaft was sunk in order to excavate the gold but less than a year later the reserves diminished. In these early days, prospecting in the volcanic belt across the bay was minimal as these rocks were thought to be barren of gold. In June of 1935, A.W. Joliffe was sent by the Geological Survey of Canada to do both geological and topographic mapping on the northwest shores of Great Slave Lake. Joliffe and fourteen undergraduate students from prairie universities crossed Great Slave Lake with an assignment to map 26 000 km^2 of land. Starting in the south of the Yellowknife Volcanic Belt they mapped northward. By the end of the summer, it was still generally believed that the volcanic rocks across the bay from the Burwash sediments were barren of gold. However, on his last traverse of the summer, Joliffe's field assistant, Neil Campbell, discovered a gold bearing quartz vein in what is now the Con Mine area. Within two years the entire Yellowknife Greenstone Belt was staked, the Con Mine was in production and the nearby Giant Mine was brought into production shortly thereafter (Padgham, 1987).

Since then, more than 14 million ounces of gold have been mined from a 2 x 8 km section of what is now called the Yellowknife Bay Formation. The city of

Yellowknife has developed a vibrant economy largely based on the mineral wealth of the Con and Giant mines. However, the current state of exploration in the area reveals that only 2-5 years of gold reserves remain in the ground. This prompted the Government of the Northwest Territories, the Geological Survey of Canada, the Department of Indian and Northern Affairs and both the Royal Oak (Giant) and Miramar (Con) mining companies to collaborate on re-examination of previous theories on the origin of these gold deposits. This collective group of researchers was organized in 1999 as Extech III: an intensive localized "exploration technology" project headed by the Geological Survey of Canada. The mandate of the Extech III project is to develop a model for the petrogenesis of the Yellowknife Camp and to apply key aspects of this model to a defined area in and around the region. The goal of this research is to extend the life of the Con and Giant mines and to aid in the discovery of new deposits.

This thesis is a contribution to this objective. It is based on a detailed mapping project re-examining the Townsite Formation, lying directly adjacent to gold mineralization in Yellowknife. This formation comprises a unique package of felsic units separating the Crestaurum and Yellowknife Bay Formations of the mafic dominated Kam Group. Due to offsets across Proterozoic faults, the Townsite Formation has been subdivided into the Niven, Brock and Vee Lake lenticles. Although an outstanding marker unit in the belt, to date detailed reconstruction of the complex history of these rocks has been unsuccessful. The present work primarily attempts to resolve the origin of the felsic Townsite lithologies and to shed light on any role these rocks may have played in gold mineralization.

1.2 Location Access and Physiography

Access to the study area can be gained via Yellowknife which is located on the West side of Yellowknife Bay on the North shore of Great Slave Lake (114° 25' W longitude, 62° 25' N latitude (Fig. 1.1). The north and northwestern portions of

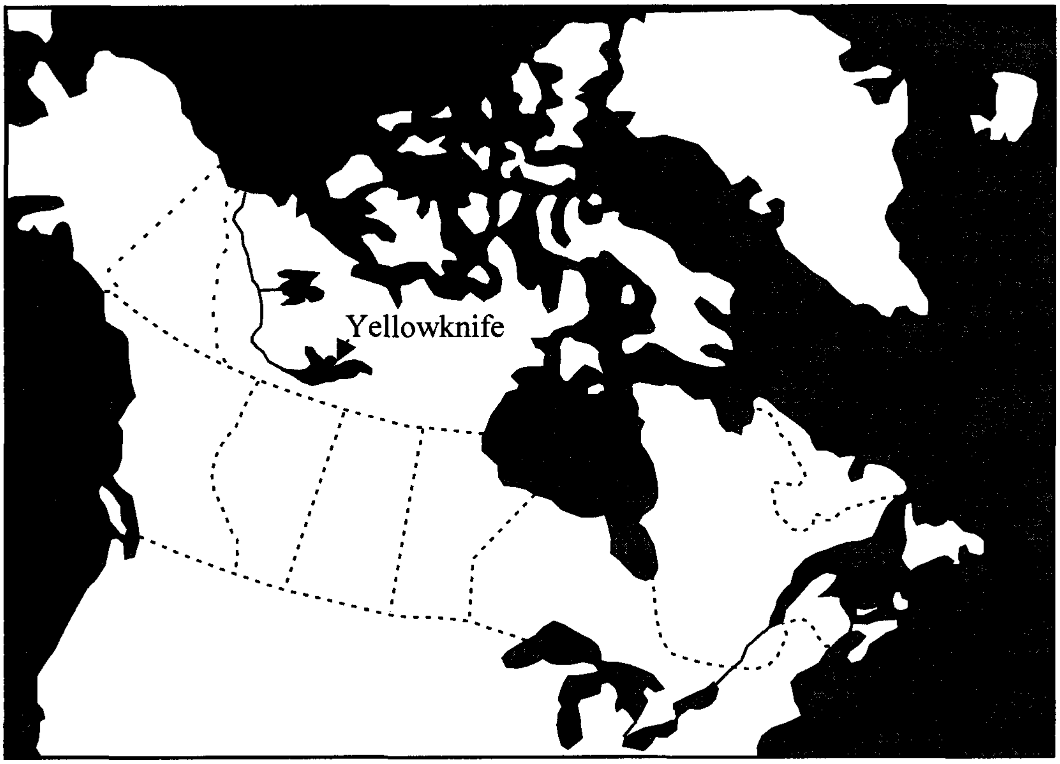

Figure 1.1 Location of the City of Yellowknife.

the city of Yellowknife are built on the Niven Lake Lenticle, hence its name the Townsite Formation. Access to rocks of the Brock Lenticle may only be gained through permission from Miramar Mining and Exploration as it is entirely on Giant Mine property. An all weather gravel road offers access to the Vee Lake Lenticle. Southern portions may be reached by foot but boat transport is ideal as the majority of outcrop exposure is best accessed from Walsh Lake. Walsh Lake is much larger and connected via a small channel to Vee Lake.

The exposure of rocks in the Yellowknife Greenstone Belt is exceptional, the Townsite Formation itself offers 80-90% exposure. The polished, lichen free outcrops are a result of repeated glacier advance and subsequent scouring and erosion. Glacial grooving left long narrow linear depressions in areas where shear deformation has weakened the rocks. This has resulted in an overall rugged terrain with 10-50 m high rocky knobs separated by drift covered swamps and lakes.

1.3 Previous Geological Investigations

Because of location in the southern Slave, its relatively small size and excellent exposure, the Yellowknife Greenstone Belt is undoubtedly one of the most well mapped Archean volcanic belts in the world. Of particular significance, its apparent layer cake stratigraphy has been tested by U-Pb zircon geochronology (Isachsen, 1992), establishing rock ages with a margin of error in most cases of less than one percent. Age dating in the Yellowknife volcanic belt has generally confirmed the deposition of some 10 km of mafic lava in a very short period 2712 – 2707 Ma. This dating has created an enigma for the Townsite Formation with respect to previously established stratigraphic relationships in the belt. Dating of the Brock and Vee Lake lenticles reveal ages of 2703+/-2 and 2705 +/- 3 Ma respectively, while zircons from the Niven Lake Lenticle, reveal ages between 2683 +/- 5 and 2726 +/-2 Ma (Pb/Pb date) (Isachsen, 1992). In an attempt to resolve this relative discordance, Isachsen did in all, thirty one analyses at three separate locations in the Niven Lake Lenticle. Although this discordant age may be explained by complex lead loss from zircons in both the correlative Brock and Vee Lake members, Isachsen (1992) suggests it is likely better explained by a mixing array between older and younger components, the older of which represents inherited zircons.

These anomalous age dates combined with the proximity of the Brock Lenticle to the Giant mine led exploration geologists at Giant to initiate detailed re-mapping of these rocks in an attempt to recognize lithologies of differing age. Grant, (1997) began this mapping project and recognized intrusive felsic and intermediate bodies in the Brock. This work was partially completed when the author began working on this thesis and over the course of the 1998/99 summer field seasons completed detailed maps (1:600, 1:1200) of all three lenticles (maps 1, 2, 3 in rear folder).

The most recent study of Townsite Formation rocks is by Cousens (2000), within the context of a regional geochemical and radiogenic isotope investigation of the entire Kam Group. Mafic to intermediate flows of the Townsite Formation revealed ε^{T}_{Nd} ranging from 1.8 to 2.7 and correspond closely to the estimate of depleted mantle at 2.7 Ga (Depaolo, 1988). It was also discovered that felsic units across all three lenticles are isotopically homogeneous with ε^{T}_{Nd} of –0.2 to –0.9. Of all of the units sampled in the Kam Group, the felsic rocks of the Townsite Formation, and the volcanic flows of the underlying Crestaurum Formation and overlying Yellowknife Bay Formation are closest in their isotopic signature.

1.4 Field Work and Methodology

Field work consisted of approximately four months of mapping in the Yellowknife Greenstone Belt. In order to attain a better understanding of the Townsite Formation, approximately one day a week was spent on geologic field trips with other geologists, both veteran and new to the belt. Mapping of the Brock Lenticle was carried out first and at the largest scale (1:600, map 2). The reasoning here was to start in the center and work laterally in order to recognize key lithological relationships linking the Brock to the Niven and Vee Lake members. Further, as a result of roasting at the Giant Mine, the Brock rocks are free of lichen and thus offer 100% exposure. Such exceptional exposure proved invaluable in establishing specific contact relationships between the different lithologies. Vee Lake, the largest of the three lenticles was mapped second followed by the Niven Lake Lenticle, both at 1:1200 (maps 1 and 3). One area in the southeastern portion of the Niven Lake Lenticle, behind the Oldtown baseball diamond, offering superb exposure of the Niven Lake lithologies was mapped at a scale of 1:20 (map 1b).

Samples were collected of all units identified in all three lenticles. The goal was to compare rock types in terms of mineralogy and texture. Representative examples of each lithology were selected for bulk chemical analysis in order to compare the rock types chemically. Key samples were also chosen for microprobe analysis in order to better understand the effects of metamorphism and retrograde alteration. Both polished rock slabs and polished thin sections were studied in order to characterize key textural features. This was especially useful for dividing pyroclastic rocks into different facies.

Chapter 2

Geology

2.1 Introduction

The Slave Structural Province is an Archean granite-greenstone terrane comprising 190 000 km^2 of the northwestern Canadian Shield (Fig 2.1). The Slave is composed of 35 – 40 % supracrustal rocks and 60 % granitic gneiss and granite. Distinguishing the Slave from other Archean cratons is the rarety of ultramafic volcanics and its sediment dominated nature. The Supracrustal rocks of the Slave, comprised of 80 % tubidic metasediments and 20 % volcanic rocks, are collectively known as the Yellowknife Supergroup (McGlynn and Henderson, 1970). Volcanic rocks of the Yellowknife Supergroup have been divided into two types known as Hacket River type and Yellowknife type (Padgham, 1985). The Hacket River type volcanic belts are found in the eastern Slave and are dominated by felsic volcaniclastic rocks. The Yellowknife type volcanic belts occur in the central and western portion of the Slave and are dominated by mafic volcanic flows. Pre-Yellowknife Supergroup rocks consist of sialic basement rocks exposed largely in the western Slave. U/Pb zircon geochronology reveals basement ages between 2.83 and 3.96 Ga, including the oldest known rocks in the world (Krough and Gibbins 1978, Nikic et al., 1980, Bowring et al., 1989).

Several geotectonic models have been invoked for the evolution of the Slave. Henderson (1970) and McGlynn and Henderson (1970), suggest the Slave evolved from a series of ensialic basins which, upon developing fractures along their margins due to rifting, focused volcanic activity, and that the volcanics were buried by siliciclastics. Fyson and Helmstaedt, (1988), Kusky (1990, 1991), Davis and Hegner (1992) and Davis and King, (1994) have favoured accretionary models for the evolution of the Slave whereby island arcs and associated basins forming accretionary prisms in the eastern Slave were subsequently intruded by granites related to terminal collision with the western Slave. Recently, Bleeker et al,. (1998) have developed a hybrid model involving components of both the ensialic and accretionary models. This model essentially consists of the formation of ensialic rift related volcanic belts in the western Slave Province followed by the docking of accretionary arcs to the eastern margin of this craton.

2.2 Geology of the Yellowknife Greenstone Belt

The Yellowknife Greenstone Belt, located in the southwestern corner of the Slave Province, is the southwesternmost of approximately 26 volcanic belts (Fig.2.1). Situated between the Western Plutonic complex to the west and metaturbidites of the Burwash Basin to the east, the Yellowknife Greenstone Belt is approximately 50 km long and 5-8 km wide (Fig 2.2). Structurally, the belt comprises a steeply-dipping, northeast-striking monoclinical successsion which youngs in a southeast direction. The southern portion of the belt has been segmented along northwesterly-trending sinistral strike-slip faults of Proterozoic age that partition the belt into a series of fault bounded blocks. The lithostratigraphic subdivisions for the belt were initially introduced by a synthesis of mapping projects carried out by Joliffe (1966), Boyle (1961) and Henderson and Brown (1966). A revised regional stratigraphic framework was proposed by Helmstaedt and Padgham (1986) and is shown in Figure 2.3.

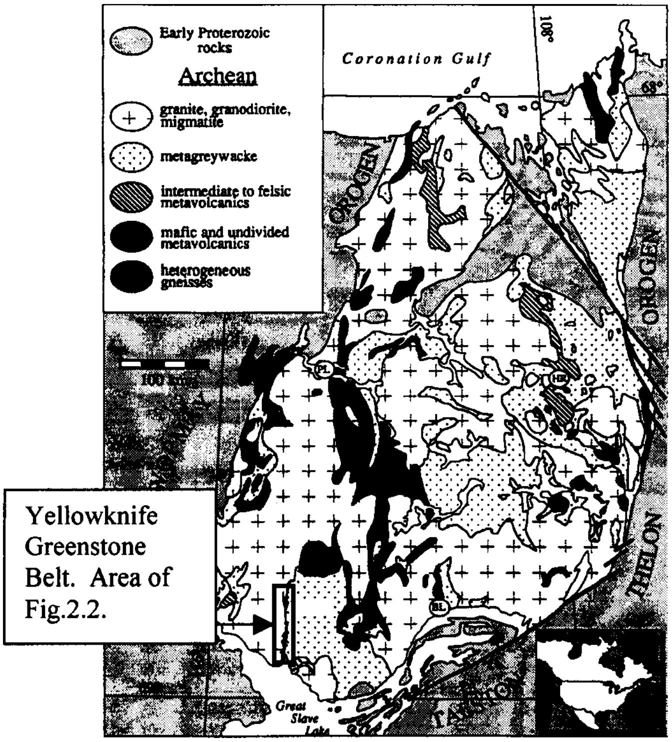

Figure 2.1 Map Showing Location of the Yellowknife Greenstone Belt and Characteristics of the Slave Structual Province, Modified from Padgham, 1985.

The Yellowknife Greenstone belt is dominated by mafic metavolcanic rocks of the Kam Group. As defined by Helmstaedt and Padgham (1986), the Kam Group consists of a 10 km thick sequence of tholeiitic basaltic flows. The Kam Group has been divided into four formations - the Chan, Crestaurum, Townsite, and Yellowknife Bay. The Kam flows are unconformably overlain by felsic metavolcanic rocks of the Banting Group. Pre-Kam rocks have been identified at the northern end of the belt and consist of a succession of quartzite-rhyolite-banded iron formation, known as the Dwyer Formation. U/Pb zircon geochronology has constrained the age of these rocks

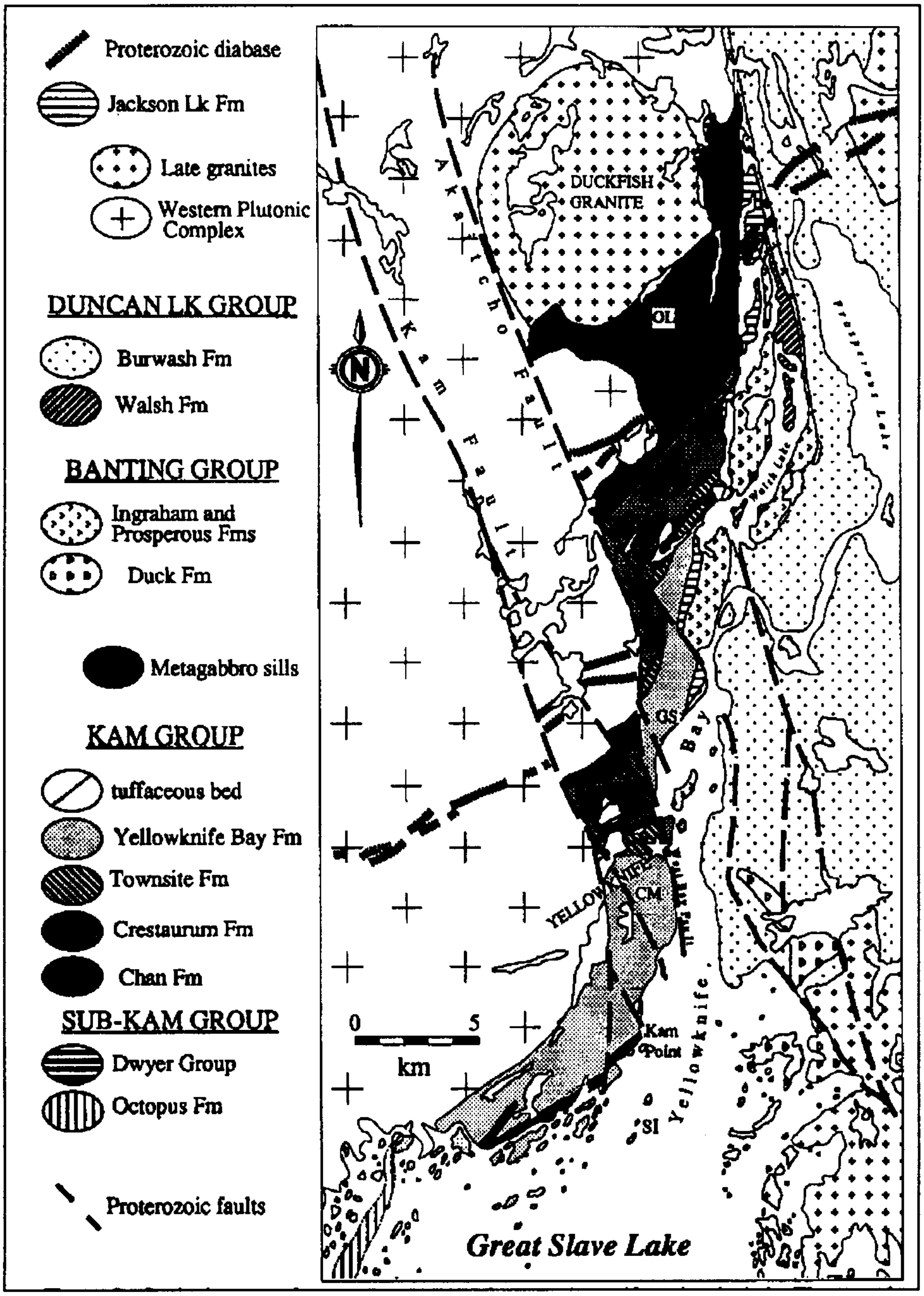

Figure 2.2 Generalized Geology of the Yellowknife Greenstone belt Modified from Henderson and Brown (1966) and Helmstaedt and Padgham (1986).

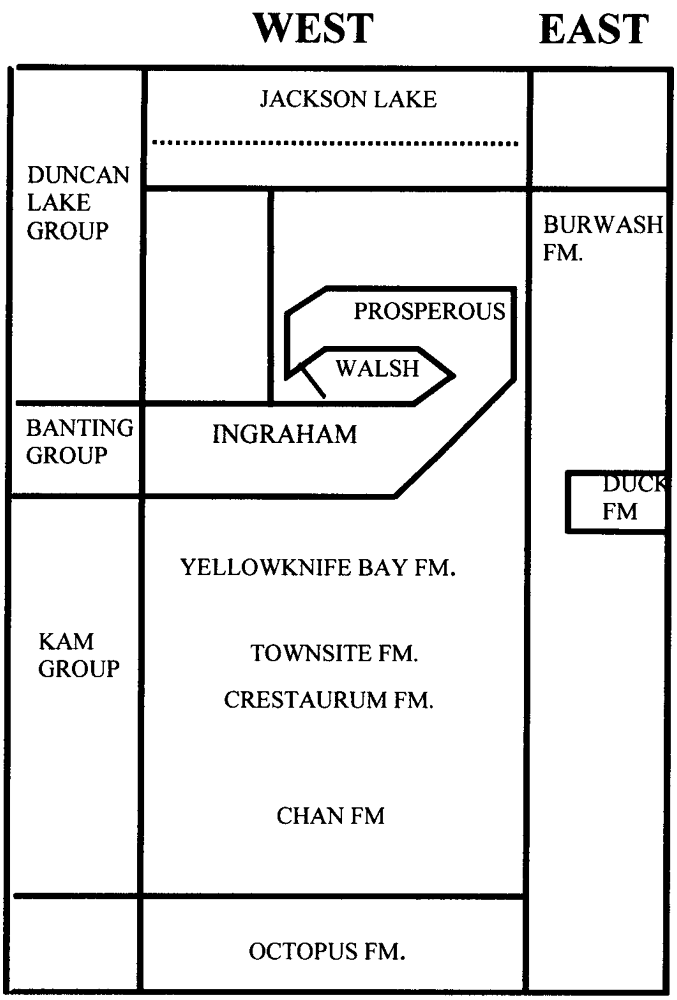

Figure 2.3 Layer Cake Stratigraphic Model for the Yellowknife Greenstone Belt. Modified after McDonald et al., 1993.

in excess of 2.9 to greater than 3.7 Ga (Isachsen, 1992). At the southwestern end of the belt, Helmstaedt et al. (1979) and Helmsteadt and Padgham (1986) identified a sequence of amphibolite-greywacke-siltstone-conglomerate and felsic pyroclastic rocks lying structurally below Yellowknife volcanic rocks. This sequence of rocks termed the Octopus Formation lies below and is in unconformable contact with the Kam

Group. Recent U/Pb zircon geochronology (Ketchum et al., 1999) tentatively suggest these rocks may be younger than previously thought and may correlate with the overlying Kam Group.

The Chan Formation is approximately 6 km thick and consists of massive and pillow basalt flows intruded by gabbroic dykes and sills. Sheeted dyke complexes in the Chan exhibiting one-way chilling resemble modern ophiolites (Helmstaedt et al 1986). The upper boundary of the Chan Formation is in conformable contact with the overlying Crestaurum Formation. This contact is marked by the Ranny Chert, a thin felsic marker unit capping Chan flows. The Ranny Chert has yielded Pb/Pb dates of between 2722 and 2818 Ma (Isachsen, 1992), suggesting a basement detrital component

The overlying Crestaurum Formation is approximately 2 km thick and is comprised of pillowed to massive mafic flows and mafic intrusive bodies. Upper Crestaurum variolitic pillowed units are capped by "cherty tuff", known as the Stock and Fox marker horizons. Henderson and Brown (1966) correlated these units with the Cemetary tuffs and used them for correlation across major Proterozoic faults within the belt. U/Pb zircon geochronology dates the Cemetary tuff at 2707 to 2713 Ma (Isachsen, 1992)

As defined, the Townsite Formation is stratigraphically above the Crestaurum Formation and stratigraphically below the Yellowknife Bay Formation. Historically the Townsite Formation has been recognized as a felsic volcanic unit, but it is redefined in the current work and is described below.

The Yellowknife Bay Formation overlies the Townsite Formation and consists of massive and pillowed variolitic flows and interflow tuffaceous sediments. Where exposed, the upper contact of the Yellowknife Bay Formation is truncated by the overlying Jackson Lake Formation but this boundary primarily occurs beneath the waters of Yellowknife Bay. The thickness of this unit is therefore unknown but is at least 5 km (Helmstaedt and Padgham, 1986). The Yellowknife Bay Formation is exceptionally well exposed along the shores of Yellowknife Bay; it is perhaps the best known example of a succession of Archean pillowed flows. Two variolitic markers known as the Negus and Yellorex flows occur within the formation. Variolitic flow - cherty tuff cycles become more prolific near the top of the formation. One of the distinctive interflow units is the Bode Tuff; a graded unit containing large, round to sub angular boulders of quartz feldspar porphyry up to 0.5 m in diameter (Henderson and Brown, 1966). This unit directly overlies the Yellorex flows and has yielded a Pb/Pb zircon date of 2704 +/- 1Ma (Isachsen, 1992).

The Kam Group is unconformably overlain by the calc- alkaline rocks of the Banting Group. These rocks are composed of intermediate to felsic pyroclastic rocks, massive flows, tuffs, and tuffaceous sediments (Helmstaedt and Padgham, 1986). The Banting Group is approximately 2 km thick and is divided into two belts termed the Ingraham Formation to the west, and the Prosperous Formation to the east. These two belts have been dated (U/Pb) at 2663 +/- 1.2 Ma and 2678 +/- 12 Ma, respectively, and are separated and conformably overlain by the Walsh Formation (Isachsen,1992). Isachsen (1992) suggests the anomalous date for the Prosperous Formation may be a result of inheritence and further work is needed therefore in order to resolve this age.

The intervening Walsh Formation is a highly deformed unit of metasediments consisting of argillite and greywacke turbidite. The Walsh is assigned to the overlying Duncan Lake Group (Helmstaedt and Padgham, 1986).

Both the Kam and Banting Groups are intruded by several generations of dykes and sills. The basalts of the Chan Formation are intruded by anorthosite sills and crosscut by sheeted gabbro dykes possibly recording an early spreading event (Helmstaedt and Padgham, 1986). The Townsite and Yellowknife Bay Formations are also intruded by various ages of gabbro sills, irregular shaped bodies and dykes. These sills are massive up to 100 m in width and extend kilometers in strike length. A swarm of quartz feldspar porphyry dykes transect the belt in the north but are absent in the south. These dykes have a 2660 Ma age (Isachsen, 1992) and may feed the Banting felsic volcanic succession.

The Jackson Lake Formation consists of a succession of crossbedded sandstones and polymictic conglomerates. It is the youngest supracrustal unit in the belt. It unconformably overlies and/or is fault bounded between the Kam and Banting Groups (Helmstaedt and Padgham, 1986). Clasts within the conglomerate include granitic to trondjhemite boulders, sub-angular to rounded quartz feldspar porphyry, angular mafic volcanic clasts, and abundant quartz sandstone boulders. Other lithologies in the Jackson Lake Formation include vein quartz, Fe-carbonate, argillite, green mica schist, and jasper (Henderson and Brown, 1966). Mueller et al. (1993) interpret the Jackson Lake Formation as being deposited as terriginous alluvial fans and/or fan deltas into fault controlled basins. They further suggest a provenance of cobbles within the conglomerates as being dominated by basalt with lesser intermediate and felsic tuff and subordinate plutonic sources. Dating of granitic cobbles at the base of the Jackson Lake Formation has yielded dates of 2605 +/- 7 Ma (Isachsen, 1992), consistent with derivation from the Western Granodiorite.

The Yellowknife Greenstone Belt is intruded in the west and southeast by large composite batholiths. The Kam Group is intruded by the Defeat Granodiorite of the Western Plutonic Complex (Atkinson, 1987). Atkinson et al. (1990), divided this complex into four main phases which from oldest to youngest consist of: (1) the Anton Complex, dated at 2642 Ma (Henderson et al., 1987); (2) the Main Defeat Suite dated at 2620 Ma; (3) the Duckfish Granite dated at 2589 + 11/-9 Ma; and (4) the Stagg Granite dated at 2585 +/- 4 Ma.

The youngest rocks in the belt are two sets of Proterozoic diabase dykes. These dykes are generally no larger than 2-4 m in width. The older Dogrib dykes trend northeast and have been dated using Rb-Sr isotopes at 2635 +/- 80 Ma (Gates and Hurley, 1973). The younger Indin dykes trend northwest and are dated (Rb-Sr) at 2049 +/- 80 Ma (Gates and Hurley, 1973).

2.3 Lithological Make-up of the Townsite Formation

The following sections describe in detail the field relationships of the various lithologies of the Townsite Formation. Descriptions start with the Niven Lake Lenticle and work north through the Brock and Vee Lake lenticles. It is also noted here that terms adopted in the field are used in order to describe certain lithologies. Detailed maps (maps 1, 1b, 2, 3) and plates of outcrops and textures aid descriptions. Detailed maps use UTM (NAD 83) coordinates. Sample location maps (Appendix C) use latitude and longitude.

2.3.1 The Niven Lake Lenticle

Volcanic flows in the Niven Lake Lenticle make up approximately 10 % of the lithologies. These flow units are discontinuous due to the dominance of intrusive phases. Those flows which have experienced hydrothermal alteration and brecciation are treated as a separate facies described in the section on hydrothermal breccias.

In outcrop the flows vary from buff green to black in colour and are generally aphanitic. Pillow selvages are rarely intact and occur as disrupted structures in what is otherwise massive greenstone. Selvages themselves are feldspar phyric with up to centimeter sized porphyroblasts occurring throughout and concentrating in pillow triple points. Variolitic textures are not preserved but pillow cores are characteristically bleached and may represent relict coalesced variolitic material. Occasionally the pillows display pipe vessicles and eyebrow structures.

Cherty tuffs are very distinct units in the Niven Lake Lenticle. These units are known as the "Trapper Tuffs" (Henderson and Brown, 1966) and have been recognized as key marker horizons in the upper Crestaurum Formation. They occur as discontinuous, poorly preserved hornfelsed lenses along the margins of gabbro sills. One well exposed outcrop can be readily viewed on the west side of the highway approximately 150 m north of the Explorer Hotel. These units are bright pink in colour, are two to three meters in width and display thin banding on freshly exposed outcrop surfaces (plate 2.1 A).

Plate 2.1

(A) Cherty tuff on the margin of a gabbro sill (left), in the Niven Lake Lentile. Note banding.

(B), (C) Quartz feldspar porphyry (pink) "back-veining" gabbro sill.

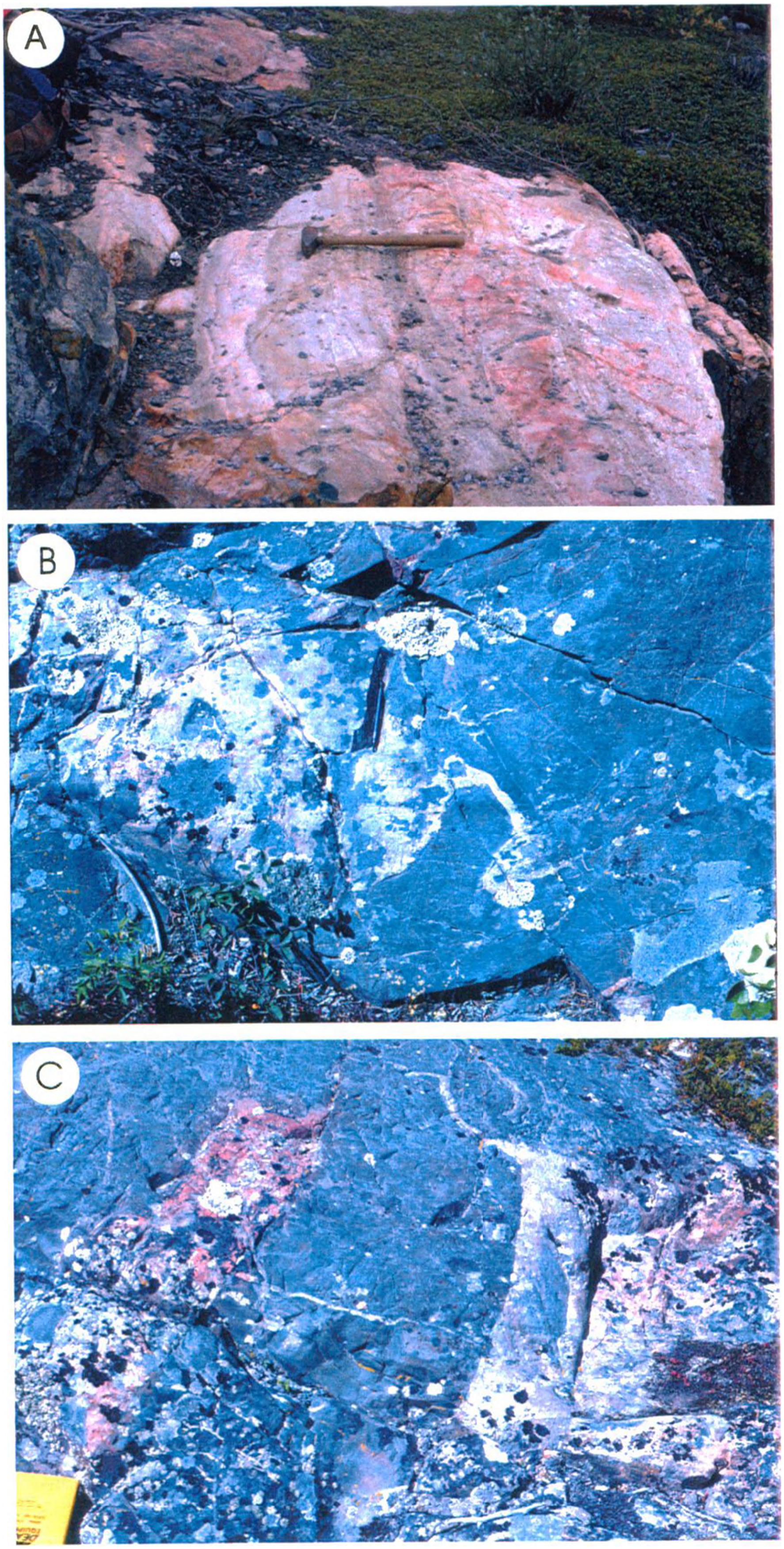
A
B
C

Intrusive feldspar porphyry makes up only a small portion of the lithologies (1%). A wedge of feldspar porphyry occurs behind the Yellowknife Racquet Club (map 1b). It is approximately 20 m long and 5 to 10 m wide, pinching out between a gabbro dyke and bordering hydrothermal breccia. Another exposure of feldspar porphyry occurring approximately 30 m to the north, is approximately 50 m long and 20 m in width. The feldspar porphyry is black in outcrop, consisting of (20%) 0.5 to 1.5 cm phenocrysts of subhedral plagioclase in an aphanitic groundmass.

Quartz feldspar porphyries make up approximately one fifth of the Niven Lake Lenticle. These outcrops are buff pink in colour, mapping out as irregular shaped bodies along the margins of gabbro sills. In terms of size, these bodies are 10 to 50 m in length by 10 to 30 m wide. The large body in the central Niven Lake Lenticle area between Frame and Niven lakes is approximately 100 m long and 40 m wide. These bodies display undulose, nonchilled contacts and locally physically interfinger with gabbro, suggesting co-existing magmas. Such a relationship is further suggested by quartz feldspar porphyry "back veining" cooling fractures along the margins of gabbro sills. (plates 2.1 B, 2.1 C).

Hydrothermal Breccias (plates 2.2 A - 2.2 D, maps 1 and 1b) are well exposed behind the baseball diamond and immediately west of Frame Lake. The breccias are distributed as blocks bordered by gabbro sills, quartz feldspar porphyry and feldspar porphyry. As shown in detail in map 1b and plate 2.2c, a pipe like breccia body is found between feldspar porphyry and brecciated pillow material.

The matrix of the breccias consists of hydrothermally milled rock flour. Pillow selvages are disrupted, discontinuous, and rarely intact. The inner cores of partial

Plate 2.2

(A) Hydrothermal Breccia behind the Oldtown baseball diamond. Light pink material represents siliceous flooding and quartz feldspar porphyry material invading volcanic flows.

(B) Hydrothermal breccia behind Oldtown baseball diamond. Shows a mixture of quartz feldspar porphyry fragments and pillow core material in a rock flour matrix.

(C) Hydrothermal breccia pipe behind Oldtown baseball diamond. Shows a mixture of quartz feldspar porphyry fragments and pillow core material in a rock flour matrix.

(D) Hydrothermally brecciated pillows behind Oldtown baseball diamond. Note partial selvage just above pencil. Fragmental material consists of pillow material in a rock flour matrix.

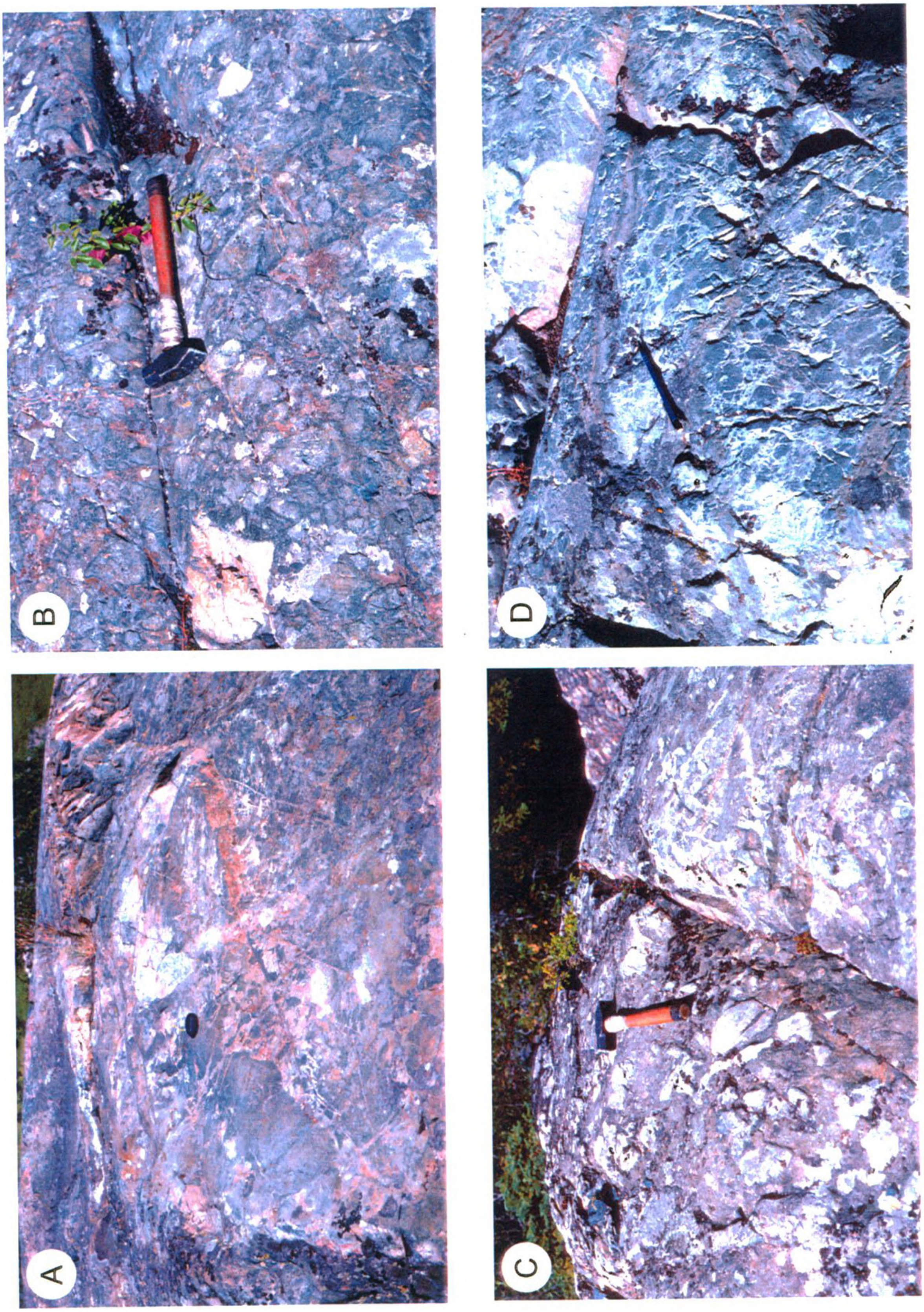
B
D
A
C

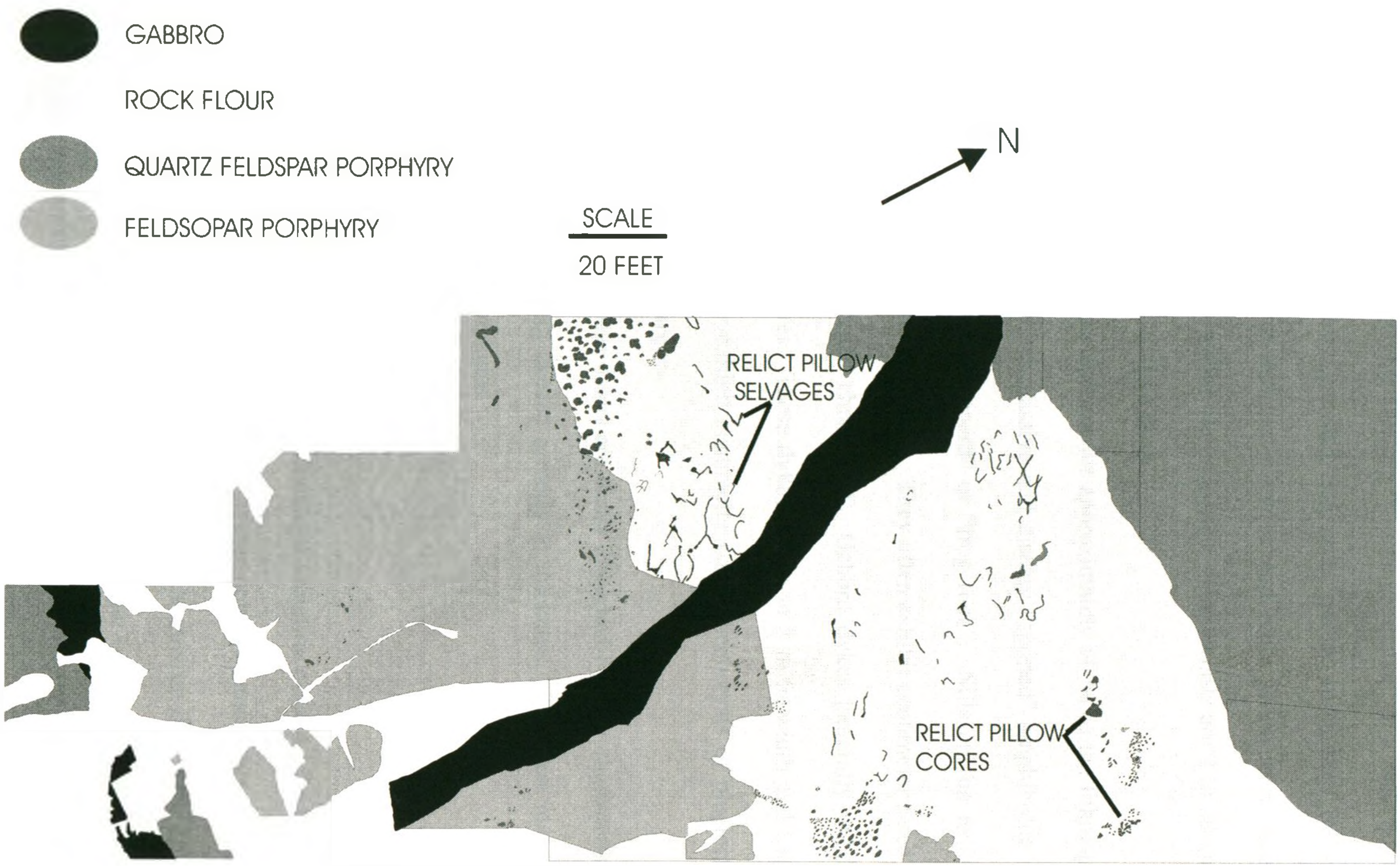

Map 1b Detailed Map Showing Relationship of Porphyries to Hydrothermal Breccia. Mapped Out Behind The Oldtown Baseball Diamond.

pillows exhibit angular fragments creating "jigsaw fit texture" in a rock flour matrix. Pillow selvages are randomly oriented and relict pillow cores may be variolitic. Angular fragments of quartz feldspar porphyry and relict pillow core material are occasionally found as clasts within the rock flour. These clasts are 2 to 50 cm in size and felsic fragments exhibit reaction rims.

Gabbro sills and dykes account for approximately 50 % of the lithology in the Niven Lake Lenticle. Sills are massive and display "spotted" amphibolite textures, leading to such field terms as "leopard" or "frog rock". Sills are up to 100 m in thickness and run up to 1 km along strike. They often exhibit centimeter sized feldspar phenocrysts where they intrude cherty tuff. Gabbro dykes generally exhibit finer grained metagabbroic textures. These dykes are up to 8 m in width and transect all lithologies. They also may exhibit centimeter sized phenocrysts of plagioclase and occasionally have chilled margins.

The Proterozoic diabase dykes are easily discerned by their characteristic rusty brown colour. These rarely exceed a meter in thickness. They are magnetic and contain minor amounts of sulphides.

2.3.2 Brock Lenticle

In the Brock Lenticle (map 2) remnants of variolitic pillowed flows (plates 2.3 A, B) host later feldspar porphyry, quartz feldspar porphyry and gabbro sills. Flows constitute approximately 1/5 of the total exposure. In outcrop they have a buff pink colour on weathered surfaces but are olive green colour on fresh surfaces. The buff pink colour is a result of bleaching due to the effects of the roaster at the Giant Mine.

Plate 2.3

(A) Relic pillow selvages in the Brock Lenticle volcanic flows. Note partial selvages just below compass.

(B) Relic pillow selvages in the Brock Lenticle volcanic flows. Note coalesced varioles just below hammer.

(C) Intact pillows in the Brock Lenticle.

(D) Recrystallized pillows in the northen Brock Lenticle . Fine lines are baked, intact selvages.

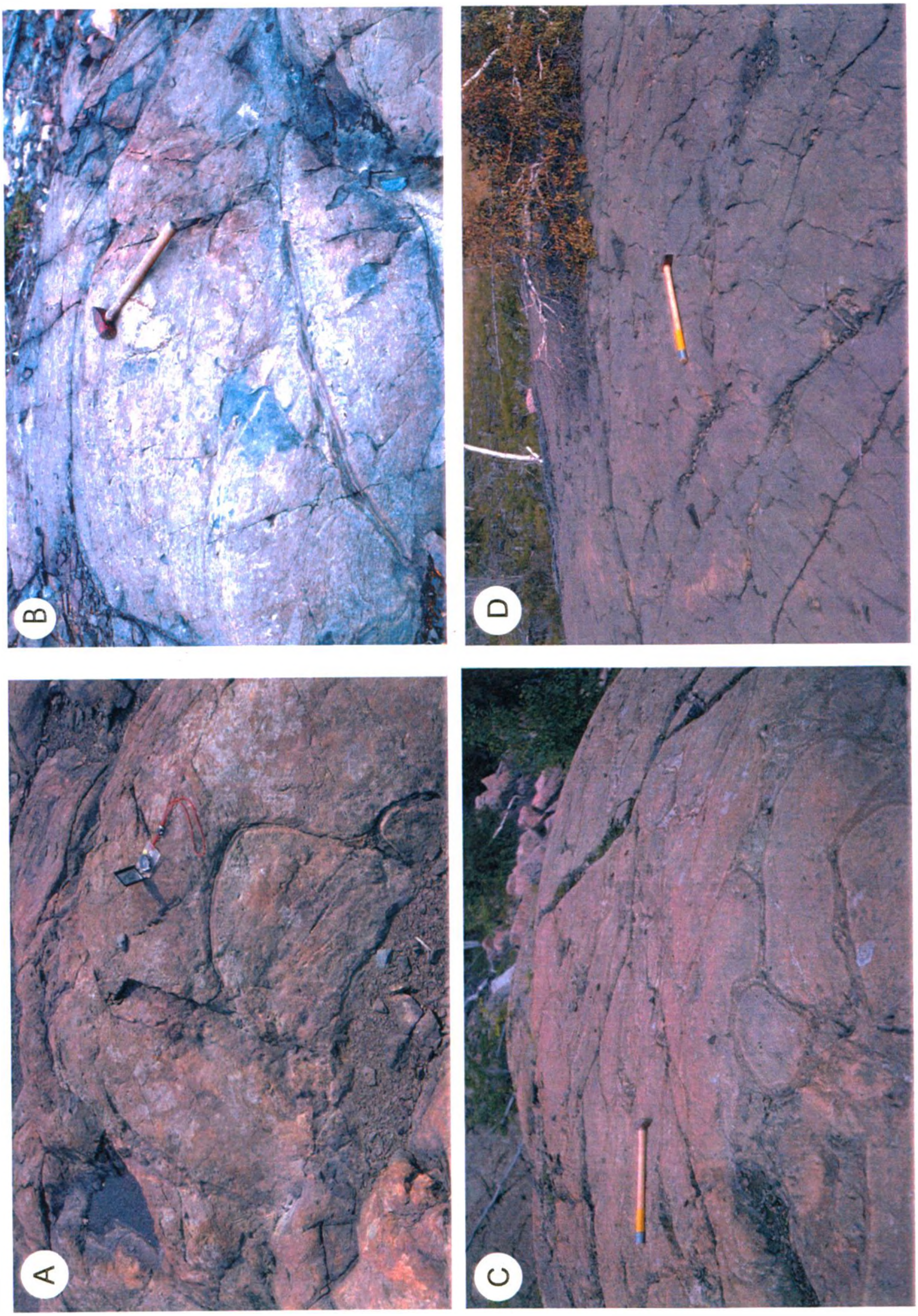
B
D
A
C

This bleaching led Henderson and Brown (1966) to interpret these outcrops as dacites. Their colouration is quite similar to the intrusive quartz feldspar porphyry. Detailed mapping reveals remnants of partial pillow selvages and variolitic textures. One outcrop in the central Brock and adjacent to the West Bay Fault reveals "ghostly" glomerophyric patches of varioles with relict pillow selvages that appear twisted and contorted. Just to the north and in fault contact with this outcrop, perfect pillows are preserved (plate 2.3 C). At the northern end of the Brock, pillowed flows are strongly recrystallized due to their proximity to gabbro sills (plate 2.3 D). These recrystallized pillowed flows were originally mapped as gabbro sills by Henderson and Brown, (1966) and Grant (1997). In the southern end of the Brock, domains of pillows have suffered shear deformation and have been flattened by a factor of fifty to one.

Cherty tuff occurs as discontinuous hornfelsed lenses along the margins of gabbro sills (plate 2.4 A). These units are one to two meters in thickness and although recrystallized, thin banding is still visible. Lapilli tuff makes up a minor component (<5%) of the lithologies in the Brock Lenticle. These rocks are observed in two outcrops: one at the northern end of the Brock Lenticle near the Vee Lake road, and the other at the base of Baker Creek where it flows into the tailings waterworks. The lapilli tuff at the north end of the Brock is an unbedded, moderately well sorted matrix supported rock with lapilli ranging in size from 5 to 15 mm (plate 2.4 B). The matrix is intermediate in composition and composed of quartz, carbonate, sericite, and chlorite. The lapilli themselves are composed mainly of carbonate followed by quartz, and sericite and are subrounded, flattened clasts. These clasts do not have reaction rims. The lapilli tuff at the mouth of Baker Creek strikes northwest, and is 10 m thick

Plate 2.4

(A) Cherty tuff (center) between gabbro sill (right) and quartz feldspar porphyry (left) at the northern end of the Brock Lenticle.

(B) Lapilli tuff at the north end of the Brock Lenticle. Note lithic fragments.

(C) Layed lapilli tuff at the mouth of Baker Creek (Brock). Dark and light bands represent intermediate and felsic units respectively.

(D) Contact between feldspar porphyry (dark unit on left) and quartz feldspar porphyry (pink material on right). Note the undulose nature of the contact. Photo taken across from UBC pit (Brock).

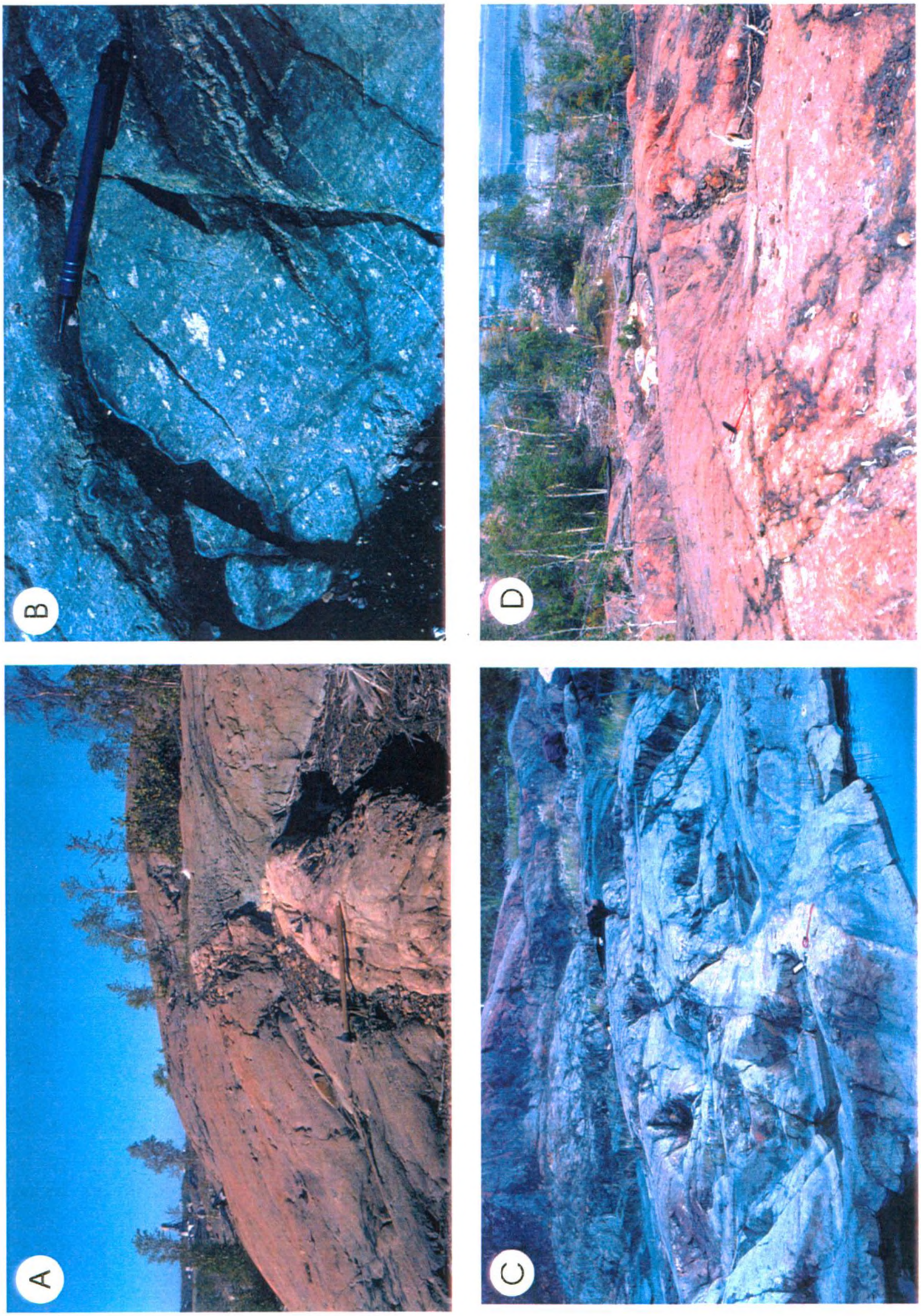
A
B
C
D

stratigraphically. This outcrop displays two distinct units: a more intermediate unit containing felsic lapilli, and a more felsic overlying unit containing intermediate clasts (plate 2.4 C). Both are of equal thickness and in sharp contact. Neither of these units have bedding and both intermediate and felsic lapilli range in size from 5-7 mm. The intermediate clasts are aphanitic and often vesicular, while the felsic clasts are quartz feldspar porphyritic. Clasts are rounded, and exhibit reaction rims.

Feldspar porphyries comprise approximately 1/5 of the rocks in the Brock Lenticle. These outcrops are greenish-grey in colour and map out as irregular sill-like bodies. They occur between quartz feldspar porphyry intrusions and mafic-intermediate flows (plate 2.4 D). Crosscutting relationships indicate feldspar porphyry predates quartz feldspar porphyry. The lack of chills combined with conformable contacts suggests a temporal association.

Quartz feldspar porphyries also comprise approximately one fifth of the Brock Lenticle. In outcrop, these rocks are a buff pink colour and occur as irregular dykes and sills ranging between ten to fifty meters in length and ten to twenty meters in width. These units are massive, lack chill margins with adjacent rocks, and display undulose contacts with gabbros. As observed in the Niven Lake Lenticle, contacts between quartz feldspar porphyry and gabbro sills appear to represent coeval melts, as fingers of quartz feldpar porphyry protrude into gabbro margins (plate 2.5 A, B).

Intrusive breccias are most prominent marginal to feldspar porphyry and quartz feldspar porphyry. Where quartz feldspar porphyry intrudes feldspar porphyry, meter sized xenolithic, stoped blocks of feldspar porphyry create “jigsaw fit texture” (plate 2.6 A, B). Excellent exposures of breccia bodies can be found approximately 40 m

Plate 2.5

(A) Quartz feldspar porphyry back veining gabbro sill in the southern Brock Lenticle.

(B) (C) Undulose contact between gabbro sill and quartz feldspar porphyry. Note the undulose and interfingering nature of the contact (southern Brock).

(C) Close-up of plate 2.5 A revealing the lack of chill margins between intrusives.

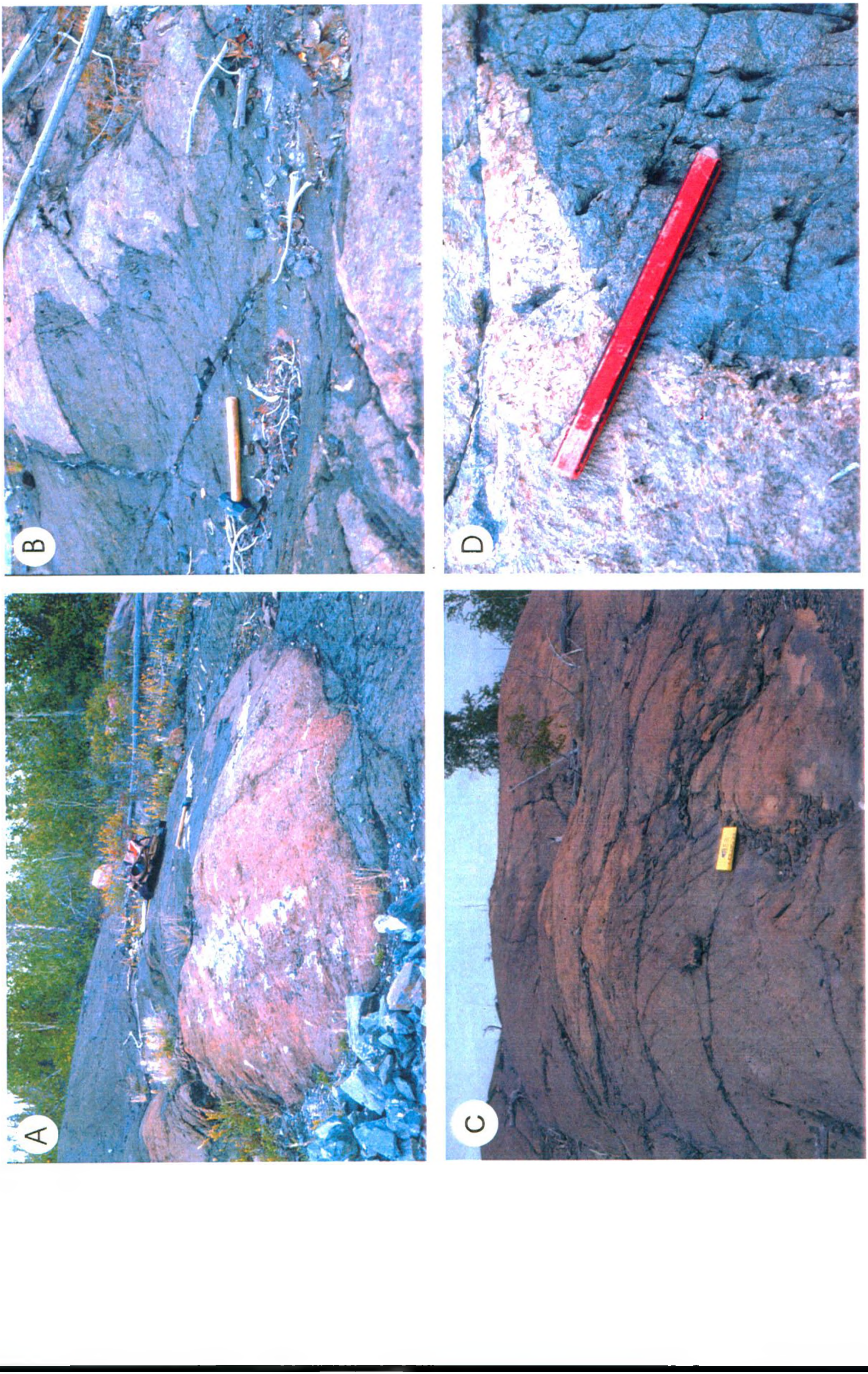

Plate 2.6

(A) Intrusive breccia, southern Brock Lenticle. Quartz feldspar porphyry (pink) is forcefully injecting feldspar porphyry material. Note gabbro sill on right is not invaded by the quartz feldspar porphyry.

(B) Close up of quartz feldspar porphyry injecting and brecciating feldspar porphyry material (northern Brock).

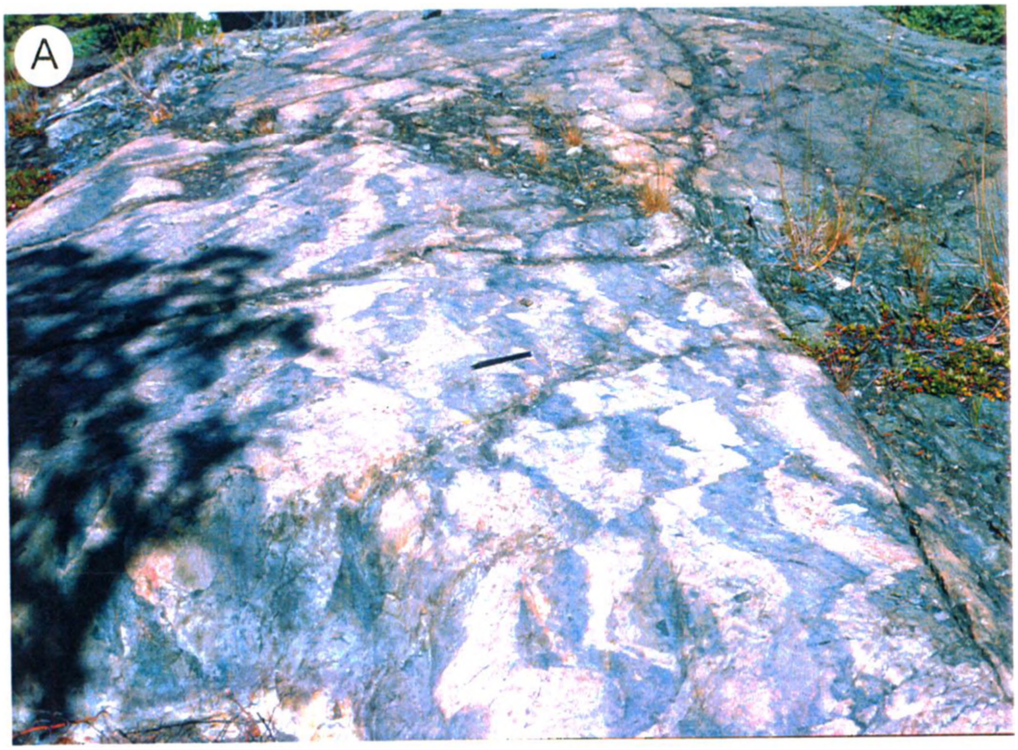
A

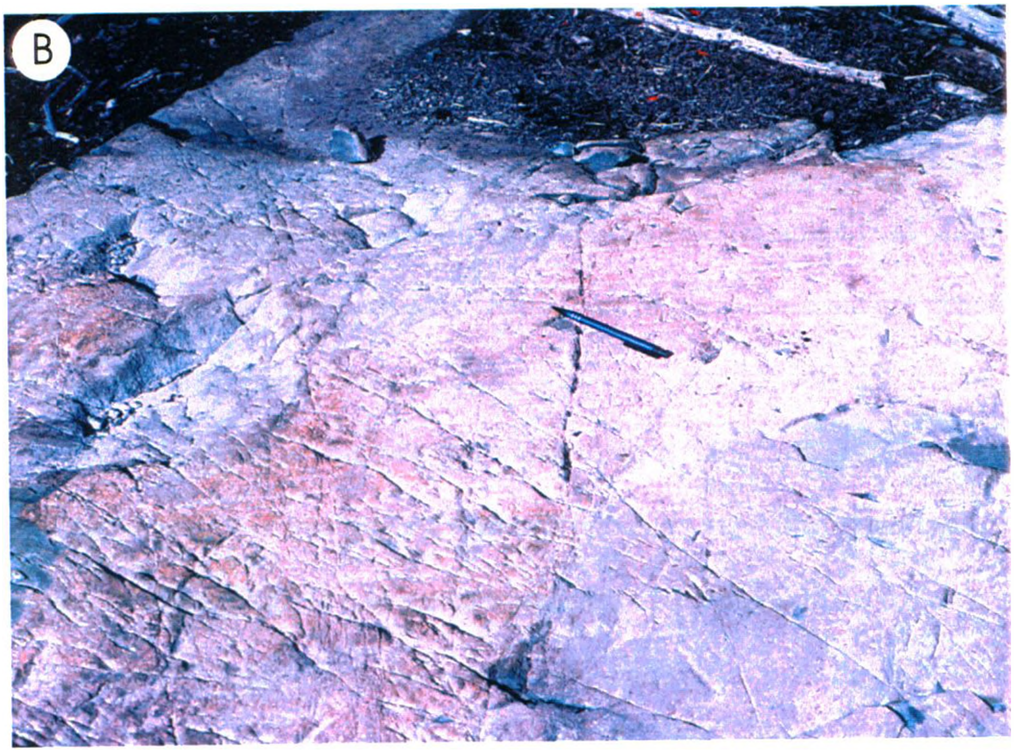
B

west of the Baker Creek reservoir. Locally, where quartz feldspar porphyry stringers invade feldspar porphyry, forceful injection produces a brecciated texture. These bodies are found at the southern end of the Brock approximately 30 m from the lower contact of the Yellowknife Bay Formation. Isolated angular blocks of quartz feldspar porphyry are also found within brecciated domains of mafic volcanics directly across from the UBC pit.

Thick (up to 30 m) gabbro sills map out along the entire length of the Brock Lenticle and comprise approximately 1/3 of the lithologies. These gabbro sills have been divided into two phases on the basis of texture. This subdivision was originally developed by mine geologists at Giant to distinguish rocks in drill core. Those sills having coarser "frog skin" textures are referred to as "old metagabbro". This phase is texturally identical to sills found at Niven, displaying similar feldspar phenocrysts where they intrude along cherty tuff horizons. Sills consisting of finer grained textures are referred to as "intermediate metagabbro". These sills are stratigraphically below old metagabbro sills and are distinguished by their dark brown appearance and epidote veining. As at Niven Lake, gabbro dykes transect the Brock gabbro sills. These dykes are two to three meters in width and cut across stratigraphy at a high angle. Occasionally, the dykes also display phenocrysts of plagioclase but are generally much finer grained than gabbro sills.

One Proterozoic diabase was identified at the northern end of the Brock Lenticle. This dyke is fine grained four to five meters in width, exhibits a rusty brown weathered surface, and is also strongly magnetic. A lamprophyric dyke occurs at the northeastern end of the Brock and cuts across lapilli tuff.

2.3.3 The Vee Lake Lenticle

A shear bounded block of pillowed flows, approximately 100 m long and 20 m wide, occurs centrally within the Vee Lake Lenticle. These flows show penetrative foliation but are not flattened. Selvages are intact, two to three centimeters in width and pillow cores often exhibit eyebrow structures. These pillows border on lapilli tuff of intermediate composition which grades upwards into tuff breccia.

Feldspar porphyries comprise only a small (5%) portion of the total exposure of outcrop in the Vee Lake Lenticle. They occur as sill-like bodies in the northwestern extension. Geometrically, they are 20 by 30 meters in dimension and have been intruded by gabbro sills. In outcrop, they appear dark grey in colour with 2-3 mm sized phenocrysts of plagioclase in an aphanatic groundmass. Pervasive deformation and penetrative foliation cause great difficulty in assessing their temporal relationship with adjacent rocks, namely gabbro and quartz carbonate sericite schist. They are, however, unconformably overlain by fanglomerates of the Jackson Lake Formation.

Vee Lake Lenticle quartz-feldspar porphyries are much more difficult to characterize than those of the Brock and Niven Lake lenticles. Since felsic rocks at Vee Lake consist of both an intrusive phase and a volcaniclastic phase, differentiating these rocks based on their contact relationships and textures is difficult due to a strong schistosity. Rocks of intrusive origin were distinguished on the basis of contact relationships at the northeast arm of Vee Lake itself. Here, a package of volcaniclastic rocks form a xenolithic "raft" within texturally massive quartz feldspar porphyry (plates 2.7A, B). In terms of their geometry, quartz-feldspar porphyry bodies occur as irregular sills and dykes up to sixty meters in length and approximately twenty to fifty

Plate 2.7

(A) Injection of quartz feldspar porphyry into pyroclastics, central Vee Lake Lenticle. White line defines the quartz feldspar porphyry boundary.

(B) Intrusive quartz feldspar porphyry bordering on pyroclastic unit in the central Vee Lake Lenticle. Black line defines contact.


A


B

meters in width. Unlike their equivalents in the Brock and Niven Lake lenticles, quartz feldspar porphyries at Vee Lake are pale green in colour as a result of sericitic alteration. Their occurrence is essentially limited to the south although much, if not all of those rocks identified as quartz carbonate sericite schist may have had an intrusive origin. Contact relationships between these rocks and gabbro sills are sharp and lack textural contrasts as a result of penetrative rock fabric.

Coarse felsic volcaniclastics at Vee Lake consist of agglomerate, pyroclastic breccia and lapilli tuff breccia. Agglomerate occurs in the central portion of the Vee Lake Lenticle as an approximately 200 m long discontinuous unit (plate 2.8 A). This unit is up to 20 m in thickness and grades both vertically and laterally into pyroclastic breccia and lapilli tuff breccia. These agglomerates are unbedded, poorly sorted and clast supported. The composition of both matrix and clasts is felsic with felsic clasts made up of quartz feldspar porphyry. Clasts are subrounded to angular, range in size from 3 cm to 50 cm, and have dark reaction rims indicating deposition while still hot.

Pyroclastic breccia (plate 2.8 B) occurs stratigraphically above the agglomerate and extends northerly along strike for approximately 500 m. This unit is up to 10 m thick and discontinuous due to offsets by faulting. This unit is poorly sorted, meter sized blocks of quartz feldspar porphyry are found sitting in a very finely bedded lapilli tuff. Clasts are stratabound suggesting that the unit is a debris flow. Blocks do not exhibit reaction rims, indicating deposition while relatively cool. The matrix is lapilli tuff breccia (plate 2.8 C) consisting of subangular clasts of felsic material. Dominant clasts include well preserved pumice, fiammi and lapilli. Lapilli are composed of

Plate 2.8

(A) Agglomerate, central Vee Lake Lenticle. Consists of volcanic bombs of quartz feldspar porphyry in a matrix of quartz feldspar porphyry. Central Vee Lake Lenticle.

(B) Pyroclastic breccia, central Vee Lake Lenticle. Consists of angular bombs of quartz feldspar porphyry in an intermediate lapilli tuff breccia matrix.

(C) Lapilli tuff breccia, central Vee Lake Lenticle. Note flattened quartz feldspar porphyry clasts hosted in intermediate matrix.

(D) Lapilli tuff, central Vee Lake Lenticle. Note bedding contact running through lens cap.

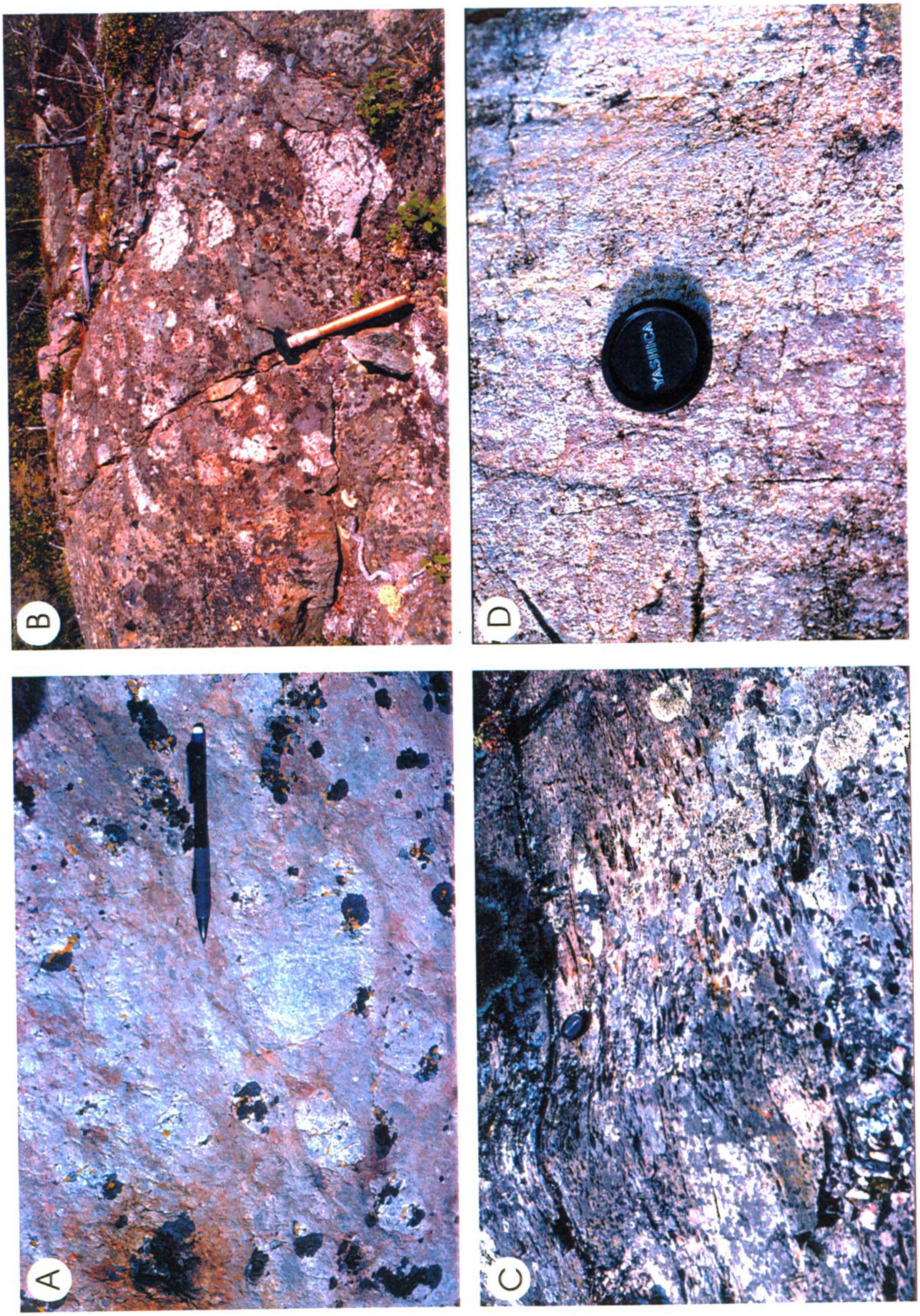
B
D
YASHICA
A
C

clusters of plagioclase, sericite, quartz and carbonate. Minor clasts include of quartz feldspar porphyry and isolated phenocrysts of quartz and feldspar.

Lapilli tuff (plate 2.8 D) overlies this pyroclastic tuff breccia. This unit is subdivided based on the absence of large quartz feldspar porphyry blocks and bombs yet it is interbedded with and gradational to lapilli tuff breccia. Gradation into straight lapilli tuff is accompanied by a greater population of plagioclase phenocryts. These crystals are tabular in habit and subhedral in form and are on average 4 mm in size. Lapilli range in size upwards to 4 mm and are composed of quartz and plagioclase phenocryst aggregates with interstitial quartz, carbonate, and sericite. Stratigraphically above and interbedded with lapilli tuff are quartz-phyric crystal tuffs (plate 2.9 A). This facies is laterally extensive and discontinuously spans the entire Vee Lake Lenticle. These tuffs are matrix supported and often well bedded. Quartz eyes are up to 2 mm in size and accessory clasts in these rocks include preserved pumice and fiami as well as the occasional lithic fragment. Plagioclase pheocrysts may or may not be present and when they occur exist as tabular equant grains 1-2 mm in size.

A volcanic sandstone occurs stratigraphically higher in the section on the western shore of Walsh Lake (plate 2.9 B, C, D). This sandstone exhibits crossbedding and appears to be the result of redeposition of lower units. Above, and in sharp contact with this unit is vitric ash tuff (plate 2.9 B, C). This outcrop is only about 4-5 mm thick and 10 m long where it dissappears into the lake. This rock consists of spindle shaped fiami in a fine grained light green/yellow matrix.

Penetrative deformation accompanied by pervasive alteration results in quartz carbonate sericite schist being the primary Vee Lake lithology type (plates 2.10A –

Plate 2.9

(A) Quartz crystal tuff, central Vee Lake Lenticle. Note laminated layering.

(B) Rock hammer spans the contact between lapilli tuff (left), volcanic sandstone (center) and vitric ash tuff (right). Taken on the shore of Walsh Lake.

(C) Close-up of contact between volcanic sandstone (left) and vitric ash tuff (right). Taken on the shore of Walsh lake.

(D) Close-up of bedded volcanic sandstone (above).

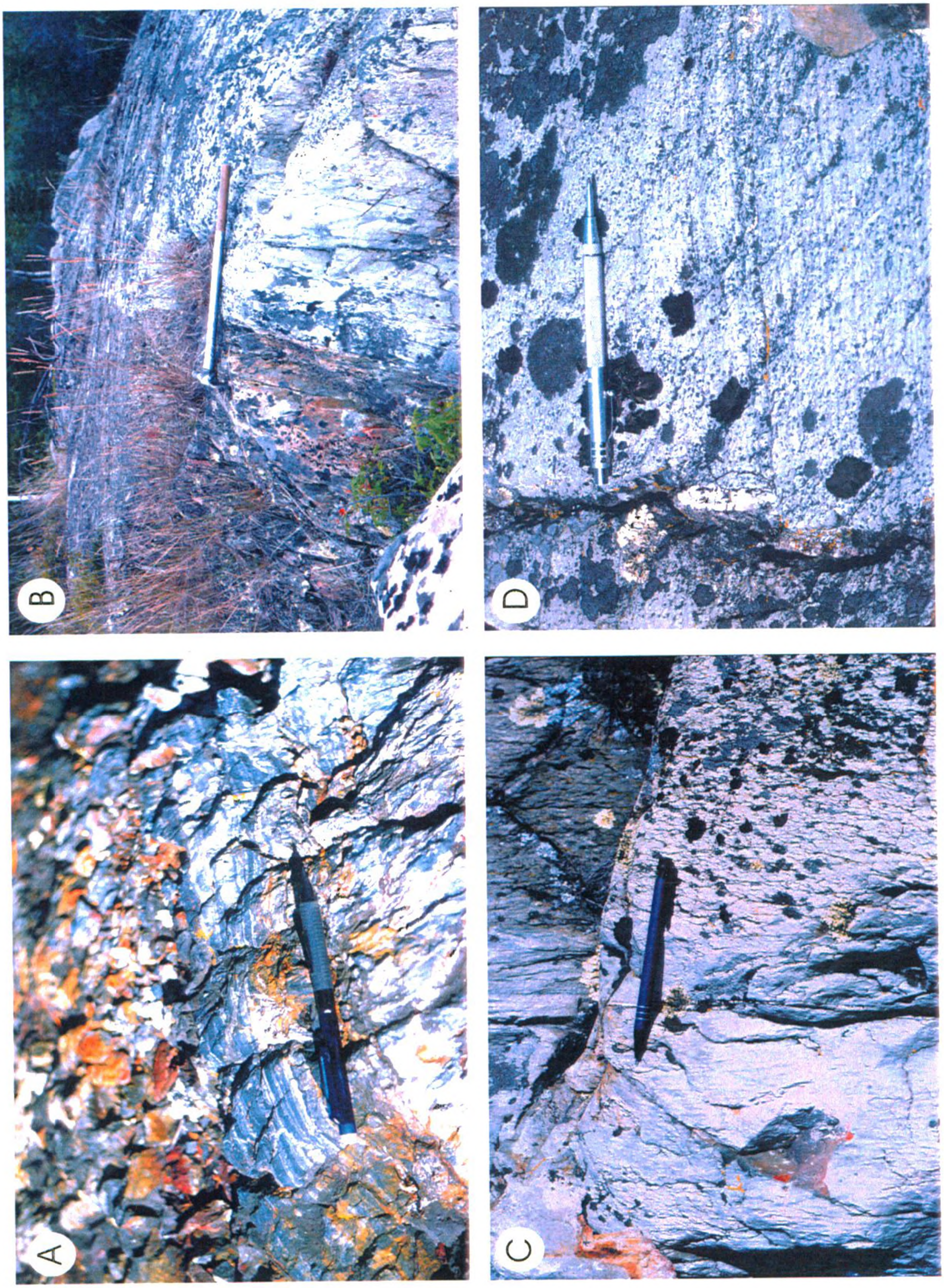

A
B
C
D

2.10C). Considering the degree of strain and alteration, it is impossible to determine an intrusive or extrusive origin for these schists. This schist is dominant in the north and northwest. It has a pinkish/yellowish colour, and has suffered grain reduction during deformation. two mm sized anhedral plagioclase and quartz phenocrysts occur in a sericitic groundmass flooded with ankerite veinlets.

Gabbro sills in the Vee Lake Lenticle are similar to those found in the Niven Lake and Brock lenticles. They are massive and occur along the entire length of this portion of the Townsite Formation. In spite of large areas in the northern portion being pervasively deformed, in much of the outcrop in the south, they exhibit spotted amphibolitic texture equivalent to those in the Brock and Niven Lake lenticles.

The north end of the Vee Lake Lenticle is pervasively transected by a suite of felsic dykes and irregular shaped bodies (plate 2.10 D). These dykes are bright green in colour and are quartz and feldspar phyric. They definitely predate the late stages of deformation as they are “pulled” into the penetrative fabric.

Plate 2.10

(A), (B), (C) Photos showing the degree of penetrative foliation in the Vee Lake Lenticle. The light green units are quartz carbonate sericite schist and may be of intrusive or extrusive origin. The dark rocks are mafic and may be flows or gabbro sills.

(D) Felsic dyke cutting gabbro sill. Jackson Lake in the background.

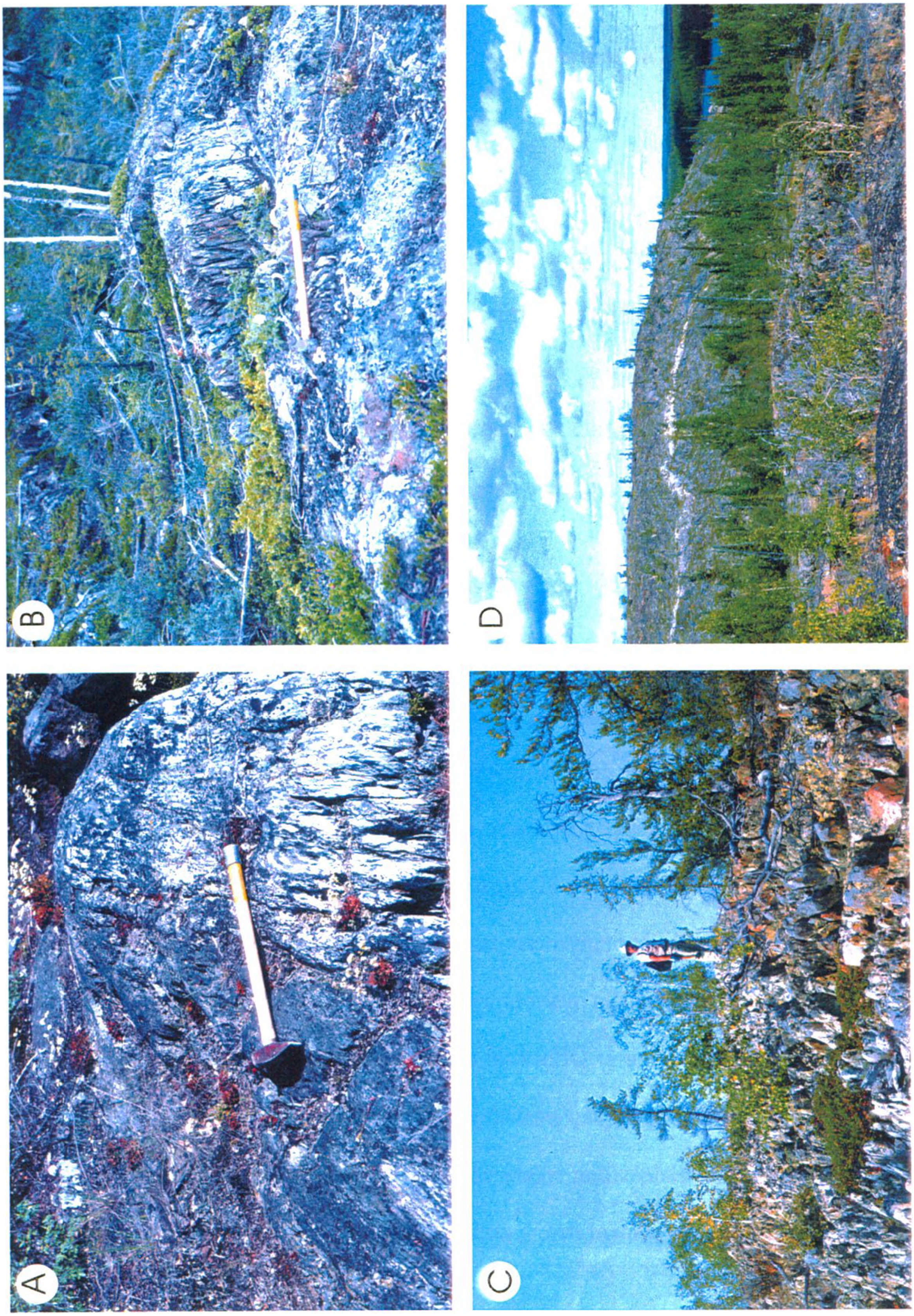
A
B
C
D

Chapter 3

Descriptive Petrography of Townsite Formation Lithologies

3.1 Introduction

Thin sections were examined using a polarizing microscope equipped with reflective light optics. Petrographic descriptions are organized from oldest to youngest lithologies, including: volcanic flows, cherty tuff, volcaniclastics, feldspar porphyry, quartz feldspar porphyry, hydrothermal breccias and gabbro sills. Each begins with lithologies in the Niven Lake Lenticle and progresses northward through the Brock to the Vee Lake lenticles respectively. Photomicrographs supplement thin section descriptions.

3.2 Volcanic Flows

Descriptions of flows are based on a study of seven thin sections. Niven Lake specimens reveal a fine grained seriate texture with amphibole (50%) as the main mafic phase. Amphibole occurs as acicular laths displaying well defined cleavage and dendridic to spherulitic porphyroblasts up to ¼ mm in size. Epidote is the second most abundant mafic phase, occurring as clear tabular grains up to ¼ mm in size. Anomolous birefringence and zoning are observed under crossed nicols. Chlorite, comprising approximately 10 %, is present as microlites interstitial to amphibole. A much finer grained groundmass consists of interstitial plagioclase, quartz, and sericite.

In the Brock Lenticle, amphibole is again the major mafic phase. These grains are anhedral in form but occur in a variety of habits which include skeletal, dendritic and spherulitic. The majority of the crystals are acicular and these are commonly disoriented. These grains partially include groundmass and show some chlorite alteration. Chlorite is the second most abundant mafic phase, occurring as patches where it replaces amphibole. Plagioclase is not abundant, occurring as tabular subhedral grains partially enclosing groundmass. Most plagioclase grains exhibit incipient alteration to sericite, carbonate and quartz.

Spherulitic masses represent varioles (plate 3.1A). The mineralogy of these masses is too fine grained to resolve microscopically but the spherules are primarily composed of secondary quartz, carbonate, and sericite. Most varioles are strongly fractured and infilled with chlorite veins and patchy chlorite. Amphibole and epidote can be observed in some nodules. The relict spherulitic to dendritic texture stem from the original variole. The fine grained groundmass is composed of quartz, sericite, carbonate and chlorite and minor plagioclase. In terms of opaque minerals, sphalerite is as abundant as is pyrite. Sphalerite appears to be associated with amphibole. Epidote is abundant in the groundmass as patchy growths as well as tabular subhedral grains which are clear and apple green in colour when viewed in plane polarized light.

In the Vee Lake Lenticle basaltic andesites display an overall aphanitic texture but in thin section they generally demonstrate a microporphyritic texture. Plagioclase phenocrysts up to 1.5 mm in length occur as prismatic, subhedral grains in a fine grained groundmass of microlitic chlorite, plagioclase, sericite and quartz. These grains display polysynthetic twinning, have normal zoning and have undergone partial resorbtion. Chlorite is the only mafic phase in the groundmass and occur as microlites.

Plate 3.1

(A) Brock Lenticle volcanic flow. Variolitic material outlined by white line.

(B) Vee Lake Lenticle pyroclastic breccia. Strongly altered pagioclase phenocryst at top of photo. Note quartz eyes hosted in a fine to medium grained hollocrystalline groundmass of quartz, sericite, plagioclase and carbonate-chlorite veins.

(C) Vee Lake Lenticle pyroclastic breccia (quartz feldspar porphyry block). This photo shows tabular and subhedral plagioclase phenocryst displaying dformation twinning.

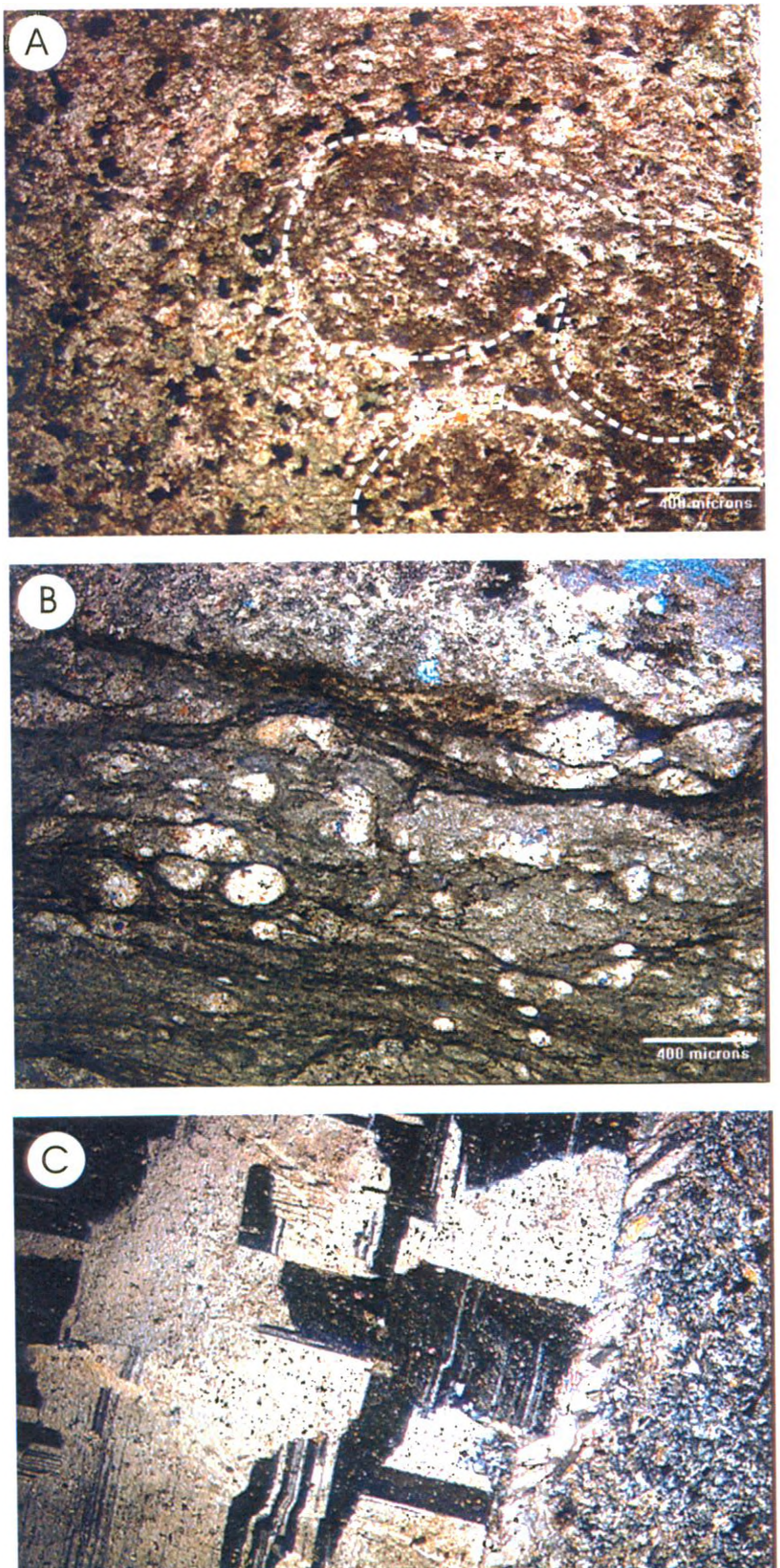
A
400 microns
B
400 microns
C
400 microns

The remainder of the groundmass consists of intergrown plagioclase, quartz, sericite and secondary carbonate.

3.3 Cherty Tuffs

Cherty tuffs occur in the Brock and Niven Lake members of the Townsite Formation but are absent in the Vee lake member. Thin sections analyzed from both lenticles are petrographically similar. In thin section, these units are massive, quartz rich and rarely display quartz and plagioclase phenocrysts.

3.4 Volcaniclastics

Agglomerates are only observed in the Vee lake lenticle. In thin section, the overall texture is porphyritic and defined by monolithic clasts almost entirely altered to sericite, with quartz eyes ranging in size from 0.5 – 2 mm. Interstitial to these clasts there exists fine grained quartz, carbonate, sericite, and minor microlitic chlorite.

Pyroclastic breccia is poorly sorted and consists of meter sized blocks of quartz feldspar porphyry sitting in a finely bedded lapilli tuff. In thin sections these blocks have similar appearance to Brock quartz feldspar porphyry. Centimeter sized plagioclase phenocrysts and quartz eyes are hosted in a fine to medium grained hollocrystalline groundmass of quartz, sericite, plagioclase and carbonate with minor patchy chlorite (plate 3.1B). The plagioclase phenocrysts are tabular in shape and subhedral in form, displaying deformation twinning (plate 3.1C).

Lapilli tuff is found at the northern tip of the Brock lenticle and is continuous throughout the Vee Lake Lenticle. At Vee Lake, however, there is a gradation from pyroclastic breccia through lapilli tuff brecccia. Gradation into uniform lapilli tuff is

Plate 3.2

(A) Lithic fragment in lapilli tuff from central Vee Lake Lenticle. (B) Crossed polars.

(C) Central Vee Lake lenticle. Pumice fragment preserved in quartz crystal tuff (lower half of photo). Note flattened vessicles. (D) Crossed polars.

(E) Quartz phyric crystal tuff from central Vee Lake Lenticle. (F) Crossed polars.

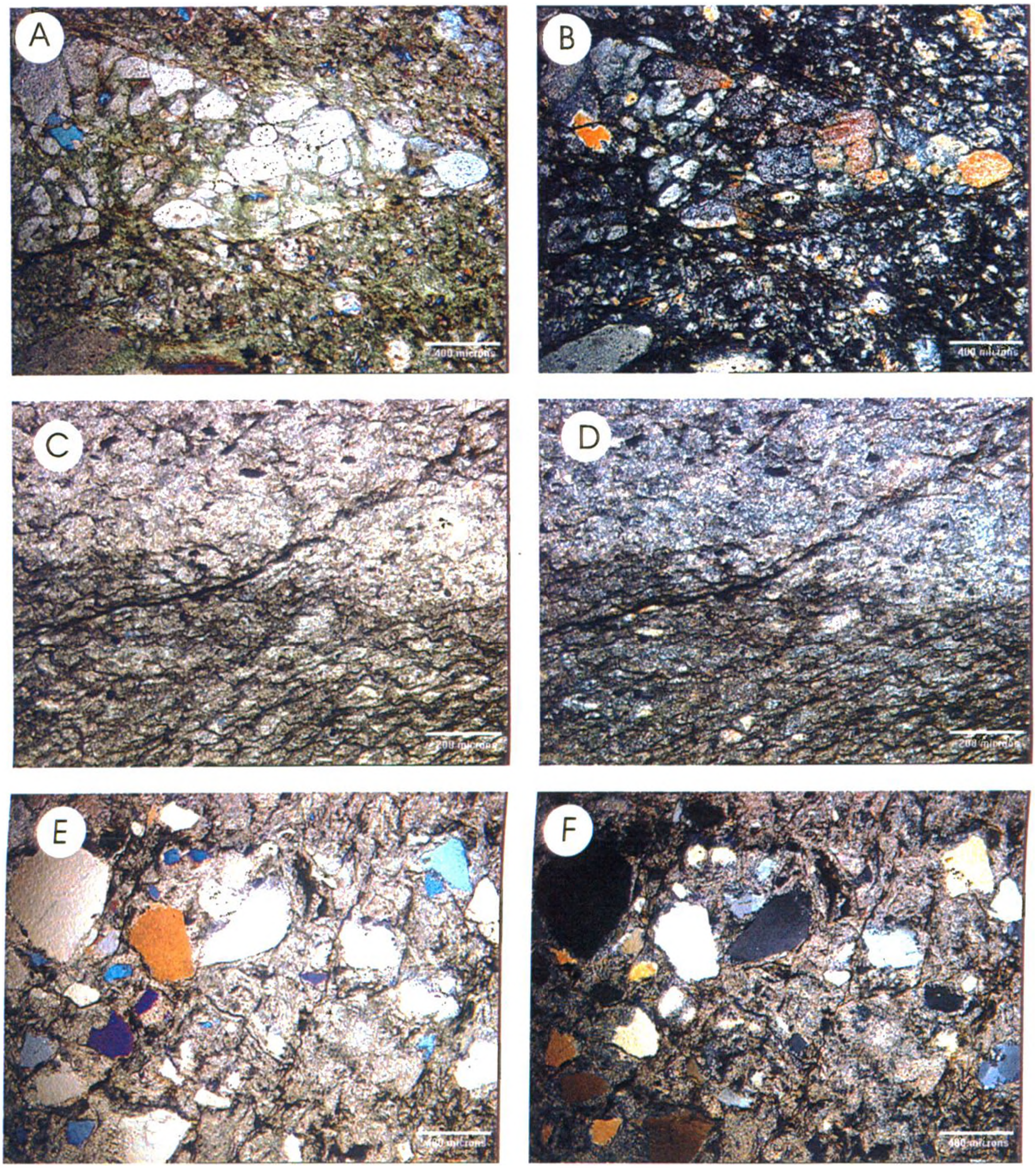
A
400 microns
B
400 microns
C
200 microns
D
200 microns
E
400 microns
F
400 microns

accompanied by a greater population of plagioclase phenocryts. These crystals are tabular in habit and subhedral in form and are on average 4 mm in size. They also display oscillatory zoning. A finer (~ 1mm) generation of plagioclase is also noted. These grains display simple twinning but are strongly altered to sericite. Lapilli range in size upwards to 4 mm and are composed of quartz and plagioclase phenocryst aggregates with interstitial quartz, carbonate, and sericite (plate 3.2A,B). The groundmass has an overall seriate texture composed of chlorite after altered glass shards, quartz and sericite altered plagioclase microlites. Where rocks are strongly altered, the groundmass is flooded with ankerite.

In the Vee Lake Lenticle quartz phyric crystal tuff occurs laterally along strike as discontinuous finely bedded lenses. In thin section, quartz eyes are up to 2 mm in size. Accessory clasts include relict pumice (plate 3.2 C,D) and fiami as well as the occasional lithic fragment. Plagioclase phenocrysts may or may not be present as tabular equant grains 1-2 mm in size (plate 3.2 E,F). Where found as rafted sediments in south/central Vee Lake they tend to be interbedded with reworked material, consisting of platy and cuspate glass shards intermixed with quartz and sericite . The very fine grained groundmass, now quartz and sericite, may derive from devitrified glass.

Occurring only as a small outcrop on the western shore of Walsh lake, vitric ash tuff consists of spindle shaped fiami in a fine grained light green/yellow matrix. Thin sections reveal sericite altered fiammi 2-3 mm in size in a ground mass of quartz,

Plate 3.3

(A) Vitric ash tuff. Sample collected at the shore of Walsh lake (Vee Lake Lenticle). Note sericitized, flattened pumice (fiami) outlined in white.

(B) Volcanic sandstone. Note prismatic chloritoid porphyrobasts in quartz rich groundmass. (C) Crossed polars.

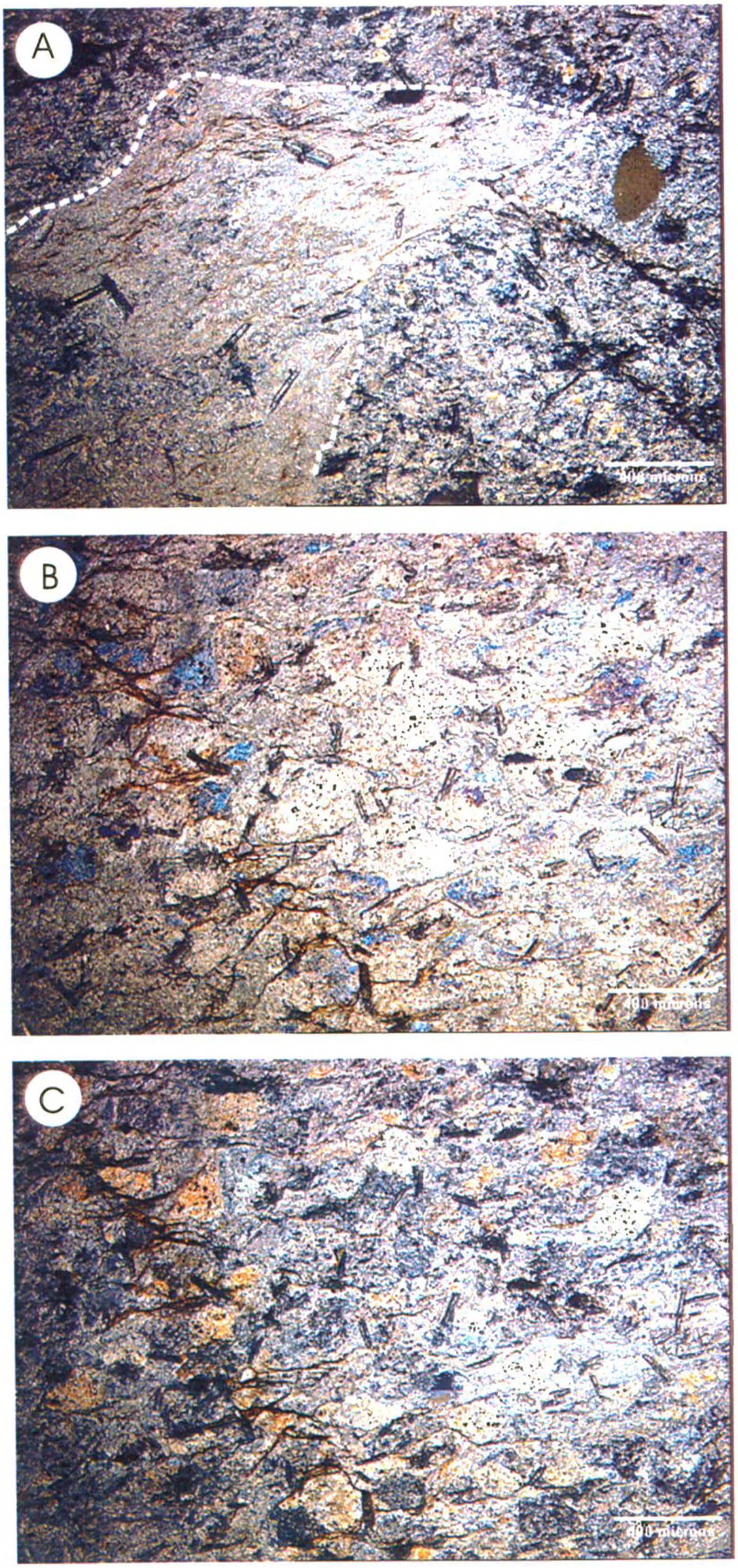
A
B
C

sericite, platy glass shards and minor chlorite (plate 3.3A). Subordinate in the groundmass are tiny microlites of feldspar and quartz. Spherulitic devitrified glass is also evident.

Crossbedded volcanic sandstone lying stratigraphically below and in sharp contact with the vitric ash tuff is medium grained, massive rock composed of equal amounts of quartz and sericite (plate 3.3 B,C). Scattered throughout the groundmass are euhedral chloritoid porphyroblasts (5%), platy glass shards and microlites of feldspar.

3.5 Feldspar Porphyry

The descriptions of feldspar porphyry from Niven lake are based on examination of two thin sections. Thin sections reveal an overall porphyritic texture with plagioclase phenocrysts in a fine to medium grained groundmass of amphibole, chlorite, plagioclase, quartz, sericite and carbonate (plate 3.4 A, B). Plagioclase phenocrysts are up to 4 mm in size and have albitic composition. These grains are subhedral in form and tabular to prismatic in habit. Twinning is rarely observed as grains are strongly altered to sericite. Secondary growths of carbonate and sericite occur along most plagioclase rims. Amphibole makes up the major mafic phase, occurring as porphyroblastic growths up to 1 mm in size with acicular, dendritic and spherulitic habits. Minor chlorite occurs as microlites in the groundmass. The remainder of the groundmass is composed of randomly oriented intergrowths of plagioclase, quartz, sericite, carbonate and apatite.

Plate 3.4

(A) Strongly altered plagioclase phenocryst from Niven Lake Lenticle feldspar porphyry. (B) Crossed polars.

(C) Brock Lenticle feldspar porphyry. Note oscillatory zoning and twinning. Also note the much finer grained groundmass in the Brock example (scale).

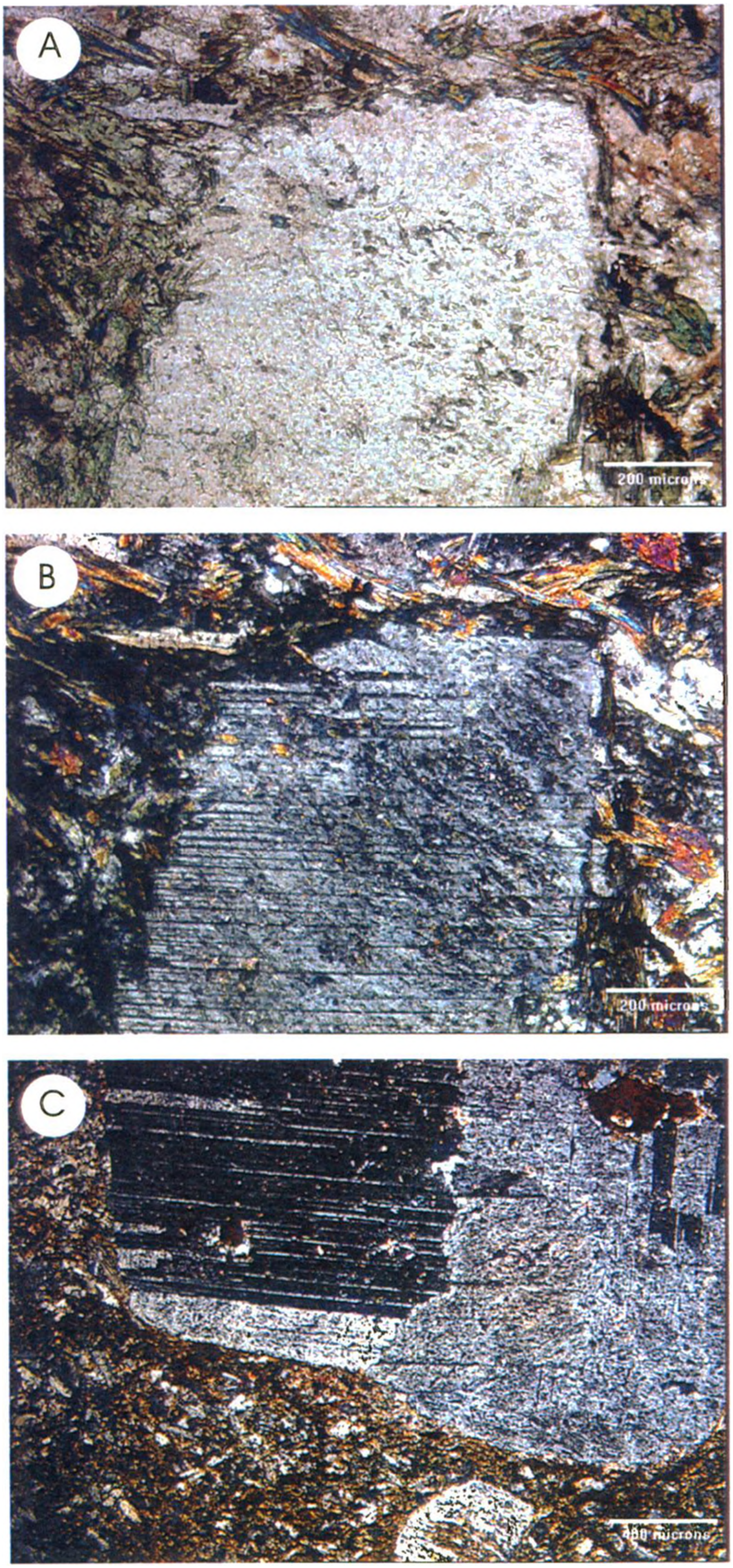
A
B
200 microns
C

Descriptions of Brock Lenticle feldspar porphyries are based on an examination of three thin sections. In thin section plagioclase is the only phenocryst phase. The groundmass is comprised of chlorite, biotite, epidote, sphene, plagioclase, sericite and quartz (plate 3.4 C). The majority of the euhedral feldspar phenocrysts are 4-6 mm in size, euhedral in form and tabular to prismatic in habit. Their composition is exclusively albitic and they comprise 20-25% of most samples. These grains often form glomeropyhric aggregates. Fractures are now infilled with secondary carbonate. Feldspar phenocrysts poikiolitically enclose minerals occuring in the groundmass. Most crystals show well developed oscillatory zoning. Biotite is ubiquitous in the groundmass of all Brock feldspar porphyry sections. These crystals show platey habit and are always partially replaced by chlorite. Sphene is also abundant throughout feldspar porphyries in the Brock, comprising 5-10% of most thin sections. These high relief grains often occur as patchy clusters <1 mm in size, are subhedral in form and tabular in habit. Most grains are fractured. Epidote occurs locally in most sections but is not ubiquitous. These are very fine grained (<1/10 mm) and display third order birefringence. Ubiquitous quartz, plagioclase and sericite make up accessory phases in the groundmass. Some sections show ½ mm sized annealed ovals of polygonal quartz. Carbonate occurs as veins and increases in areas where rocks are sheared. Opaques include pyrite, ilmenite and chalcopyrite.

Feldspar porphyries from the Vee Lake Lenticle appear dark grey in colour with 2-3 mm sized phenocrysts of plagioclase in an aphanitic groundmass. Cut and polished slabs reveal grey prismatic plagioclase phenocrysts as large as 5 mm in size. Here they appear as dark grey prismatic grains. Albite phenocrysts occur in a fine grained groundmass. Larger plagioclase phenocrysts are tabular to prismatic subhedral grains that are overprinted by moderate sericite alteration. Some grains are entirely replaced by sericite. Those that have undergone least alteration display excellent lamellar twins and oscillatory zoning. The groundmass is comprised of fine (<1 mm) albite phenocrysts (50%) and chlorite (50%). Chlorite shows dark brown to blue interference and occurs interstitially to microphenocrystic plagioclase. In some sections chlorite replaces biotite. Trace sphene and epidote occur throughout the groundmass. Trace opaque phases include ilmenite and chalcopyrite.

3.6 Quartz Feldspar Porphyry

The descriptions of quartz feldspar porphyries are based on the examination of a total of twelve thin sections. In hand sample Niven Lake Lenticle quartz feldspar porphyries exhibit well preserved porphyritic texture defined by plagioclase and quartz phenocrysts. Cut and polished slabs of this rock reveal plagioclase phenocrysts between 2 and 8 mm and smokey grey quartz eyes between 2 and 3 mm, hosted in dark grey aphanitic groundmass. In thin section the overall porphyritic texture is defined by plagioclase phenocrysts with subordinate quartz eyes (plate 3.5 A). The groundmass is fine grained and composed of biotite, minor chlorite, quartz, plagioclase, sericite, carbonate and sphene. The plagioclase phenocrysts are 2-10 mm in size, strongly sericitized and display lamellar twins. In most sections plagioclase phenocrysts make up 20-25% of the rock and range from tabular to prismatic in habit and subhedral to euhedral in form. They show normal zoning and have andesine composition. Rare

Plate 3.5

(A) Niven Lake Lenticle quartz feldspar porphyry. Note strong (quartz, sericite) alteration of plagioclase phenocryst and quartz eye at lower left.

(B) Brock Lenticle quartz feldspar porphyry. Photo displays quartz eyes, and smaller generation plagioclase rich groundmass. Note subhedral to anhedral plagioclase phenocrysts altered to sericite along microfractures.

(C) Vee Lake Lenticle quartz feldspar porphyry. Plagioclase grains display deformation twinning.

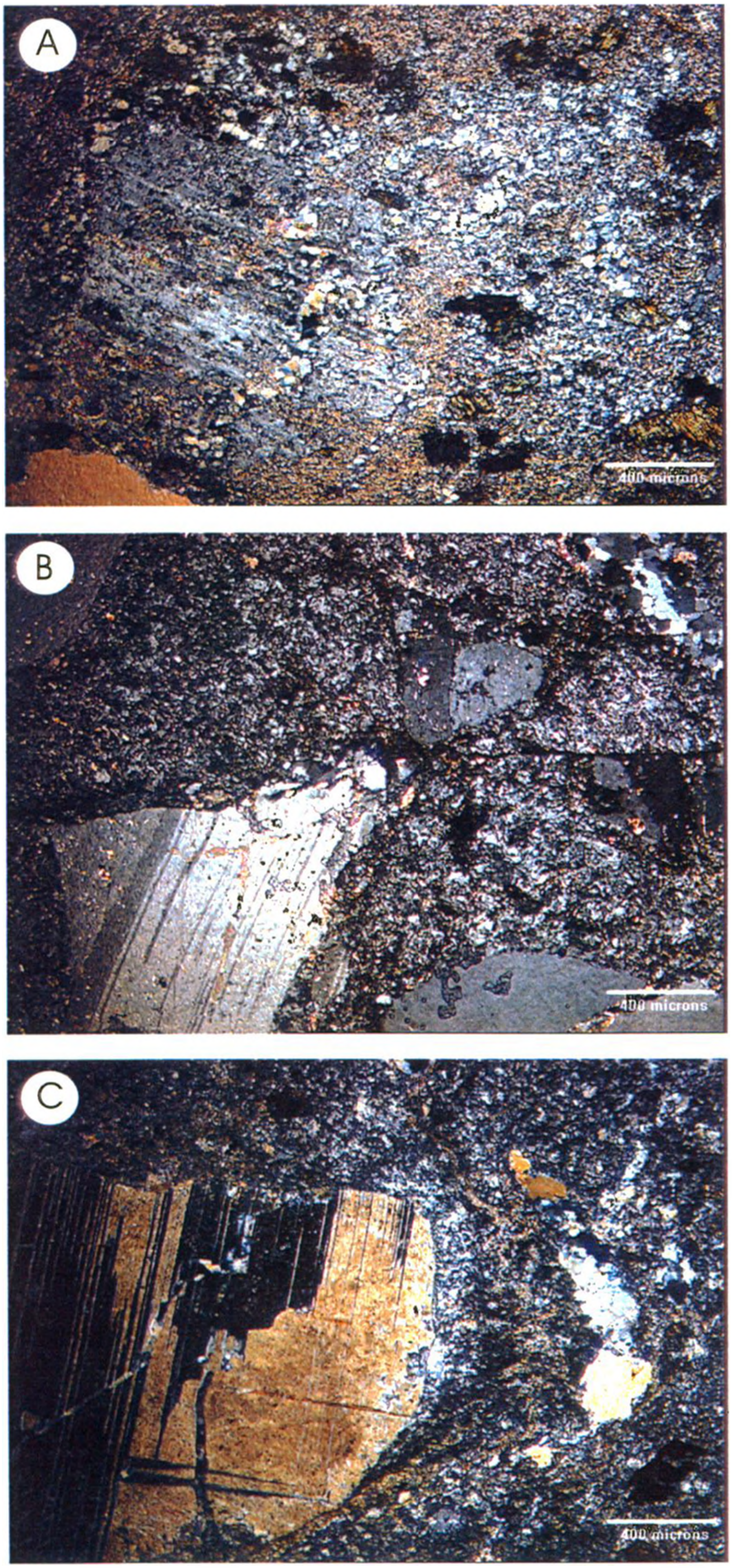
A
400 microns
B
400 microns
C
400 microns

(2%) quartz eyes are 1-3 mm in size and display embayed grain boundaries. These grains are generally clear and have undulatory extinction.

Patchy biotite makes up approximately 20% of these rocks and occurs as .25 to .50 mm equant tabular grains. Sphene makes up approximately 5% modally and occurs in close association, with the biotite. Chlorite is rare, and only occurs where it replaces biotite. The remainer of the groundmass consists of a finely intergrown assemblage of quartz, sericite and carbonate together with microlites of plagioclase and apatite. In order of abundance, quartz makes up approximately 30%, carbonate 10%, sericite 5% apatite and plagioclase 5%. Ilmenite occurs as a minor opaque phase rarely associated with sulphides.

In cut and polished slabs Brock Lenticle quartz feldspar porphyry intrusives reveal prismatic euhedral to subhedral feldspar phenocrysts up to 8 mm in length and smokey grey quartz eyes 2-3 mm in diameter hosted in an aphanitic dark grey siliceous groundmass. In thin section, Brock Lenticle quartz feldspar porphyries exhibit microporphyritic textures characterized by plagioclase and quartz eye phenocrysts in a fine grained groundmass (plate 3.5 B). There are two distinct populations of plagioclase phenocrysts: those which are 5-8 mm in size and a smaller generation ranging between 0.5 and 1.5 mm. The macrophenocrysts are euhedral to subhedral in form, tabular to prismatic in habit and comprise approximately 25%. Depending on their degree of alteration, they usually display lamellar twinning, are albite to oligoclase in composition and display normal zoning. Alteration is incipient to pervasive with sericite, quartz and chlorite. The microphenocrystic generation of plagioclase comprises up to 10%, are prismatic in habit but generally show subhedral to anhedral form. These grains commonly display simple twins and poikiolitically enclose sericite and minor apatite. The quartz eyes are 2-3 mm in size and comprise approximately 5%. These grains are usually smokey grey in colour and display undulatory extinction. Some grains display microfracturing with fine grained quartz aggregates infilling these fractures.

Chlorite is ubiquitous throughout the groundmass and occurs as microlites and as patches and veins, comprising up to 15% of most thin sections. Chlorite is dark green to bright green in plane polarized light often spatially associated with carbonate. Quartz, apatite and secondary carbonate and sericite comprise approximately 70% of the groundmass. In some sections the groundmass is almost entirely cryptocrystalline quartz. Sphene (comprising 1-2%) is observed in most sections and occurs as 1-2 mm subhedral tabular grains that often occur in clusters. Opaques are minor and consist of pyrite and ilmenite.

Weathered hand samples of Vee Lake quartz feldspar porphyry intrusives show 2-3 mm plagioclase and quartz phenocrysts in a siliceous groundmass. Cut and polished slabs reveal greenish-grey subhedral to anhedral plagioclase phenocrysts and smokey grey quartz eyes in a very dark groundmass. Thin sections display an overall porphyritic texture with plagioclase and quartz grains hosted in a fine grained groundmass (plate 3.5 C). Areas of shearing, such as northeast of Gold Lake, display the most intense alteration of groundmass. Feldspar phenocrysts may be anywhere from 2-10 mm in size, are subhedral in form and have tabular to prismatic habit. Plagioclase phenocrysts are albite in composition and range between 10 and 40 modal %. Although sericite alteration is moderate to high, lamellar twins are readily discernable. Quartz eyes ranging between 2-3 mm are less abundant, comprising 5-10 modal %. These grains are clear and typically equant, display undulatory extinction, and are rarely fractured. Samples having a greater intensity of alteration have chlorite-carbonate veinlets. In less altered samples, 5-10 % chlorite is ubiquitous throughout the groundmass. Throughout the groundmass carbonate, sericite, and apatite comprise approximately 5% each. In less altered samples quartz makes up as much as 65% of the remaining groundmass component. Pyrite is common and may comprise 2% of the more altered samples.

3.7 Hydrothermal Breccias

Mafic pillowed units bordering on massive quartz feldspar porphyry are characteristically bleached (silicified-albitized) and commonly exhibit brecciation textures. Breccias are readily observed at the eastern end of the Niven Lake Lenticle (behind the Racquet Club) and through the southern and central portions of the Brock. Breccia types range from fragmented wall rocks with blocks hosted in hydrothermally cemented rock flour, through heterolithic mixes with both volcanic and porphyry blocks. Monolithic breccias occur in the Brock where quartz feldspar porphyry is host to meter sized blocks of feldspar porphyry creating a "jigsaw" like texture. In thin section (plate 3.6a,b,c,d), the rock flour is almost entirely composed of quartz or a mixture of chlorite, sericite, and quartz. Both macro and microscopic fragments of mafic and felsic material are found in this rock flour matrix.

Plate 3.6

(A) Niven Lake Lenticle hydrothermal breccia. Note mixed felsic (light areas) and mafic (dark green areas) hosted in a hydrothermally milled rock flour.

(B) From the same area as (A), this photo shows rock flour being comprised of randomly oriented chlorite and amphibole grains in a micro quartz aggregate.

(C) From the same area of (A) and (B) shows the boundary (white line) between mafic material and rock flour. Note the extremely fined grained nature of the siliceous rock flour. (D) crossed polars.

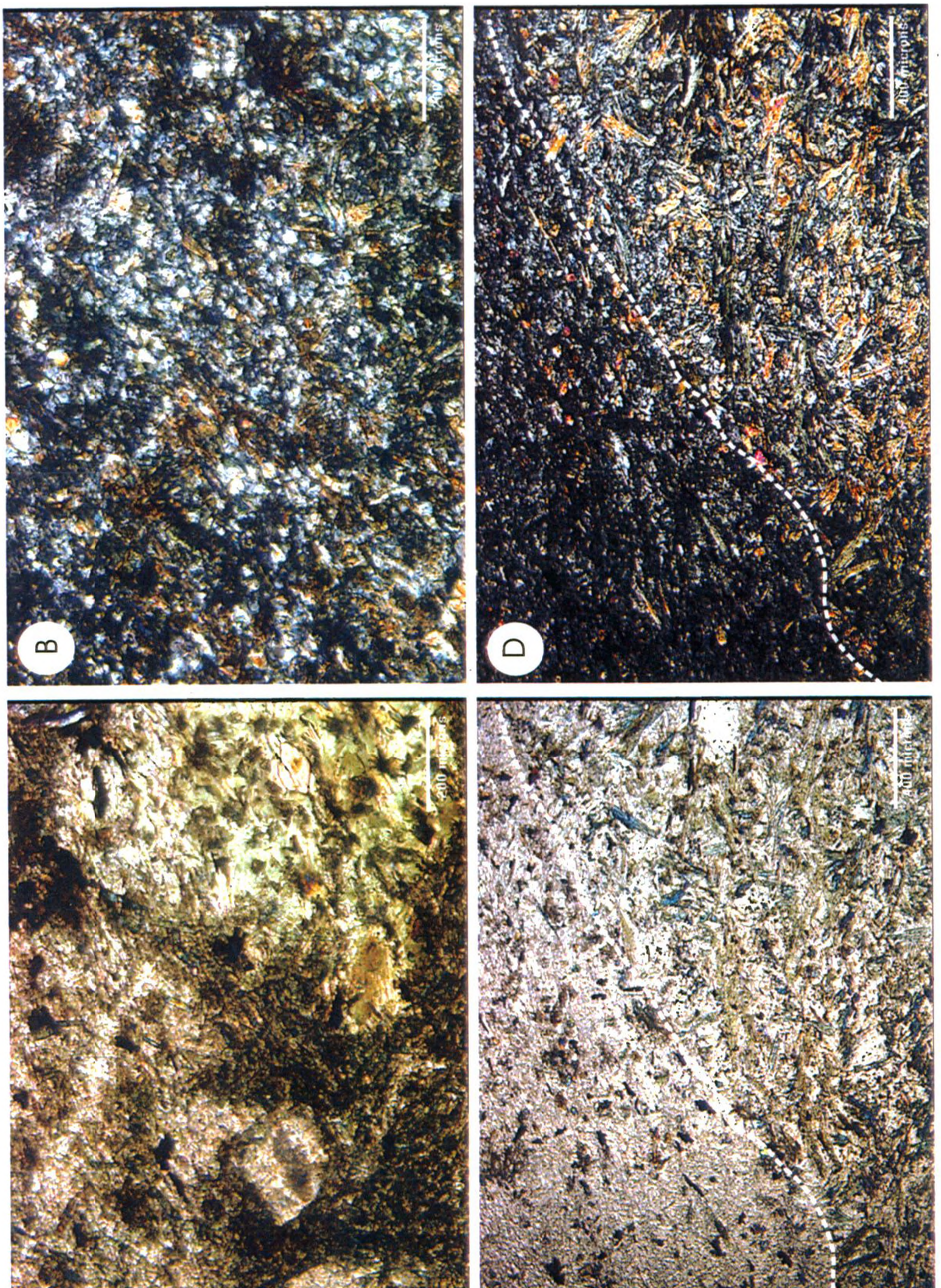
A
B
C
D
200 microns

3.8 Gabbro Sills

The description of gabbro sills in the Niven Lake Lenticle is based on four thin sections. In thin section, these sills are melano to mesocratic in colour (plate 3.7 A). These rocks are largely composed of randomly oriented blades of highly altered amphibole up to 5 mm in size. Interstitial to amphibole are fine grained aggregates of quartz and microlites of chlorite, epidote and plagioclase that together make up approximately 15%. Amphiboles are anhedral in form and partially enclose fine grained interstitial material. In some samples 80 % of individual amphibole grains are altered to prehnite, 5 % to chlorite and 5 % to epidote. Prehnite displays bright second and third order birefringence and high relief.

The rare plagioclase phenocrysts occurring proximal to cherty tuff units at the margins of sills are 95 % altered to sericite. Groundmass plagioclase, preserved as microlites with simple twins, are oligoclase to labradorite in composition. Gabbro sills display minor carbonate flooding, comprising 5 % in thin section.

Gabbro sills in the Brock are thinner than those at Niven. The old metagabbro is texturally identical to the sills at Niven Lake, exhibiting coarse amphibole and rare feldspar phenocrysts where they intrude along cherty tuff horizons. In thin section (plate 3.7 B) they differ markedly in their mineralogy and abundance of plagioclase. Plagioclase up to 2 mm in size comprise 15 %. These grains are subhedral, tabular to prismatic in habit and have andesine to labradorite composition. Although substantially altered to sericite, lamellar twins are still discernable. Amphibole is well preserved in these rocks and prehnite is absent. Amphiboles are up to 5 mm in size and have acicular to dendritic habit and are partially altered to chlorite and epidote. Chlorite

Plate 3.7

(A) Niven Lake Lenticle gabbro sill. Note the alteration of amphibole to prehnite (P).

(B) Brock Lenticle gabbro sill (old metagabbro). Note amphibole coarsely altered to chlorite.

(C) Brock Lenticle sill (intermediate metagabbro), note chlorite alteration along cleavage.

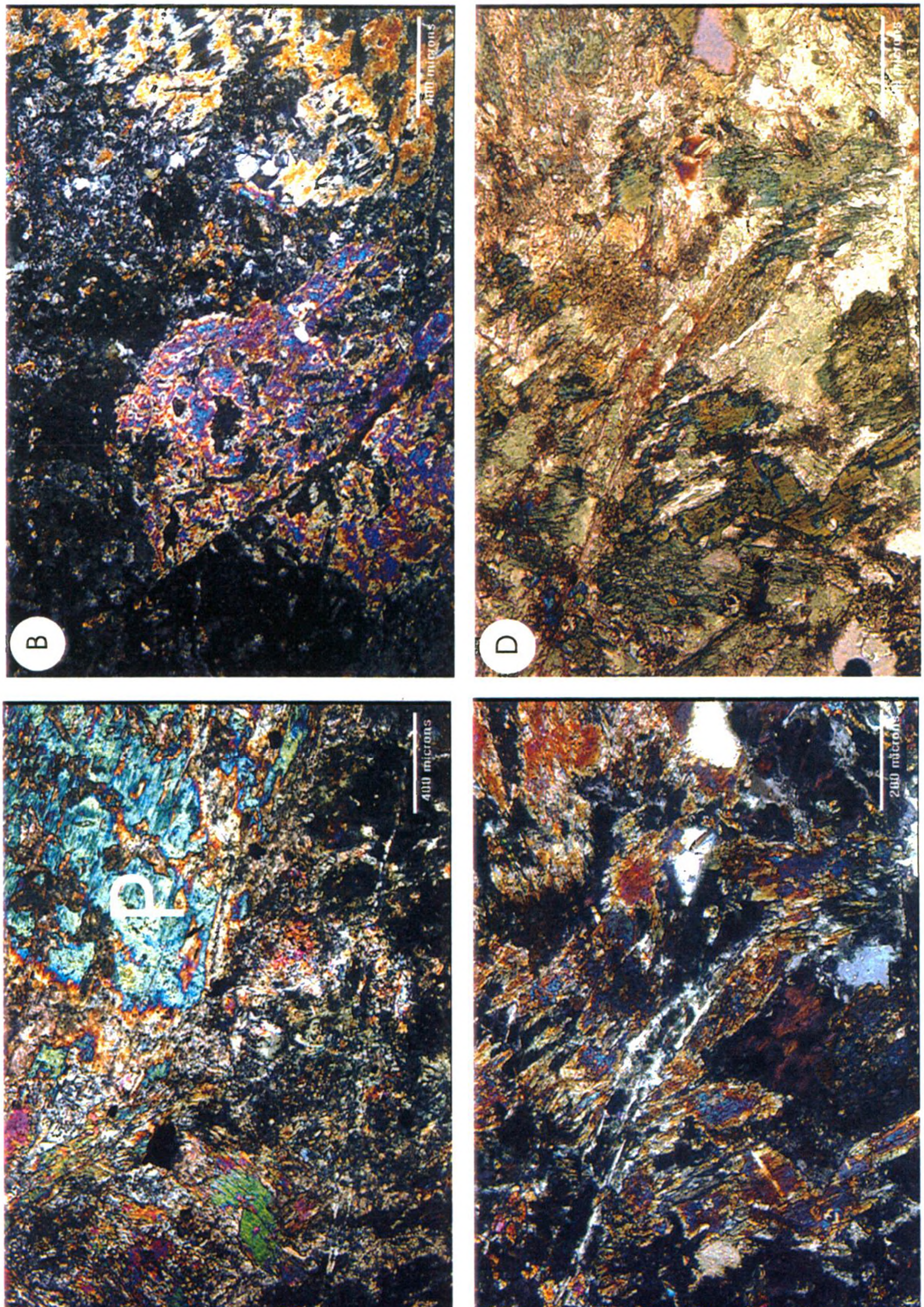
A
P
400 microns
B
C
200 microns
D

occuring as a patchy replacement of amphibole and intergrown with epidote, plagioclase, quartz and carbonate, comprises approximately 15 %.

Thin sections, of intermediate metagabbro (plate 3.7 C, D), exhibits coarse amphibole 1 – 2 mm in size. These grains are 50 % altered to chlorite and epidote. Albite to andesine plagioclase up to 1 mm in size make up 15 % of these sections, occurring as prismatic grains, subhedral in form, interlocking with amphibole. The fine grained groundmass is composed of quartz , sericite , epidote and carbonate. Sphene is an accessory phase.

Similar to the Brock, both intermediate and old metagabbro sills occur in the Vee Lake lenticle. Here textures are masked due to penetrative deformation and alteration. Where identifiable, textural characteristics are essentially equivalent to those in the Brock Lenticle. The coarse amphibole is entirely altered to chlorite. Most are carbonate (ankerite) flooded and some contain patchy ilmenite. Coarse albitic plagioclase occurs up to 2 mm in size in composition and occur as tabular prismatic laths. Rare quartz eyes occur in a groundmass of fine grained quartz, epidote and chlorite.

Chapter 4

Geochemistry

4.1 Bulk Rock Geochemistry

4.1.1 Introduction

Major oxide and trace element compositions were determined at Actlabs and the laboratory of the Ontario Geological Survey at Sudbury. Major oxides were determined by ICP at Actlabs and by WD-XRF at the Ontario Geological Survey at detection level of 0.001%. Trace elements were determined by ICP-MS at both labs at a detection level of parts per million. Results of these analyses are given in appendix A. Sample locations are given in Appendix C.

4.1.2 Major Element Geochemistry of the Townsite Formation

Major element trends in Townsite Formation rocks are shown for CaO, Na_2O, Fe_2O_3, MgO, and TiO_2 versus SiO_2 (Fig. 4.1). Plots of CaO vs SiO_2 and Na_2O vs SiO_2 show compositional differences among intermediate, and felsic rocks. CaO shows linear decrease as SiO_2 increases. Gabbro sills have the highest weight percent CaO followed by volcanic flows, feldspar porphyry and quartz feldspar porphyry. Decrease in CaO is paralleled by increase in Na_2O, reflecting the modal amount of plagioclase.

MgO and Fe_2O_3 (total) both show depletion with increasing SiO_2 content. Gabbro sills show the highest weight percent MgO and Fe_2O_3 followed by volcanic flows, feldspar porphyry and quartz feldspar porphyry. The plot of TiO_2 vs SiO_2 shows only a slight decrease in weight percent TiO_2 between mafic and felsic rocks. Volcanic flows and feldspar porphyry show the highest TiO_2 content with Vee Lake feldspar porphyry exhibiting the highest concentration. Gabbro sills followed by quartz feldspar porphyry exhibit the lowest TiO_2 concentration, with evident depletion accompanying increasing SiO_2 content in quartz feldspar porphyry.

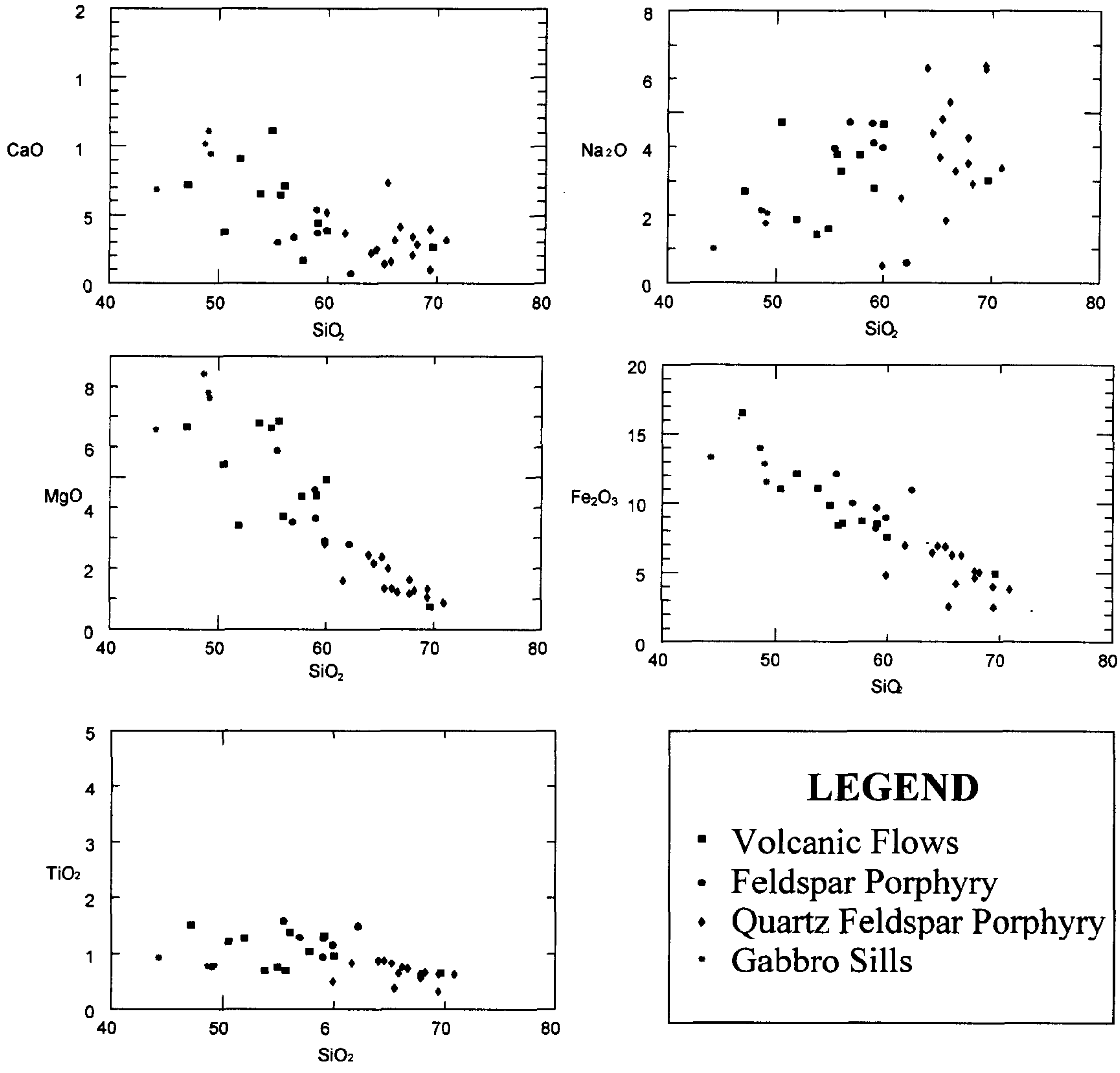

Figure 4.1. Major Element Trends of Townsite Formation Rocks

4.1.3 Geochemical Classification of Rocks in the Townsite Formation

Townsite Formation lithologies as plotted on Jensen's (1976) cation discrimination plots are shown in (Fig. 4.2). These were also plotted on the discriminant of Winchester and Floyd (1977) where the ratio of Zr/TiO_2 is plotted against Nb/Y (Fig. 4.3). The geochemical data is presented for the individual lenticles, starting with Niven Lake and moving northward to Vee Lake.

On the Jensen cation plot the mafic lithologies at Niven Lake are classified as high magnesium tholeiites. Hydrothermal breccia consisting of brecciated pillowed flows on the flanks of intrusive quartz feldspar porphyry and gabbro sills are classified as high iron tholeiite, indicating secondary iron enrichment. Gabbro sills at Niven Lake are classified as high magnesium tholeiites. Feldspar porphyry plots as calk-alkaline basalt and quartz feldspar porphyry as tholeiitic rhyolites which approach a calc-alkaline dacite composition. On the Winchester and Floyd plot, Niven Lake rocks show a slight variance in rock classification. Mafic flows plot as andesites, feldspar porphyries as andesite to andesite/dacite and quartz feldspar porphyries plot exclusively as rhyodacite/dacite. Hydrothermally brecciated pillows plot as andesite/basalt as do gabbro sills.

On a Jensen cation plot, the Brock litholigies show basically similar tholeiitic to calc-alkaline rocks as at Niven Lake. Mafic flows of the Brock lenticle show a larger compositional range plotting as calc-alkaline basalts, high magnesium tholeiites and high iron tholeiites. Feldspar porphyries straddle the line between tholeiitic andesites and calc-alkaline basalts. Quartz feldspar porphyries also straddle this line but plot as tholeiitic rhyolites to calc-alkaline dacites, or as tholeiitic dacites to calc-alkaline

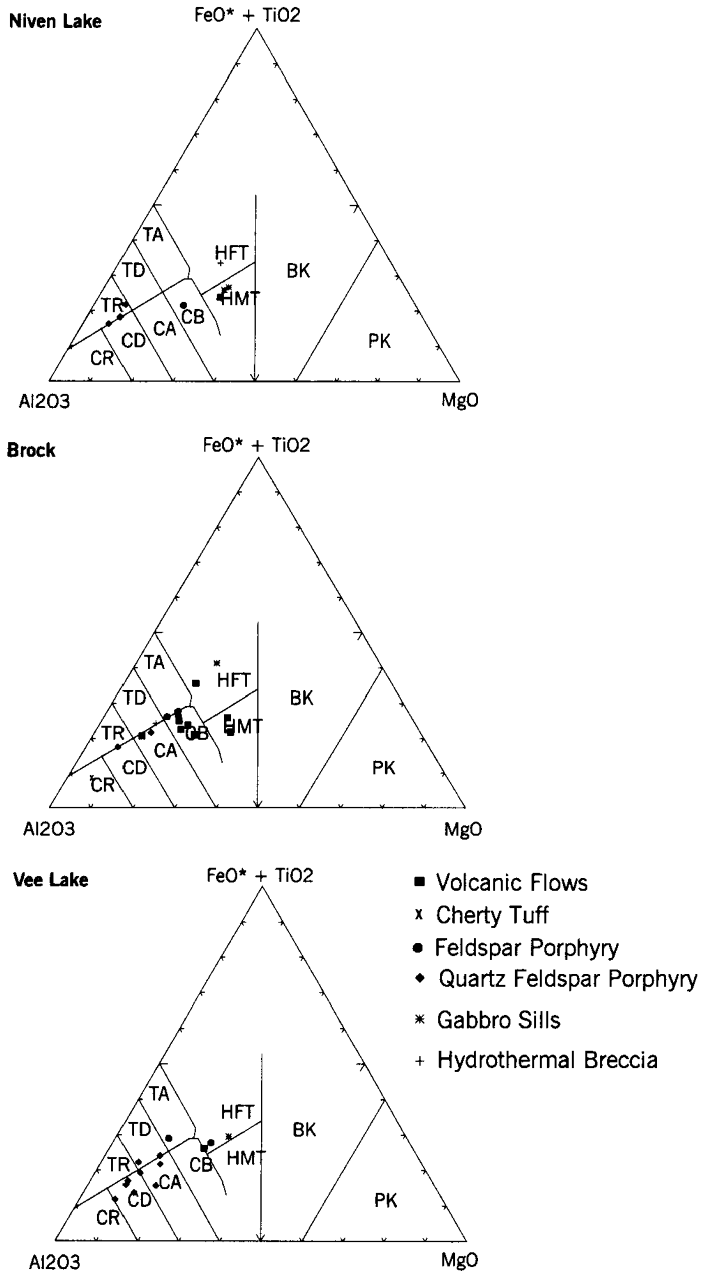

Figure 4.2 Geochemical classification of Townsite Lithologies (After Jenson, 1976)

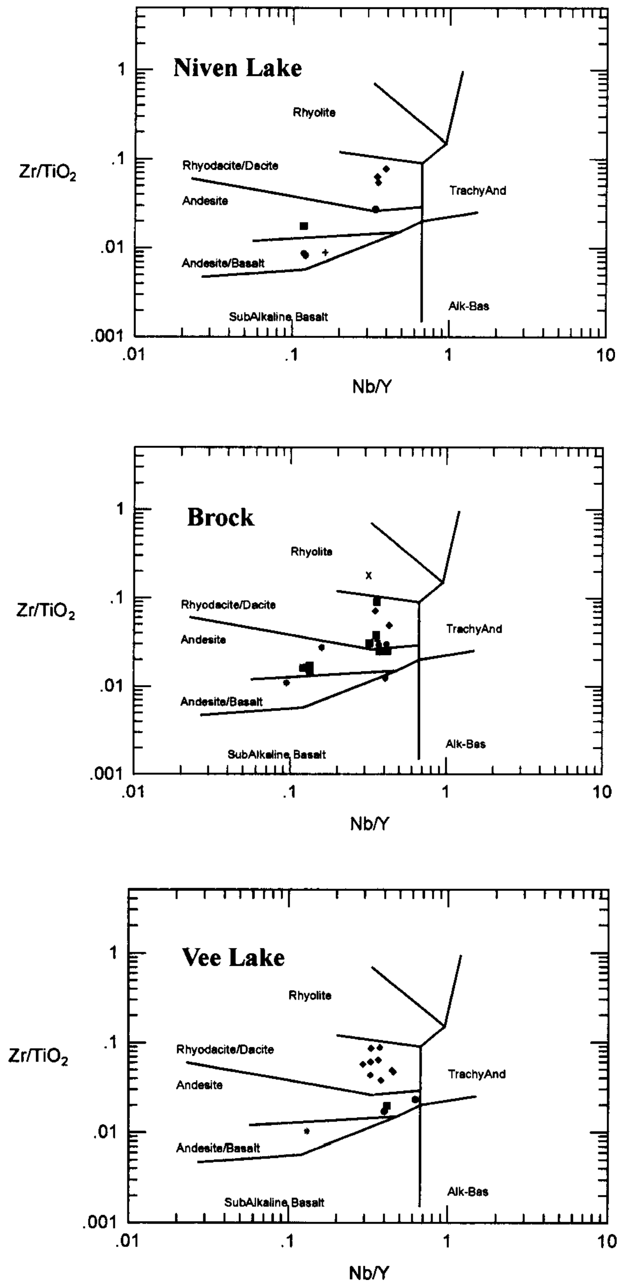

Figure 4.3 Geochemical Classification of the Townsite Formation Lithologies, After Winchester and Floyd, 1977 (Symbols Same as on Previous Diagrams)

andesites. One sample of cherty tuff from the upper Crestaurm Formation was analyzed for comparison with quartz feldspar porphyries and plotted as a calc-alkaline rhyotite. A sample of hydrothermal breccia was selected for analysis from the Brock Lenticle and plots as tholeiitic dacite to calc-alkaline rhyolite. Gabbro sills of the Brock Lenticle plot as high-iron tholeiites. On a Zr/TiO_2 versus Nb/Y plot, these same samples appear more felsic in composition. This shift is especially pronounced in pillowed flows as these plot between andesite to dacite composition. Feldspar porphyries plot as dacites while quartz feldspar porphyry plots as rhyodacite/dacite. The cherty tuff again plots as rhyolite. Hydrothermal breccia plots as dacite. Gabbro sills show an andesite/basalt composition, appearing more andesitic.

Pillowed flows from Vee Lake straddle the line between calc-alkaline basalt and high iron tholeiite on a Jenson plot. Feldspar porphyry exhibits a greater range of composition, ranging from tholeiitic andesite to high iron tholeiite. Quartz feldspar porphyry also displays a broad compositional range in the calc-alkaline field, from calc-alkaline dacite through tholeiitic dacite to calc-alkaline andesite. Gabbro sills exhibit a high iron tholeiite composition. Like the Brock suite Vee Lake lithologies show felsic affinity on a Zr/TiO_2 versus Nb/Y plot. Both pillowed flows and feldspar porphyries exhibit andesitic composition. The quartz feldspar porphyry analyses form a tight cluster in the rhyodacite/dacite field. Gabbro sills plot on the andesitic side of andesitic basalt.

4.1.4 Trace Element Geochemistry of Rocks in the Townsite Formation

Townsite formation incompatible and compatible trace elements were plotted on Harker diagrams (Fig. 4.4) in order to distinguish trends in trace element behaviour for different lithologies of the Townsite Formation. Incompatible elements which show obvious enrichment or depletion include Zr, Rb and Ba (ppm).

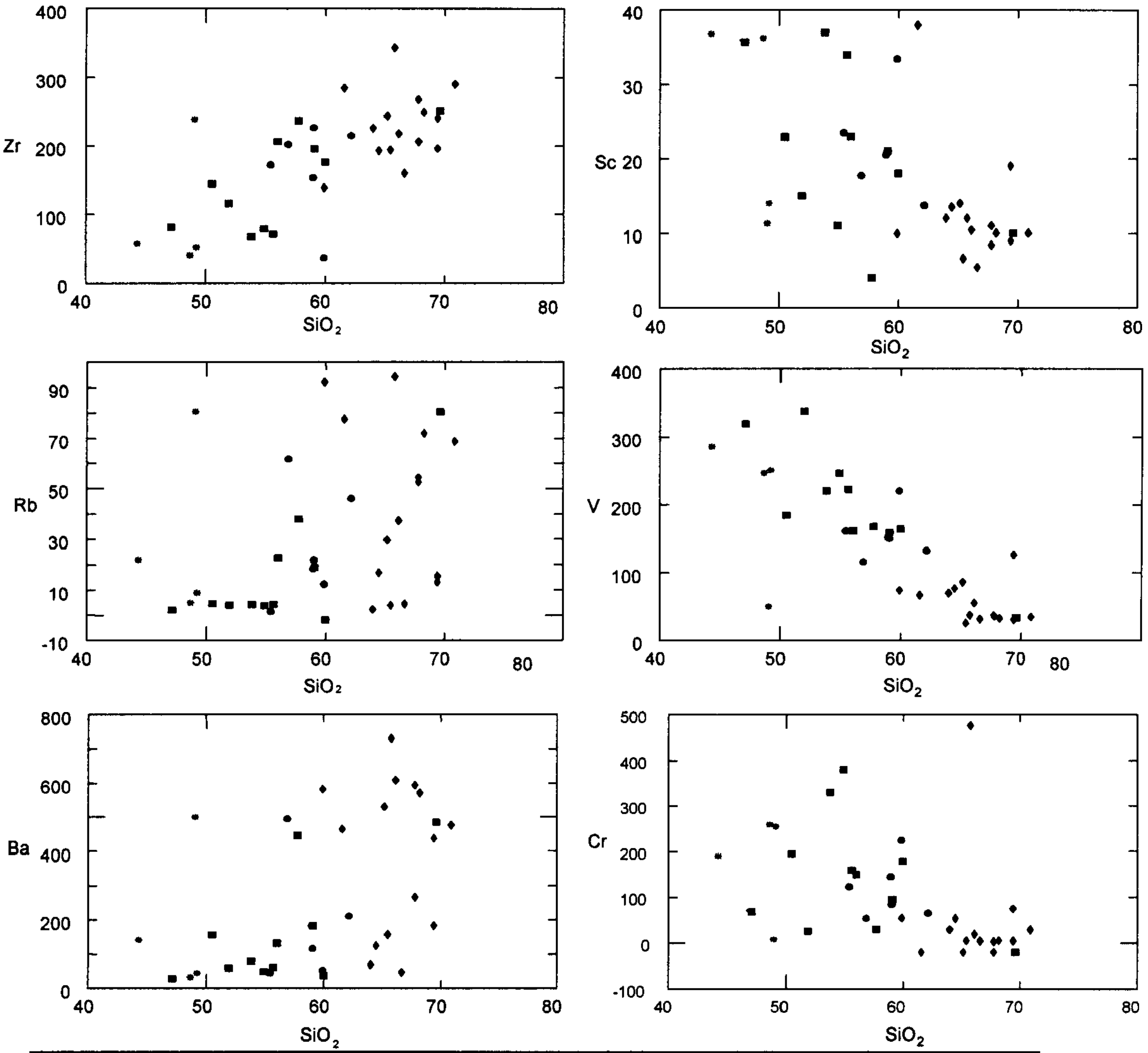

Figure 4.4. Trace element trends for Townsite Formation Rocks (symbols same as on previous diagrams)

Zr is strongly enriched in felsic rocks relative to mafic. Gabbro sills show the lowest concentrations followed by volcanic flows, feldspar porphyry and quartz feldspar porphyry. Rb and Ba also exhibit a general enrichment with increasing SiO_2. In both of these plots quartz feldspar porphyry is divided into two groups with high and low concentrations of Ba and Rb at SiO_2 concentrations between 60 and 70 weight percent. The anomalously high group reflects the mobility of these elements during subsequent metamorphic/hydrothermal overprinting.

The transition metals Sc, V, and Cr (ppm) plotted against SiO_2 (wt%) show marked depletion with increasing SiO_2. Cr decreases in concentration from gabbro sills through volcanic flows, feldspar porphyry and quartz feldspar porphyry respectively. Sc concentrations exhibit sharp depletion with increasing SiO_2 especially between mafic to intermediate rocks. Vanadium and chromium both show a linear decrease with increasing SiO_2, decreasing from gabbro sills to volcanic flows, feldspar porphyry, and quartz feldspar porphyry.

Primitive-mantle normalized spidergram patterns for Townsite formation rocks are displayed in figures 4.5 – 4.7. Separate plots of volcanic flows, feldspar porphyry, quartz feldspar porphyry and gabbro sill data are shown for each of the Niven Lake, Brock, and Vee Lake Lenticles. Niven Lake volcanic flows show flat primitive mantle-normalized patterns. Two samples are plotted: one showing a negative Nb anomaly is enriched in Th, while the other lacking a negative Nb anomaly is not enriched in Th. Only one sample of feldspar porphyry was analyzed from the Niven Lake lenticle and this shows marked Nb depletion, a slight depletion in Ti, Th enrichment and is LREE-enriched. Two samples of quartz feldspar porphyry were analyzed and show parallel patterns ie; depleted in Nb and Ti, enriched in Th, and marked LREE enrichment.

Gabbro sills from Niven Lake do not display REE enrichment. Their REE pattern is flat.

Niven Lake Lenticle

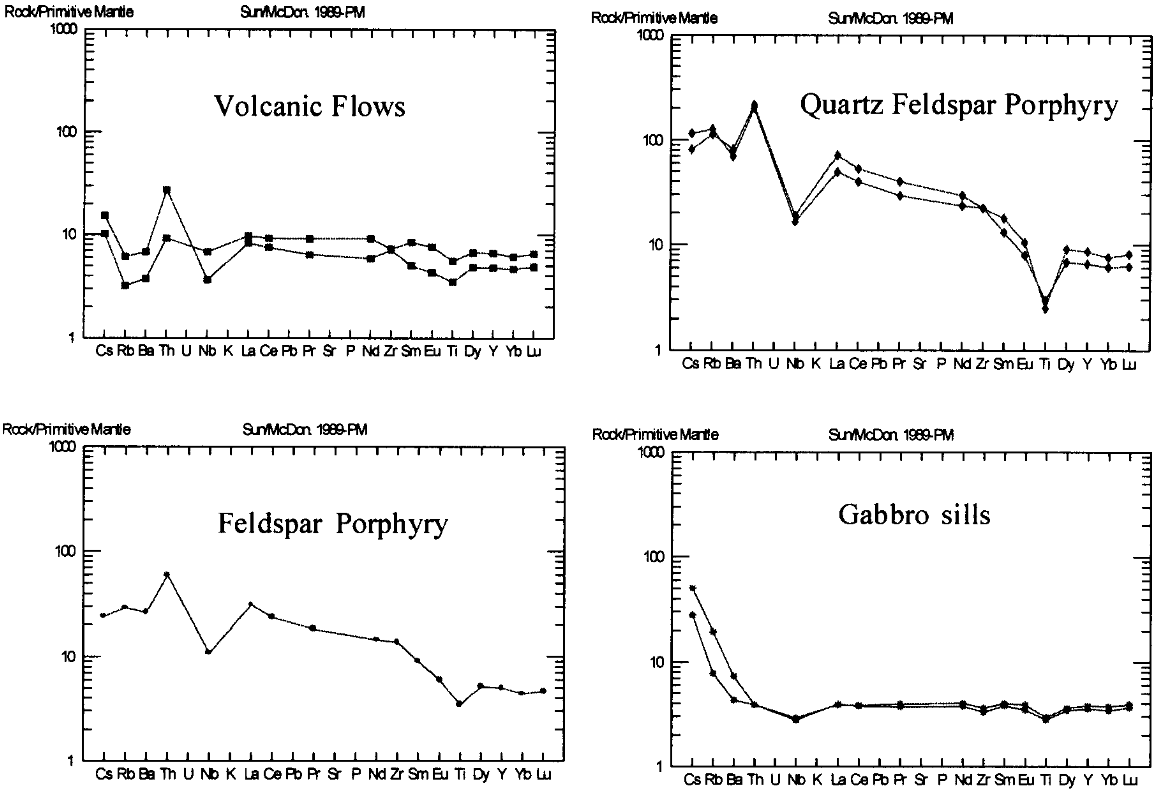

Figure 4.5. Spider Diagrams for Niven Lake Lithologies (Sun and McDonough, 1989)

The Brock Lenticle volcanic flows show strong Nb depletion and are Th enriched. Some samples show anomalous LREE-enrichment and represent those rocks which lie directly adjacent to gabbro sills and quartz feldspar porphyry intrusions. Those volcanic flows with flatter REE patterns were sampled from the upper Crestaurum Formation for comparison. These rocks generally show a slight enrichment in Zr and one sample demonstrates slight Eu enrichment. Ti is slightly depleted in all samples. Brock feldspar porphyries display highly consistent incompatible element patterns; these samples show strong Nb-Ti depletion, Th enrichment and are highly LREE-enriched. Brock quartz feldspar porphyries show parallel patterns. These samples are slightly more LREE-enriched than the feldspar porphyries with which they are spatially associated. Ti depletion is more pronounced in quartz feldspar porphyry than in feldspar porphyries. Gabbro sills show only slight depletion in Nb-Ti and their REE pattern is extremely flat, with subtle HREE-enrichment.

Brock Lenticle

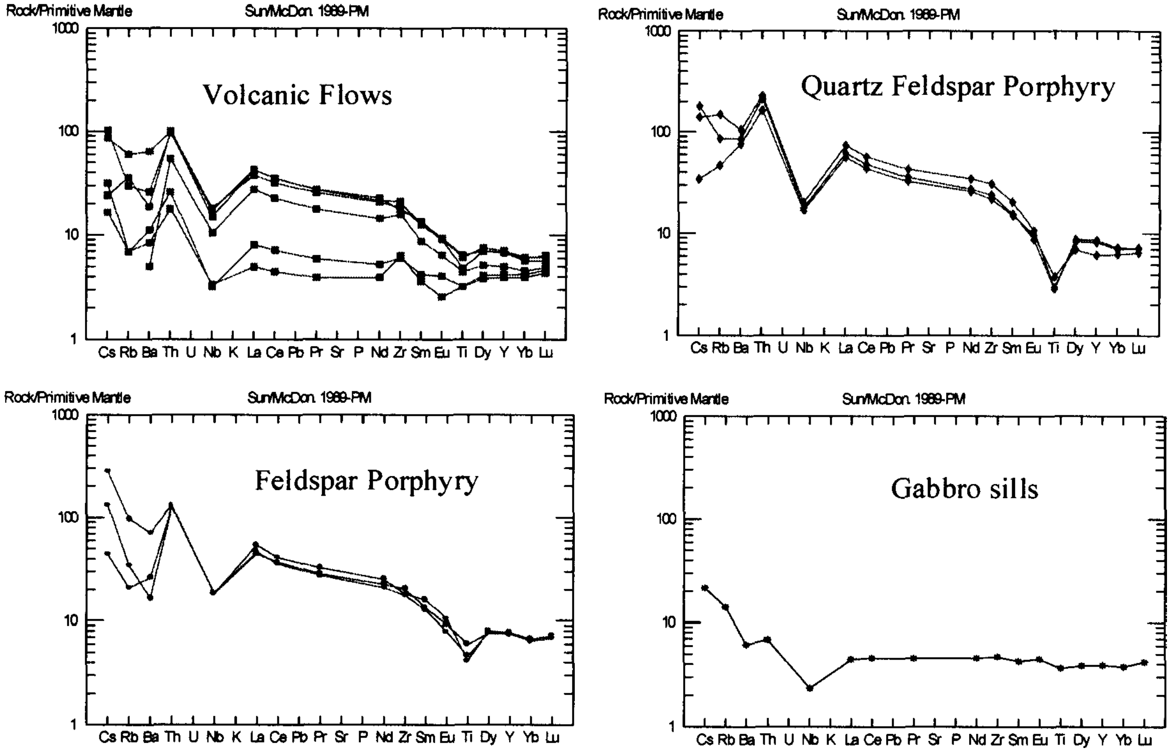

Figure 4.6. Spider Diagrams for Brock Lithologies (Sun and McDonough, 1989)

Volcanic flows from the Vee Lake Lenticle show a slight depletion in Nb-Ti and enrichment in Th. These rocks are similar to several Brock flows in demonstrating

LREE-enrichment. Feldspar porphyries from Vee Lake show enrichment in Th and a slight depletion in Nb. Rb and Ba show very strong depletion in one sample, likely the result of secondary remobilization. These rocks show LREE-enrichment and one sample displays anomalous enrichment in Zr and the other a depletion in Ti. Several samples of quartz feldspar porphyry were analyzed from the Vee Lake Lenticle and these show consistent patterns. One sample of lapilli tuff and one of quartz carbonate sericite schist were also added for comparison. All are highly depleted in Nb-Ti and enriched in Th and exhibit well defined LREE-enrichment. The gabbro sills from Vee Lake show markedly different patterns relative to gabbros in the Niven lake and Brock lenticles. These rocks show Nb-Zr enrichment, and are markedly HREE-enriched.

Vee Lake Lenticle

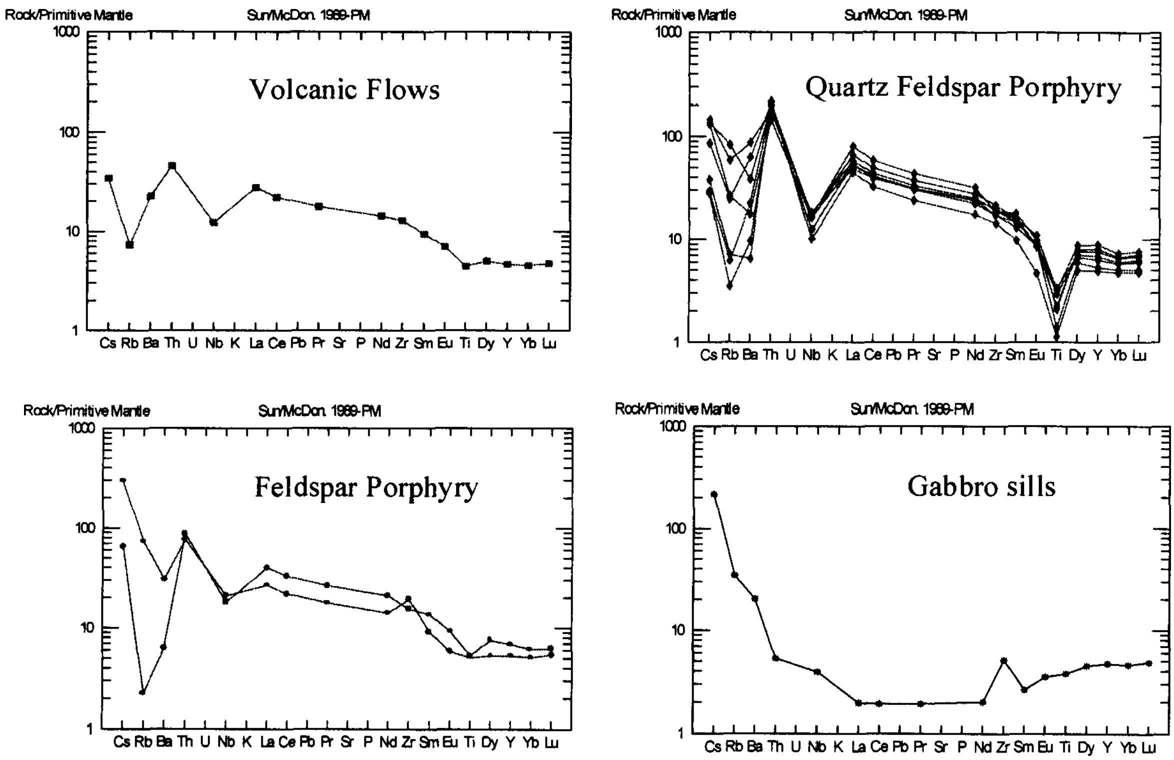

Figure 4.7. Spider Diagrams for Vee Lake Lithologies (Sun and McDonough, 1989)

Quartz feldspar porphyries are plotted on; Rb vs Y+Nb and Rb vs Yb+Ta discrimination diagrams and are plotted in figure 4.8 (after Pearce et al.,1984). The plot of Rb vs Y+Nb shows that Vee Lake quartz feldspar porphyries typify volcanic arc setting while the Brock and Niven Lake samples plot within a volcanic arc to within plate setting. The Nb vs Y plot shows Niven Lake and Brock samples between volcanic arc/syn-collisional to within plate, while Vee Lake quartz feldspar porphyries plot exclusively as volcanic arc to syn-collisional. Plots of Rb vs Yb + Ta, and Ta vs Yb both show quartz feldspar porphyries from Niven , Brock and Vee Lake as plotting within the volcanic arc field.

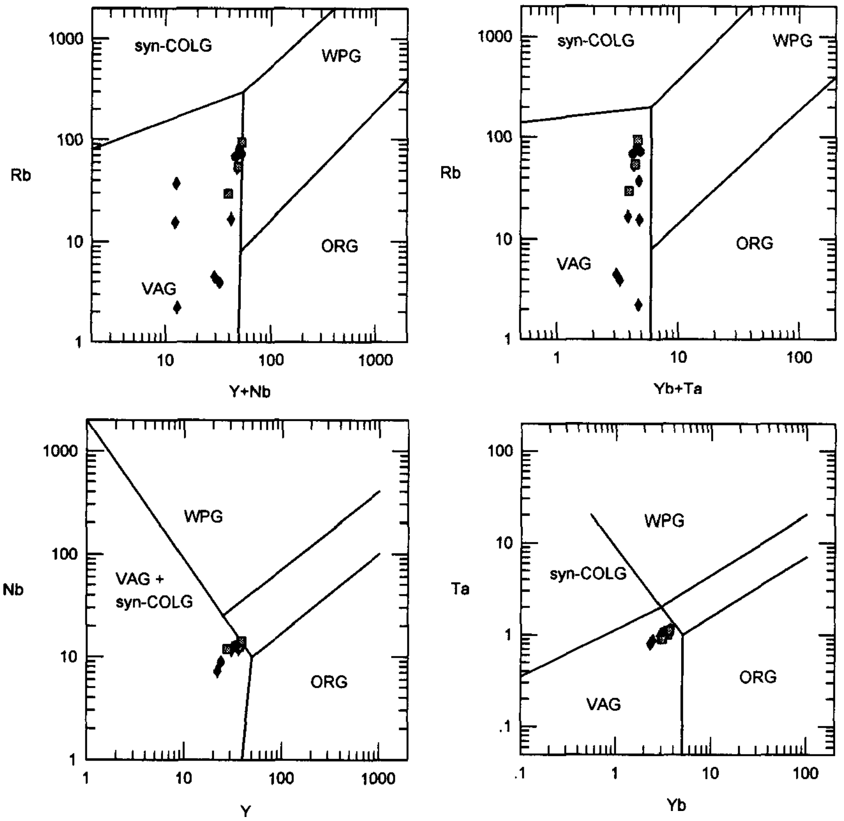

Figure 4.8 Discrimination Diagrams for Quartz Feldspar Porphyry Intrusive phases. Diamonds Represent Vee Lake Lenticle, Squares the Brock Lenticle and Circles the Niven Lake Lenticle (After Pearce et al., 1984).

Post orogenic granites cannot be distinguished from volcanic arc and syncollisional granites on these diagrams. However, such settings can be distinguished on the Hf-Rb-Ta diagram after Harris et al. (1986). Quartz feldspar porphyries from the Townsite formation have been plotted on these diagrams (Fig. 4.9a). On a ternary plot of Hf - Rb/10 - Ta x 3, Niven Lake and Brock samples range from volcanic arc to within plate. Vee Lake quartz feldspar porphyries range between within plate and ocean ridge.

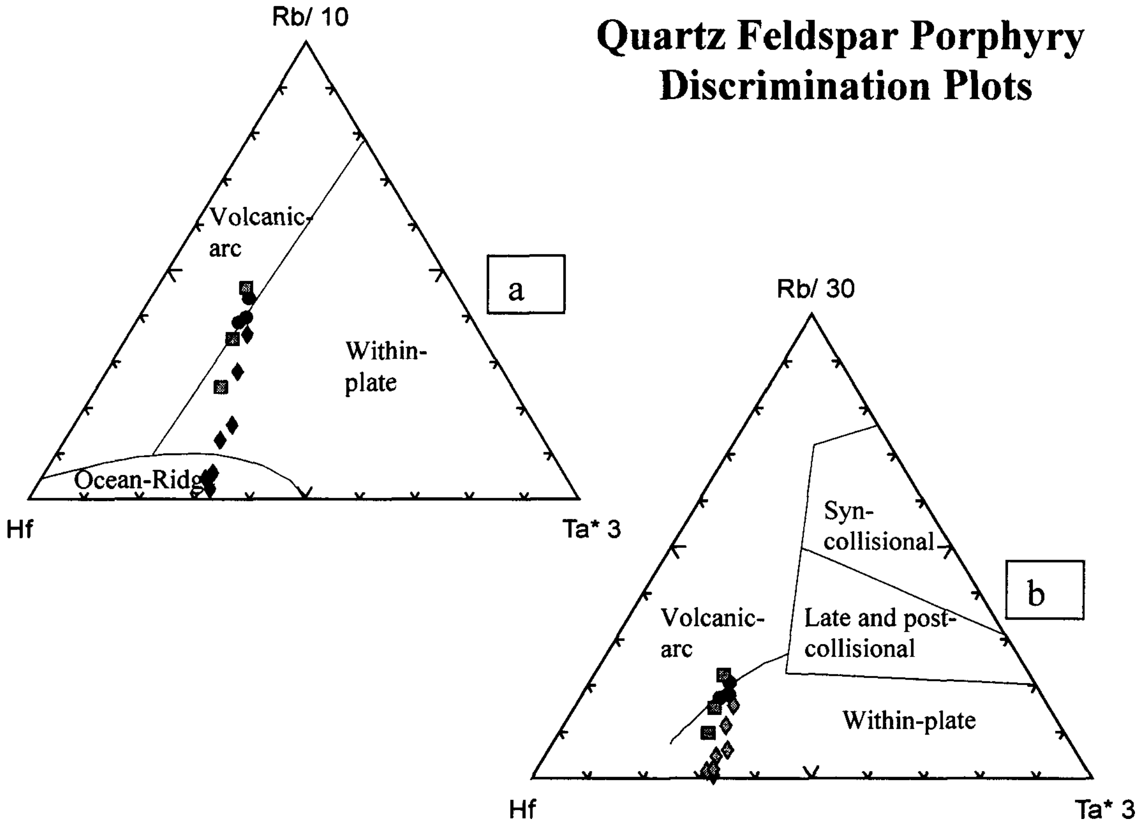

Figure 4.9 a,b. Discrimination Diagrams for Quartz Feldspar Porphyry intrusive Phases. See Text for Explanation. Symbols same as in previous. (Harris et al., 1986)

A modification of this diagram (Harris et al., 1986) which, expands the field of collisional granites, has quartz feldspar porphyry from Niven Lake and Brock straddling the line between the volcanic arc and within-plate fields, while those from Vee Lake plot exclusively within plate (Fig. 4.9b).

4.2 Mineral Chemistry

4.2.1 General Statement

Microprobe analysis were preformed on amphibole, biotite, chlorite, and plagioclase. The mineral compositions of these species were determined in order to determine compositional variation in these minerals in different rock types, as well as define ambient metamorphic conditions and the effects of retrograde hydrothermal alteration. Mineral analyses were performed on carbon-coated polished thin sections using a JEOL JXA-8600 electron probe xray microanalyser. This probe is equipped with four wavelength dispersive spectrometers (WDS) and one energy dispersive spectrometer (EDS). Calibration was on natural mineral standards at an accelerating voltage of 15kV and a probe current of 10nA. A counting time of 20 seconds on peak and background was used for all mineral analyses.

4.2.2Amphibole

The major element chemistry of amphiboles occuring in gabbro sills and mafic to intermediate flows of the Townsite formation have been plotted on the $Mg/(Mg + Fe^{2+})$ versus Si classification diagram of Leake et al., (1997, Fig.10,). Amphiboles were analysed in mafic/intermediate flows and gabbro sills from the Niven Lake and

Brock lenticles. Brock volcanics range in composition from magnesiohorneblende to actinolite while Niven Lake amphiboles are exclusively magnesiohorneblende. The change from the Brock actinolite to Niven Lake magnesiohornblende indicates higher grade rocks at Niven Lake, from mid-greenschist to epidote amphibolite facies metamorphic conditions.

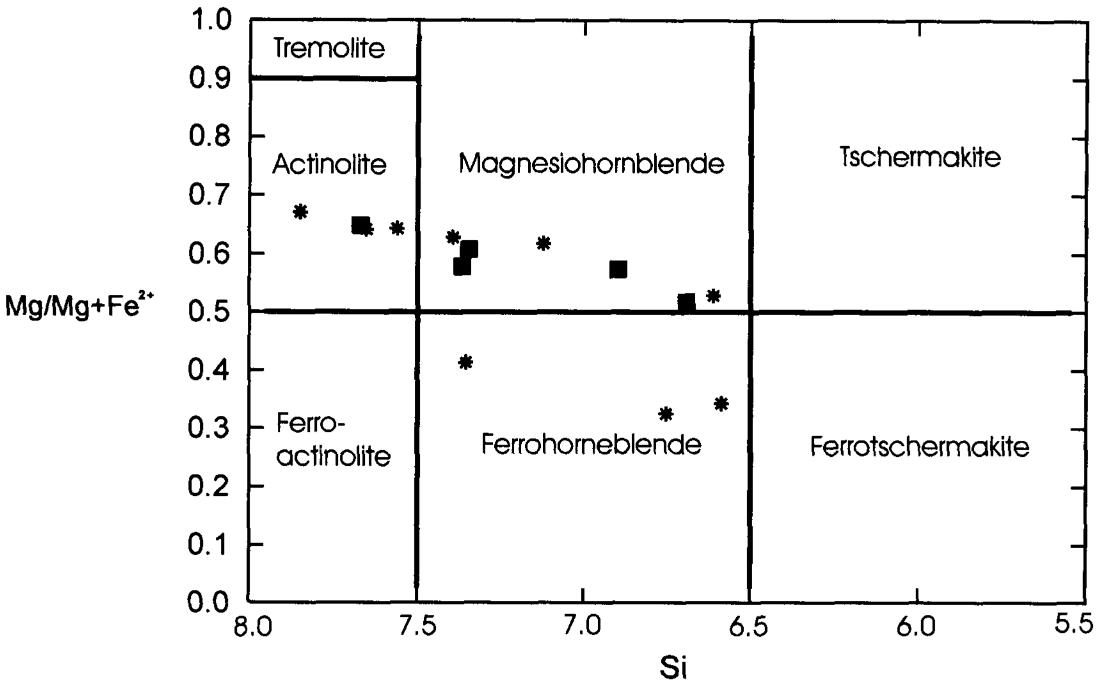

Figure 4. 10. Classification of Amphiboles in Gabbro Sills and Volcanic Flows of the Townsite Formation (After Leake et al., 1997). Astrix Represent Gabbro Sills and Squares Represent Volcanic Flows.

The gabbro sills show a similar trend. Niven Lake sills range in composition from high to low Si magnesiohorneblende. Brock sills have amphibole compositions ranging between actinolite to ferrohornblende. Those sills with classic "frog rock" texture (old metagabbro) contain actinolite and thus are lower in metamorphic rank than adjacent intermediate gabbro sills. Thus old metagabbro is a likely precursor to intermediate metagabbro. Noteably, however, the old metagabbro sills at the Brock are lower in Fe and higher in Si contents than texturally similar Niven Lake sills. This again reflects the higher grade of metamorphism at Niven Lake.

4.2.3 Biotite

Biotite was analyzed in feldspar porphyry from the Brock Lenticle and in quartz feldspar porphyry from the Niven Lake Lenticle. These biotites are classified on the plot of Al^{VI} vs Mg/(Mg+Fe) of Guidotti , 1984 (Fig 4.11).

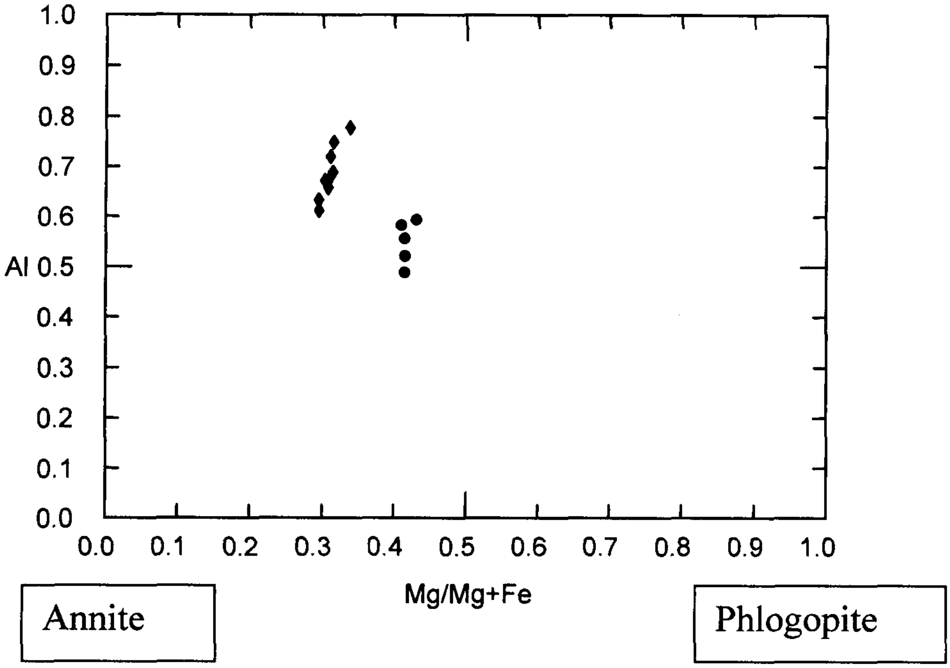

Figure 4.11. Classification of Biotites for Niven Lake Quartz Feldspar Porphyries and Brock Feldspar Porphyries (After Guidotti, 1984).

Niven Lake quartz feldspar porphyry biotites are more aluminum rich and higher in Fe than biotites from feldspar porphyry in the Brock. Niven Lake biotites also show a slight increase in Ti relative to those from the Brock. This combined with their higher

Al and Fe contents reflects the more fractionated quartz feldspar porphyry host at Niven Lake.

4.2.4 Chlorite

Chlorite species were analyzed in mafic/intermediate volcanic flows, feldspar porphyries, quartz feldspar porphyries and gabbro sills. Chlorites are classified using the nomenclature of Hey (1954, Fig 4.12). Niven Lake mafic volcanics have chlorites which are exclusively ripidolite in composition. These chlorites are lower in iron than those from mafic volcanics in the Brock and Vee Lake lenticles. Chlorites from the Brock Lenticle pillowed flows range in composition from ripidolite to pynochlorite. This range in composition occurs within individual samples. Vee Lake pillowed flows have chlorites which are lower in Si but are exclusively ripidolite in composition.

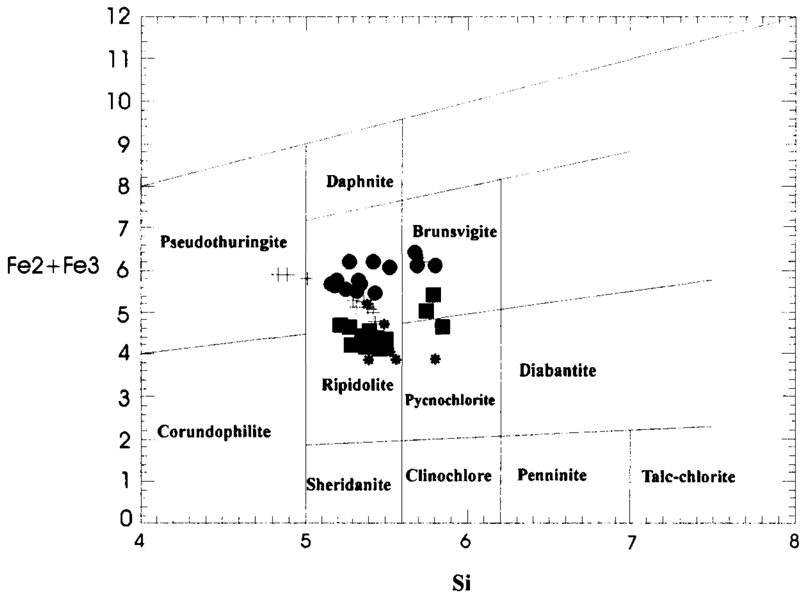

Figure 4.12. Classification of Townsite Formation Chlorites (After Hey, 1954). Squares represent volcanic flows, circles quartz feldspar Porphyry, Crosses Feldspar Porphyry, and Astrix Gabbro Sills.

Feldspar porphyry chlorites from Niven Lake are exclusively brunsvigite in composition and are thus higher in Si and Fe than chlorites in felspar porphyry from the Brock and Vee Lake lenticles. Chlorites from Brock feldspar porphyries are exclusively ripidolite in composition and in terms of Si and Fe contents fall in between chlorites from feldspar porphyries from Niven and Vee Lakes. The Vee Lake feldspar porphyry chlorites, however, range between relatively high and low Fe contents between outcrops. This indicates varying degrees of alteration between sample sites.

Chlorites from Niven Lake quartz feldspar porphyry range in composition from ripidolite to brunsvigites and are higher in their Fe content relative to chlorites from the Brock and Vee Lake lenticles. Brock quartz feldspar porphyry also have chlorites ranging from ripidotite to brunsvigite but are generally lower in Si and iron than those from Niven Lake. Vee Lake quartz feldspar porphyry are exclusively ripidolite in composition and lower in Fe contents than those from Niven and Brock.

Chlorites from Niven Lake gabbro sills are ripidolite to pynochlore in composition. Chlorites from the Brock gabbro sills are ripidolite in composition with old metagabbro exhibiting relatively higher Fe and Si than those from intermediate metagabbro than those from Niven Lake. Vee lake gabbro sills also contain chlorite of ripidolite composition but these chlorites are generally lower in Fe and Si than those from the Niven Lake and Brock lenticles.

There is a general trend with chlorite in more felsic lithologies displaying higher Fe contents than more mafic lithologies. However, highly altered mafic samples from Vee Lake and Niven Lake show Fe contents comparable to those found in quartz feldspar porphyries in all three lenticles.

4.2.5 Feldspar

Feldspar was analysed from mafic/intermediate flows, feldspar porphyry, quartz feldspar porphyry, and gabbro sills in the Townsite Formation. All feldspars analyzed are plagioclase, when plotted on a feldspar ternary diagram they plot between albite and anorthite end members (Fig. 4.13 a, b, c).

Secondary alteration of plagioclase to sericite +/- prehnite in mafic volcanics at Niven Lake made it impossible to get accurate stoichiometry from these feldspars. Plagioclase from Brock pillowed flows range in composition from albite to andesine. These compositions vary within individual samples and show no systematic variation with respect to sample location. Vee Lake flows contain plagioclase that are exclusively albite in composition reflecting greenschist metamorphism.

Plagioclase from feldspar porphyries sampled in the Niven Lake, Brock and Vee Lake lenticles are exclusively albite in composition, reflecting pervasive sodium metasomatism.

Plagioclase from quartz feldspar porphyries in the Niven Lake lenticle have andesine composition while those from Brock quartz feldspar porphyry range from albite to oligoclase. Vee Lake quartz feldspar porphyry plagioclase are exclusively albite. This progressive increase in Ca/Na moving from Vee Lake through Brock and south to the Niven Lake lenticle reflects the increase in metamorphic grade from greenschist at Vee Lake to epidote-amphibolite at Niven.

Plagioclase compositions from gabbro sills throughout the Townsite are variable. Samples from Niven Lake have compositions ranging from oligoclase to labradorite. Brock sills show plagioclase compositions ranging from albite to labradorite with old metagabbro plagioclase being more calcic, ranging between andesine and labradorite with intermediate metagabbro exhibiting exclusively metamorphic plagioclases ranging between albite and andesine. Noteably, the lower Ca plagioclase in the intermediate metagabbro is accompanied by the strong epidotization of these rocks. Vee Lake gabbro sills contain plagioclase having exclusively albite composition, a further reflection of greenschist metamorphism.

Niven Lake Feldspars

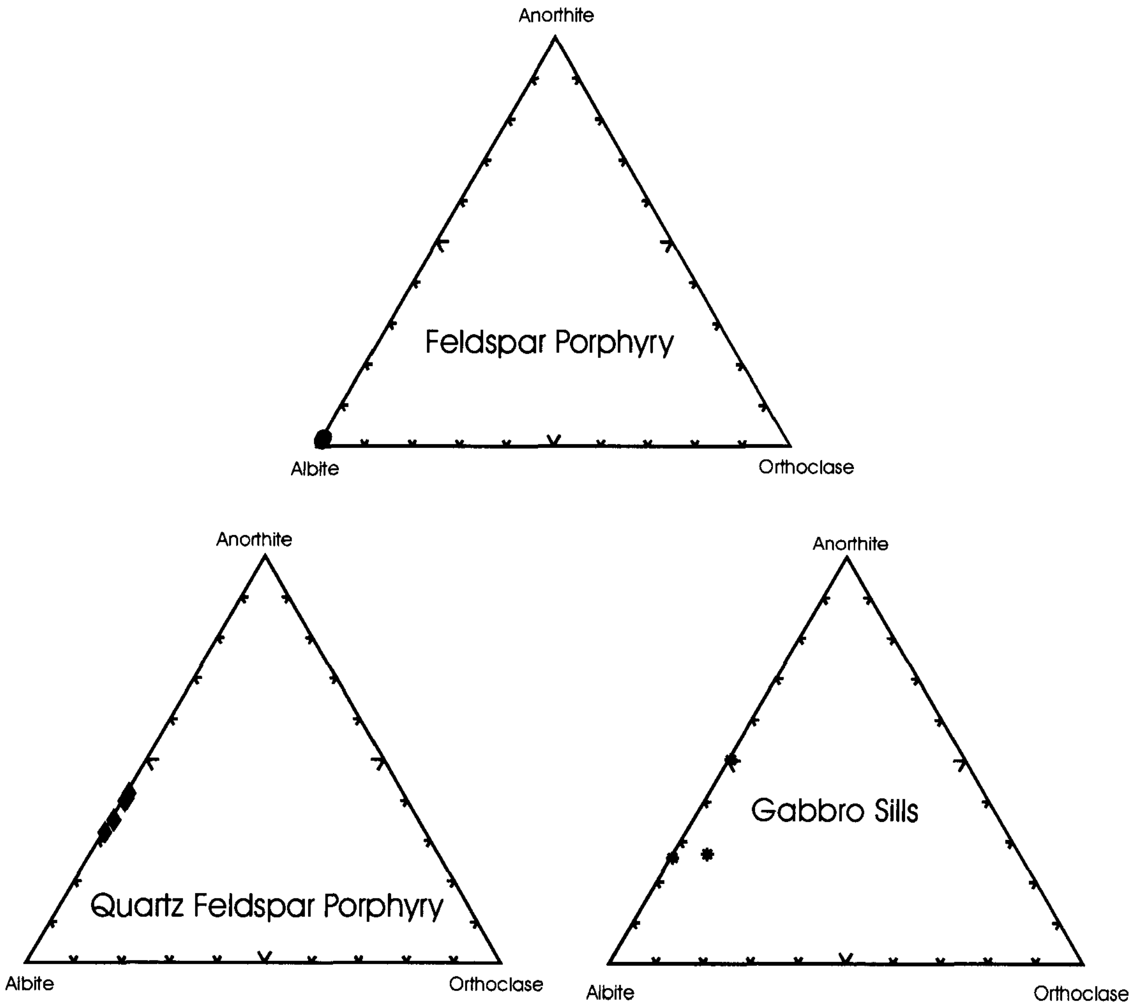

Classification of Niven Lake Lenticle Feldspars

Brock Lenticle Feldspars

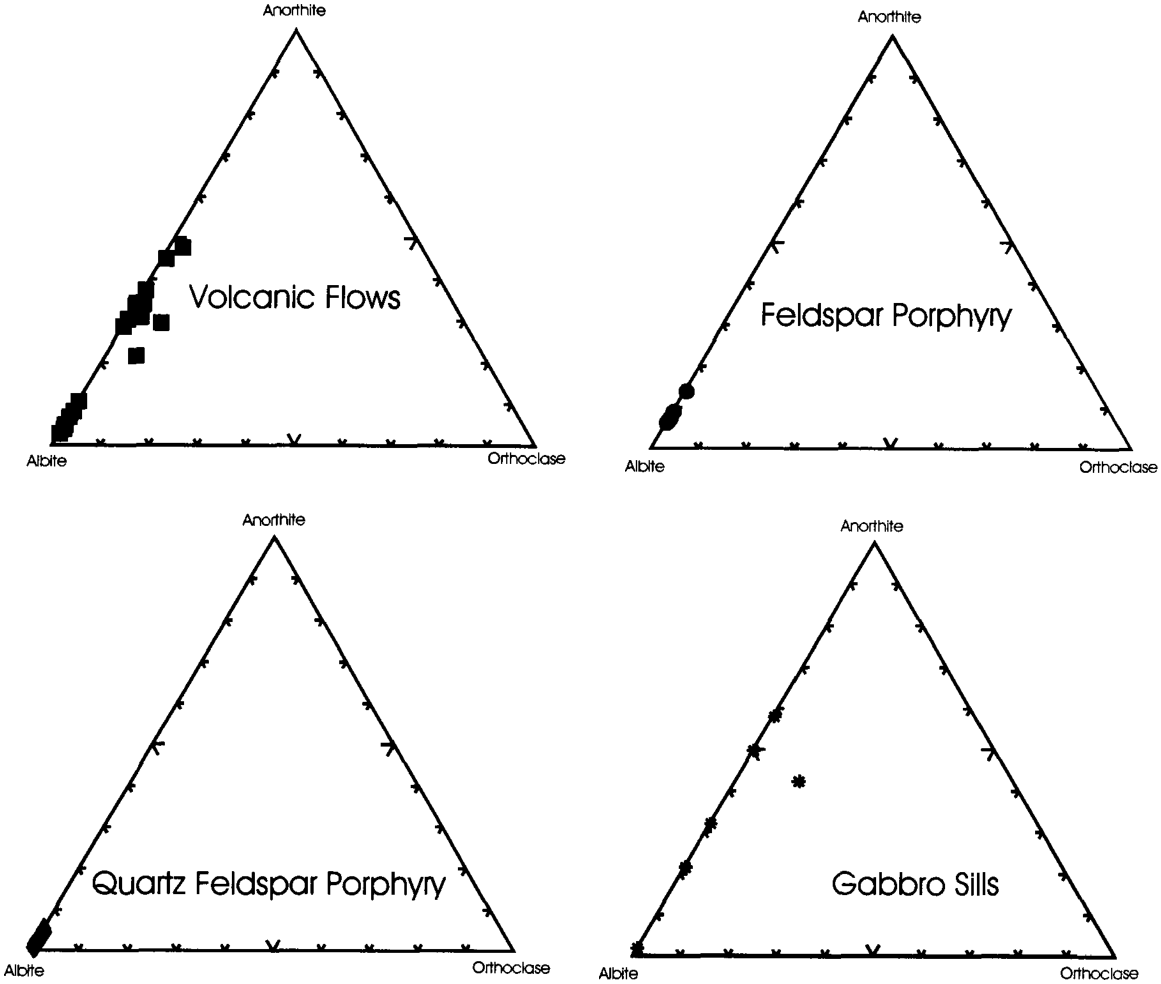

Figure 4.13b Classification of Brock Lenticle Feldspars

Vee Lake Lenticle Feldspars

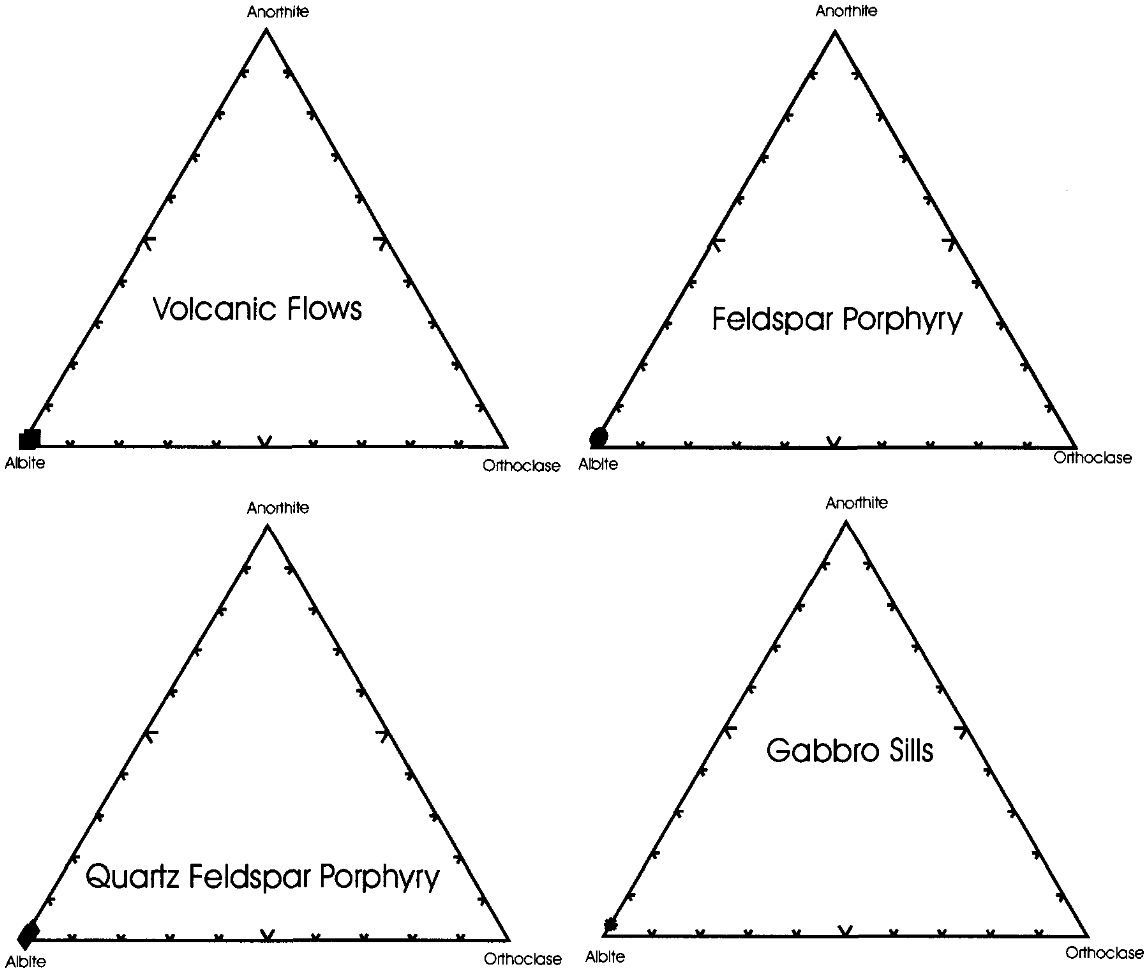

Figure 4.13c Classification of Vee Lake Lenticle Feldspars

Chapter 5

Discussion

5.1 Introduction

Detailed mapping of the Townsite Formation demonstrates an intimate association of quartz feldspar porphyry intrusions and gabbro sills. The felsic intrusions are associated with pyroclastic rocks over the northern third of the extent of the Townsite. The following discussion presents an interpretation of the results of mapping integrated with analytical work. It focuses on the geological setting, the petrogenesis of the quartz feldspar porphyry intrusions and considers the possible metallogenic significance of quartz intrusive feldspar porphyries in the Yellowknife gold camp.

5.2 Geological Setting

The Yellowknife Greenstone Belt defines the Yellowknife "type" volcanic belts that have been recognized throughout the west-central Slave Province on the basis of their high mafic/felsic rock ratios (Henderson,1981, Padgham, 1985) and bimodal association of tholeiitic volcanic flows with calc-alkaline felsic units. Models proposed for the origin of the Yellowknife-type greenstone belts include: intracratonic rifting of ensialic basins (Henderson, 1985, Bleeker, 1988), seafloor spreading centres in marginal basins (Helmstaedt et al, 1986a, MacLachland and Helmstardt, 1995), oceanic island and island arc/back arc basins (Helmstaedt, 1986). Kusky, (1990,1991) envokes an accretionary model for the Slave Province whereby ophiolitic slivers (ie: the Yellowknife-type greenstone belts), ocean sediments and greywackes typical of arc trench settings, are contained in fold-thrust belts characteristic of modern accretionary prisms. Kusky's plate tectonic model is essentially similar to models proposed for the Abitibi and other greenstone belts in the Superior Province. (Dimroth, 1982, Hodgson, 1986).

The Yellowknife Greenstone Belt is unique in terms of its excellent exposure. Its essential make up is a tholeiitic dominated succession of volcanic flows (Kam Group) which are unconformably overlain by and/or tectonically juxtaposed against mixed mafic/intermediates of the Duncan Lake Group. Later intrusive phases include; quartz feldspar porphyry , gabbro sills and dykes. Following tilting of the belt, the belt was subject to transpressional deformation accompanying the unroofing of granites. This is recorded in the deposition of the Jackson Lake Formation which is similar in appearance and is also thought to be similar in origin to the Timiskiming-type sediments of the Abitibi Greenstone Belt .

In their geochemical study of the Yellowknife Greenstone Belt, Cunningham and Lambert (1989), concluded that due to problems of element mobility during metamorphism, Archean greenstones do not plot with any consistency on geochemical diagrams used to discriminate among modern tectonic settings. Such problems notwithstanding, Cousens (2000) notes that Kam Group volcanic rocks plot in the ocean floor basalt field, and Banting Group rocks in the convergent margin field. On the basis of isotopic systematics of the Kam Group, Cousens (2000) proposed that the Kam flows most closely resemble modern back arc basin basalts. This setting allows for submarine lavas forming in proximity to a continent of older basement rocks. This is consistent with trace element and isotope data which indicate that the lavas have been contaminated by continental crust.

At present, there is no consensus of opinion as to the specific setting of the Yellowknife type greenstone belts. Furthermore, as increasingly detailed investigations are carried out, the simple layer cake stratigraphy as established by Henderson and Brown (1967) is being brought into question. The present investigation focuses attention on problems with the historical interpretation of the Townsite Formation as a felsic volcanic member separating the Crestaurum and uppermost Yellowknife Bay Formation of the Kam Group. The felsic rocks of the Townsite Formation are intrusive feldspar and quartz feldspar porphyry bodies. Contact relationships indicates that these porphyry bodies syn-date the intrusions of major gabbro sills into the base of the Yellowknife Bay Formation. Although somewhat speculative due to marked discordance, the work of Isachsen (1992) suggests a quartz feldspar porphyry/gabbro silling event at 2683 Ma, some twenty million years after Kam volcanism (2705-2712 Ma).

The quartz feldspar porphyry intrusions have an associated pyroclastic apron over the northern third (Vee Lake Lenticle) of the Townsite Formation. Quartz feldspar porphyry intrusions and associated volcanic breccias, lapilli tuffs and crystal tuffs have identical bulk rock trace element compositions, supporting the interpretation that the quartz feldspar porphyry are related to the volcanic facies.

Detailed mapping combined with lithogeochemistry suggests quartz feldspar porphyries were generated by partial melting of volcanic flows at the time of gabbro silling. The injection of massive high magnesium to high iron gabbro sills caused high heat flow within the immediate environs of magma conduits. This resulted in the partial melting of wet basaltic andesite to produce an intermediate melt (feldspar porphyry) which subsequently evolved to a dacitic melt (quartz feldspar porphyry) by fractional crystallization. The detailed contact relationships among mafic volcanics, feldspar porphyry, quartz feldspar porphyry and gabbro sills provide evidence for this model. The absence of chill margins on intrusive phases combined with undulose contacts, interfingering and back veining of quartz feldspar porphyry into gabbro sills suggest the existence of coeval melts. The occurrence of the relic “variolitic” pillows marginal to quartz feldspar porphyry intrusions represent reservoirs of the partial melts. Hydrothermal breccias indicate wet melts at high crustal levels where phreatic injection has produced mixed litholigies consisting of clasts of quartz feldspar porphyry, feldspar porphyry and disrupted variolitic pillowed flows hosted in milled rock flour.

Over the northern third of the Townsite Formation, hydrothermal breccias give way to pyroclastic venting. The lithic lapilli tuff occurring in the northeastern portion of the Brock Lenticle and the volcanic breccias, lapilli tuffs, and crystal tuffs in the Vee Lake Lenticle is indicative of eruptions. The coarse pyroclastics, occurring centrally in the Vee Lake Lentile are vent proximal facies. The lack of bedding in the breccias indicates explosive eruptive conduits. Reaction rims on quartz feldspar porphyry clasts in this facies suggests they were still hot when deposited. The layering in coarse lapilli tuff breccia suggests debris flow with large blocks of quartz feldspar prophyry carried down slope. The graduation from lapilli tuff breccia to lappilli tuff suggests a gradation away from vent proximal facies. The presence of lapilli tuffs exhibiting unbedded microbreccia textures suggests continuous deposition as subaqueous debris flows.

Capping crystal tuffs represent a distal facies. The preservation of pumice with discernable vesicles in crystal tuff suggests direct deposition. Interbeds of reworked volcaniclastics suggests an environment where epiclastic processes overlapped. Sharp contact between units and the presence of crossbeds in sandstone indicate an epiclastic origin.

5.3 Petrogenesis of Quartz Feldspar Porphyry

Prior et al., (1999) compared lithologies formed by the partial melting of crustal rocks in Iceland and other modern axial rift zones with the Archean Kidd Creek rhyolites at Timmins. The REE patterns and high field strength element contents of the Kidd Creek rhyolite are remarkably similar to rhyolites formed in settings undergoing seafloor spreading. The quartz feldspar porphyry and related pyroclastics of the Townsite Formation show a broadly similar trace element pattern: a particularly close similarity occurs with the Whitsunday rhyolite, Queensland, Australia. Ensialic back arc rhyolites (eg: the Deception Island rhyodacite and the Rocas Verdes plagiogranite) also show a strong geochemical affinity with Kidd Creek rhyolites and a similar pattern to the felsic intrusive/extrusive rocks of the Townsite Formation. Similar cases of rift related felsic melts have been documented in the Ambler District of northern Alaska as well as at Myra Falls, British Columbia (Barrett & Maclean, 1999). Generating wet felsic partial melts from hydrated basaltic andesites is considered the most feasible method of petrogenesis for the felsic lithologies of the Townsite Formation. As reported by Beard and Lofgren (1990) experimental dehydration melting and water saturated melting of basaltic and andesitic greenstones and amphibolites at 1,3, and 6.9

kb at 800-1000°C yields mildly peraluminus to metaluminous granodioritic to trondhjemitic melts of similar composition to Townsite Formation felsics.

The trace element patterns for quartz feldspar porphyry from the Townsite Formation reveal fractionation of Nb from La and Th between parental mafic rocks and felsic melts. This fractionation may occur as a result of a Nb-phase such as rulite or sphene remaining as a residual phase (Tatsumi et al., 1985). During production of wet melts, fluids readily dissolve K, Rb, Sr, U, Pb, Th and the light REE , but not Nb, Ta, Zr, and Ti. These latter high field strength elements have low solubilities in aqueous fluids and are prone to retention by phases such as rutile (Tatsumi et al., 1985).

The partial melt produced from basaltic andesite, fractionated to form intermediate feldspar porphyry. Collectively the trace element patterns for volcanic flows, feldspar porphyry and quartz feldspar porphyry from the Niven Lake, Brock and Vee Lake Lenticles show progressive enrichment and fractionation of light REE as the melt evolves. Of particular significance, comparison of upper Crestaurum variolitic flows with remnant flows in the Brock reveal progressive light REE enrichment. The partial melts enriched in light REE are progressively fractionated from feldspar porphyry to quartz feldspar porphyry.

Significantly the recent ε_{Nd} work on the Kam Group demonstrates that of all the units in the Kam Group, the Townsite felsic rocks are the closest in composition to basaltic andesites (Cousens, personal communication). A sample of quartz feldspar porphyry from the Niven Lake Lenticle yielded ε_{Nd} values of –0.2 while values for pillowed volcanics from the Crestaurum and Yellowknife Bay Formations yield values of 0.1, 0.7, and –2.9 respectively. Such isotopic signatures corroborates buffering of feldspar porphyry – quartz feldspar porphyry melt chemistry by bordering greenstones.

5.4 Metallogenic Significance of the Townsite Formation in the Yellowknife Gold Camp

It is here proposed that the Townsite Formation was formed during an aborted rifting event of the Kam mafic platform some twenty million years after the cessation of ocean floor volcanism (Fig 5.1). The high level emplacement of massive gabbro sills created high heat flow and partial melting of juvenile crust. These melts are expressed as the feldspar and quartz feldspar porphyry intrusions. Associated hydrothermal breccias demonstrate phreatic injection into immediate wall rocks adjacent to these melt bodies. Preservation of related pyroclastics in the northern third of the Townsite Formation identifies a "Townsite rift association", the affiliated pyroclastic facies only preserved proximal to the Jackson Lake unconformity. As depicted, the southern extension of the Townsite Formation exposes the deeper "intrusive" roots, the northern extension the associated pyroclastic volcanic facies.

To date, the significance of this "aborted" 2680 m.y. rift has been overlooked in metallogenic studies of the Yellowknife Camp. It has long been recognized that the economic segments of the gold-bearing Campbell and Giant shear systems occur where these shears directly impinge on " the Townsite Formation" (Fig.5.2). Given the close association of auriferous shears to intrusive quartz feldspar porphyries in the Townsite one might readily speculate that the globally recognized quartz feldspar porphyry/gold association might well apply to Yellowknife as well. The spatial association of

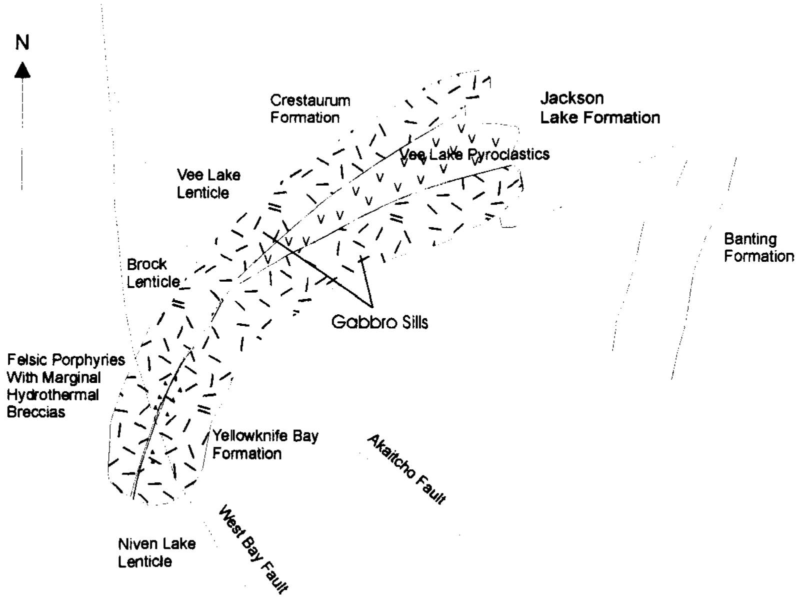

Figure 5.1 Interpretation of the Townsite Formation as an Aborted Rift System

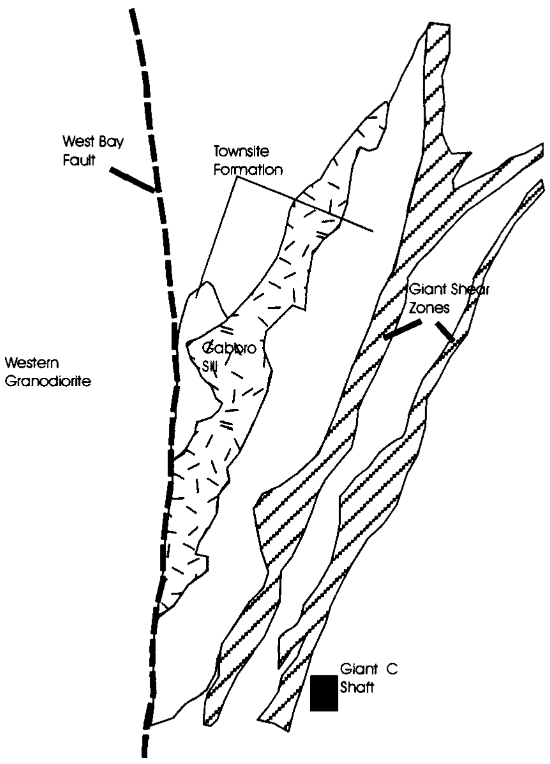

Figure 5.2 Gold Bearing Strands of the Giant Shear System Impinging on the Brock Lenticle of the Townsite Formation (After Henderson and Brown, 1966)

porphyries to lode gold deposits in modern and ancient settings has led many researchers to advocate porphyry gold models of genesis (Cameron and Hattori, 1985, 1987, Mason, 1986, Kuhns, 1994, Sillitoe, 1997). The physical processes which allow gold concentration in these deposits rely upon initial water concentration within magmas and the nature of magma emplacement. Rapid emplacement at shallow levels allows for partitioning of gold into a fluid. This is represented by high gold concentrations found within hydrothermal breccias at many deposit sites.

At the Con Mine the most economic segments of the Campbell shear is that connecting the hangingwall/footwall offsets of the Niven Lake Lenticle. At the Giant Mine the major gold bearing stopes occur where the Giant shears impinge directly on Brock Lenticle quartz feldspar porphyry bodies. The apparent lack of gold in the northern Vee Lake Lenticle remains unexplained as in this pyroclastic facies shearing is penetrative. Either gold is strictly related to intrusive quartz feldspar porphyry bodies and does not occur north of the Vee Lake intrusive bodies or the nature of gold concentration in the Townsite pyroclastic facies may differ, ie: is more "epithermal in signature" and still to be identified as a target type.

Although the close spatial relation of gold-bearing segments of shears to quartz feldspar porphyry intrusions strongly argues for a genetic tie, the work to date on the Yellowknife shear-hosted lode gold ores strongly favours late concentration in post-peak metamorphic high strain zones preferential to a main structural break separating the Kam and Duncan Lake Groups. A genetic tie of gold to Townsite quartz feldspar porphyry bodies supplies an important endogenous porphyry gold source, thus favouring local gold remobilization into late shears during subsequent prograde metamorphic/retrograde hydrothermal overprints.

Chapter 6

Conclusions

6.1 Summary

The results of detailed mapping of the Townsite Formation challenges previous interpretations of the Townsite as a simple conformable felsic volcanic succession within the mafic dominated Kam Group. Contact relationships reveal intrusive relationships for feldspar porphyry and quartz feldspar porphyry bodies. Associated hydrothermal breccias in the south give way to associated pyroclastic facies in the north. Related pyroclastics range from vent proximal breccias grading laterally into distal tuffs. Undulose, non-chilled contacts between quartz feldspar porphyry and massive gabbro sills indicate that they are coeval melts. The origin of the felsic melts is therefore linked to high heat flow attending the emplacement of gabbro sills. The geochemistry of remnant pillowed flows, feldspar porphyry and quartz feldspar porphyry is consistant with the felsic magmas being generated through partial melting of hydrated mafic flows of the Kam Group.

The transition from intrusive quartz feldspar porphyry in the southern Niven Lake and Brock lenticles to vented pryoclastics in the northern Vee Lake Lenticle combined with coeval silling of massive gabbros is consistent with the Townsite Formation developing as an aborted rift setting. On the basis of age dating by Isachsen (1992), the age of felsic melt generation, emplacement of high level porphyry bodies, formation of hydrothermal beccias and pyroclastic facies together with gabbro silling is considered to postdate Kam volcanism by approximately twenty million years. Immobile trace element patterns for the Townsite porphyries and related pyroclastics are consistent with wet partial melting of juvenile crust in both modern and ancient rifting environments.

6.2 Key Results

(1) The Townsite Formation of the Kam Group is reinterpreted from being a stratigraphic unit to signifying an aborted rift setting which postdated Kam volcanism by approximately twenty million years.

(2) The generation of felsic magma is linked to high heat flow within the hydrated Kam platform, attending emplacement of high level gabbro sills.

(3) From south to north the Townsite rift changes character from an intrusive setting with felsic porphyry bodies and related hydrothermal breccias to an extrusive setting of vent proximal to distal pyroclastics.

(4) The recognition of rift-related quartz feldspar porphyry intrusions in the Yellowknife Greenstone belt suggests that the globally important porphyry gold association is present and this genetic relationship should be factored into existing metallogenic models for the shear zone hosted lode gold deposits.

6.3 Recommendation for Further Work

(1) Although Isachsen's (1992) geochronology reveals age discrepancies for the Townsite Formation, except for his attemps to date the main Niven Lake quartz feldspar porphyry body no additional geochronological results are available on the

intrusive/extrusive phases in the Brock or Vee Lake lenticles. Isachsen's work should be extended to better document the aborted rift setting as hypothesized.

(2) The present study did not focus on the critical metallogenic problem of tying gold mineralization to quartz feldspar porphyry intrusions. An investigation attempting to link gold concentration to initial mineralization within the environs of subvolcanic porphyry bodies, with late remobilization into post-peak metamorphic shear zones, would supply new directions for ongoing exploration strategies in the Yellowknife gold camp.

REFERENCES

Atkinson, D.J., 1987. Report on preliminary mapping and geochemistry of the Western Plutonic Complex. *In* Exploration Overview, 1987. *Edited by* C.E. Ellis, NWT Geology Division, NAP, INAC, p19.

Atkinson, D.J., and van Breeman, O. 1990. Geology of the Western Plutonic Complex, Southwestern Slave Province: Late Achean crustal granites and gold mineralization in the Yellowknife District. In Exploration and Mining Overview, 1990. *Edited by* S.P. Goff, NWT Geology Division, NAP, INAC, p20.

Barrett, T.J., and MacLean, W.H., 1999. Volcanic sequences, lithogeochemistry and hydrothermal alteration in some bimodal VMS systems. In Short course manual: Volcanogenic massive sulphide deposits.

Beard and Lofgren, 1990. Dehydration melting and water saturated melting and Basaltic and andesitic greenstones and amphibolites at 1,3 and 6.9 kb. *In* Journal of Petrology, 32: 365-401.

Bleeker, W. and Ketchum, J., 1998. Central Slave basement complex, Northest Territories: contrasting basement/cover relationships on western and south western flanks of the Sleepy Dragon Complex. *In* Current Research 1997-c; Geological Survey of Canada. P27-37.

Bowring, S.A., and Williams, I.S., Compston, W., and Podosek, F.A., 1989. Remnants of earths oldest known continental crust, Slave Province, NWT, Canada. *In* Exploration Overview, 1989. Edited by J. Brophy. NWT Geology Division, NAP, INAC, 27p.

Boyle, R.W., 1961. The geology, geochemistry, and origin of the gold deposits of the Yellowknife District. In Geological Survey of Canada, Memoir 310, 193p.

Cameron, E.M., and Hattori, K., 1985. The Hemlo gold deposit, Ontario; a geochemical and isotopic study. *In* Geochimica a Cosmochimica acta 49, 2041-2050.

Cameron, E.M. and Hattori, K., 1987. Archean gold mineralization and oxidized hydrothermal fluids. *In* Economic Geology, 82, 1177-1191.

Cousens, B.L., 2000. Geochemistry of the Archean Kam Group, Yellowknife Greenstone Belt, Slave Province, Canada. *In* Journal of Geology, 108, no.2.

Cunningham, M.P., and Lambert, R. St. J. 1989. Petrochemistry of the Yellowknife volcanic suite at Yellowknife, NWT. Canadian Journal of Earth Sciences, 26: 1630-1645.

Dapalolo, D.J., 1988. Neodynium Isotope Geochemistry. Berlin, Springer, 154p.

Davis, W.J., and Hegner, E., 1992. Neodynium isotopic evidence for the tectonic assembly of Late Archean crust in the Slave Province, northwest Canada; contributions to minerology and petrology, V.111, p.493-504.

Davis, W.J., and King, J.E., 1994. Geochemistry and evolution of Late Archean Plutonism and its significance to the tectonic development of the Slave Craton; Pre Cambrian Research, v.67, p.207-241.

Dimroth, E., Imreh, L., Rocheleau, M and Goulet, N, 1982. Evolution of the south central part of the Archean Abitibi Belt, Quebec, Part 1: stratigraphic and paleogeoraphic Model; Canadian Journal of Earth Sciences, v19, p. 1729-1758.

Fyson, W.K., and Helmstaedt, H. 1988. Structural patterns and tectonic evolution of supracrustal domains in the Archean Slave Structural province, Canada. Canadian Journal of Earth Sciences, 25: 301-315.

Gates, T.M., and Hurley, D.M. 1973. Evaluation of Rb-Sr dating methods applied to Matachewan, Abitibi, Mackenzie and Sudbury dike swarms in Canada. Canadian Journal of Earth Sciences, 10:900-919.

Grant, 1997. Unpublished map of the Brock Formation. Royal Oak Mines.

Guidotti, C.V., 1984. Micas in metamorphic rocks, *In* Micas, Reviews in Minerology, v.13, p.357-468.

Harris, N.B.W., Pearce, J.A., and Tindle, A.G., 1986. Geochemical characteristics of collision-zone magmatism . *In* Coward, M.P., and Reis, A.C. (eds), *Collision Tectonics.* Spec. Publ. Geol. Soc., v.19, 67-81.

Helmstaedt, H., King, J., and Goodwin, J.A 1979. Multiple dykes in the lower Kam Group, Yellowknife Greenstone Belt. *In* Proceedings of the Gold Workshop. Edited by R.D. Morton, Yellowknife N.W.T., pp 232-249.

Helmstaedt, H., and Padgham, W.A. 1986a. A new look at the stratigraphy of the Yellowknife Supergroup at Yellowknife, N.W.T. – implications for the age of gold-bearing shear zones and Archean basin development. Canadian Journal of Earth Sciences, 23: 454-475.

Helmstaedt, H., and Padgham, W.A. 1986b. Stratigraphic and structural setting of gold-bearing shear zones in the Yellowknife Greenstone Belt. In Gold in the Western Shield. Edited by L.A. Clark. CIM Symposium, volume 38, pp. 322-346.

Helmstaedt, H., Padgham, W.A., and Brophy, J.A. 1986. Multiple dykes in Lower Kam Group, Yellowknife Greenstone Belt: evidence for Archean sea-floor spreading?. Geology, 14: 562-566.

Henderson, J.B. 1970. Startigraphy of the Yellowknife Supergroup, Yellowknife Bay Prosperous Lake areas, District of Mackenzie. Geological Survey of Canada, Bulletin 246, 12 p.

Henderson, J.B. 1981. Archean basin evolution in the Slave Province, Canada. *In* Precambrian Plate Tectonics. *Edited by* A. Krone, Amsterdam, Elsevier, pp. 213-235.

Henderson, J.B. 1981. Geology of the Yellowknife-Hearne Lake area, District of Mackenzie: A segment across an Archean basin. *In* Geological Survey of Canada, Memoir 414, 135p.

Henderson, J.F., and Brown, I.C. 1966. Geology and structure of the Yellowknife Greenstone Belt, District of Mackenzie. Geological Survey of Canada, Bulleting 141, 87 p.

Hey, M.H. 1954. A new review of chlorites. Mineralogical Magazine, 30: 272-292.

Hodgson, C.J. 1986. Abitibi Greenstone Belt, Ontario, Canada; Transactions of the institution of Mining and Metallurgy, v95, p.B 183-194.

Isachsen, C.E., 1992. U-Pb zircon geochronology of the Yellowknife volcanic belt and subjacent rocks, N.W.T., Canada: constraints on the timing, duration, and mechanics of greenstone belt formation. PhD thesis, Washington University, 164p.

Jensen, L.S., 1976. A new cation plot for classifying subalkalic volcanic rocks. Ontario Department of Mines, Miscellaneous Paper 66.

Ketchum, K., Bleeker, W., and Jackson, V., 1999. Field relations and U-PB geochronology of the central Slave cover group in the Yellowknife Greenstone Belt and central Slave basement complex at Point Lake. 27th Yellowknife Geoscience Forum, Program and Abstracts of talks and posters. Indian and Northern Affairs, Northwest Territories Geology Division, Canada, p.32-33.

Krough, T.E., and Gibbins, W.1978. U-Pb isotopic ages of basement and supracrustal rocks in the Point Lake area of the Slave Structural Province. *In* Geological Association of Canada Program with Abstracts, 3: 438.

Kuhns, R.J., Sawkins, F.J., and Ito, E., 1994. Magmatism, metamorphism in the Golden Giant mine; Economic Geology, 89, 720-756.

Kusky, T.M. 1990. Tectonics of a late Archean arc/continent collision in the Slave Province, Northwest Territories, Canada. Third International Archean Symposium, Perth. Extended Abstracts Volume, pp. 452-454.

Kusky, T.M., 1991. Structural development of an Archean orogen, Western Point Lake, Northwest Territories. Tectonics, 10: 820-841.

Leake, B.E., Wooley, A.R., Arps, C.E., Bitch, W.D., Gilbert, M.C., Grice, J.D. Hawthorne, F.C., Kato, A., Kisch, H.J., Krivovichev, V.G., Linthout, K., Laird, J., Mandarino, J.A., Maresch, W.V., Nickel, E.H., Rock, M.S., Schumacher, J.C., Smith, D.C., Stephenson, N.C., Ungaretti, L., Whittaker,E.J., and Youzhi, G., 1997. Nomenclature of amphiboles: report of the subcommittee on Amphiboles of the International Mineralogical Association, Commission on New Minerals and New Names: American Mineralogist, vol. 82, p.1019-1037.

MacLachlan, K., and Helmstaedt, H., 1995. Geology and geochemistry of an Archean mafic dike complex in the Chan Formation: basis for a revised plate-tectonic model of the Yellowknife greenstone belt. *In* Canadian Journal of Earth Sciences 32: 614-630.

Mason, R and Melnik, N. 1986. The anatomy of an Archean gold system – the Mctyre-Hollinger complex at Timmins, Ontario, Canada; *in* Proceedings of Gold'86 an International Symposium on the Geology of Gold Deposits, Konsult International Inc, Toronto, p. 40-55.

McGlynn, J.C., and Henderson, J.B. 1970. Archean volcanism and sedimentation in the Slave Structural Province. *In* Symposium on basins and geosynclines of the Canadian Shield. *Edited by* A.J. Baer. Geological Association of Canada, Special Paper 70-40, pp. 31-40.

Mueller, W., Doucer, P., Donaldson, J.A., and Padgham, W.A. 1993. Preliminary interpretation of the late Archean Jackson Lake Formation, Slave Province, Canada. In Exploration Overview 1993. Edited by S.P. Goff. NWT Geology Division, NP 40 pg.

Nikic, Z., Baasgaard, H., Folinsbee, R.E., Krupicka, J., Leech, A.P., and Saski, A. 1980. Boulders from the basement, the trace of an ancient crust. *In* Selected Studies of Archean Gneisses and Lower Proterozoic Rocks, Southern Canadian Shield. *Edited by* G.B. Morey and G.N. Hanson. Geological Society of America. Special Paper 182: 169-175.

Padgham, W.A. 1985. Observations and speculations on supracrustal successions in the Slave Structural Province. In Evolution of Archean Supracrustal Sequences. Edited by L.D. Ayers, P.C. Thurston and K.D. Card. Geological Association of Canada, Special Paper 28, pp. 133-151.

Padgham, W.A. 1987. The Yellowknife Volcanic Belt: setting and stratigraphy. *In*Yellowknife Guide Book. *Edited by* R.D. Morton, Geological Association of Canada, pp. 11-20.

Pearce, J.A., Harris, N.B.W., and Tindle A.G., 1984. Trace element discrimination diagrams for the tectonic interpretation of granitic rocks. Journal of Petrology, 25, 956-983.

Prior, G.J., Gibson, H.L., Watkinson, D.H., Cook, R.E., and Hannington, M.D., 1999. Rare earth and high field strength element geochemistry of the Kidd Creek Rhyolites, Abitibi Greenstone Belt, Canada. Evidence for Archean felsic volcanism and massive sulfide ore formation in an iceland-style rift environment. *In* The Giant Kidd Creek Volcanogenic Massive Sulfide Deposit, Western Abitibi Subprovince, Canada. P 457-483.

Sillitoe, R.H., 1997. Characteristics and controls on the largest gold rich porphyry copper and epithermal gold deposits in the circum Pacific Rim. Australian Journal of Earth Sciences. V 44, p 373-388.

Sun, S.S., and McDonough, W.F., 1989. Chemical and isotopic systematics of oceanic basalts:implications for mantle composition and processes. *In*: Saunders A.D. and Norry, M.J., (eds), Magmatism in Ocean Basins. Geol. Soc. London. Spec. Pub. 42, pp. 313-345.

Tatsumi, 1986. Chemical characteristics of fluid phase released from a subducted lithosphere and origin of Archean magmas evidence from high pressure experiments and natural rocks. Journal of Volcanology and Geothermal Research. v29: p 293-309.

Winchester, J.A., and Floyd, P.A., 1977. Geochemical discrimination of different magma series and their differentiation products using immobile elements. *Chemical Geology. v. 20, 325-343.*

APPENDIX A

WHOLE ROCK GEOCHEMISTRY

Major Oxide Geochemistry

Analyte		SiO2	Al2O3	MnO	MgO	CaO	Na2O	K2O	P2O5	TiO2	Fe2O3	LOI	TOTAL
Units		wt%	wt%	wt%	wt%	wt%	wt%	wt%	wt%	wt%	wt%	wt%	wt%
Detection Limit		0.01	0.01	0.01	0.01	0.01	0.01	0.01	0.01	0.01	0.01	0.05	n/a
CF9833v	Quartz Feldspar Porphyry	64.50	12.95	0.07	2.16	2.46	4.39	0.79	0.21	0.86	6.89	4.47	99.75
CF98VR1	Gabbro Sill	44.28	13.16	0.20	6.57	6.83	1.00	1.00	0.07	0.93	13.30	13.17	100.51
CF98NR2	Gabbro Sill	48.66	15.22	0.20	8.43	10.15	2.12	0.37	0.06	0.78	13.95	0.91	100.85
CF997n	Quartz Feldspar Porphyry	68.22	14.59	0.06	1.27	2.82	2.90	2.11	0.21	0.66	5.01	1.79	99.64
CF999n	Feldspar Porphyry	58.96	15.13	0.19	4.60	5.38	4.68	0.78	0.17	0.94	8.16	1.05	100.04
CF9910n	Breccia	47.12	14.20	0.29	6.66	7.19	2.69	0.22	0.11	1.51	16.47	3.44	99.90
CF9916v	Quartz Feldspar Porphyry	69.43	13.77	0.05	1.32	0.98	6.28	0.72	0.19	0.63	3.99	1.96	99.32
CF9922v	Quartz Feldspar Porphyry	66.13	13.74	0.10	1.33	3.14	5.30	1.10	0.20	0.75	4.19	3.45	99.43
CF9925v	Quartz Feldspar Porphyry	64.01	13.69	0.06	2.44	2.18	6.31	0.22	0.21	0.87	6.41	2.82	99.22
CF9926v	Volcanic Flow	50.49	15.19	0.14	5.43	3.75	4.71	0.19	0.21	1.22	11.02	7.67	100.02
CF9927v	Quartz Feldspar Porphyry	65.44	10.21	0.14	1.33	7.31	4.79	0.25	0.09	0.37	2.56	6.63	99.12
CF9934v	Feldspar Porphyry	62.15	15.80	0.05	2.79	0.70	0.58	1.84	0.34	1.49	10.95	3.65	100.34
CF9935v	Feldspar Porphyry	55.42	15.12	0.14	5.88	2.98	3.97	0.06	0.30	1.58	12.12	3.55	101.12
CF9937v	Quartz Carbonate Sericite Schist	59.91	14.52	0.09	2.80	5.17	0.47	3.38	0.18	0.49	4.78	8.94	100.73
CF9942v	Lapilli Tuff	67.79	13.09	0.05	1.62	3.37	3.52	1.52	0.17	0.56	5.10	4.04	100.83
CF9949n	Quartz Feldspar Porphyry	66.61	14.34	0.08	1.22	4.10	3.29	2.27	0.23	0.73	6.23	0.79	99.89
CF9950n	Gabbro Sill	49.05	14.92	0.18	7.81	11.09	1.74	0.64	0.06	0.75	12.85	1.04	100.13
CF9954b	Feldspar Porphyry	59.87	14.45	0.10	2.90	3.88	3.98	2.06	0.25	1.16	8.93	1.54	99.12
CF9955b	Feldspar Porphyry	56.88	14.44	0.11	3.52	3.36	4.71	0.48	0.26	1.29	9.99	4.68	99.72
CF9948v	Quartz Feldspar Porphyry	69.41	12.10	0.06	1.05	3.92	6.38	0.19	0.07	0.31	2.51	3.57	99.57
CF982 b	Quartz Feldspar Porphyry	67.78	14.18	0.05	1.16	2.03	4.26	1.74	0.22	0.62	0.84	2.79	99.44
CF9818b	Quartz Feldspar Porphyry	65.18	14.54	0.09	2.35	1.37	3.69	1.33	0.27	0.82	1.09	2.33	98.80
CF9814b	Volcanic Flow	56.03	14.32	0.21	3.71	7.10	3.29	0.71	0.31	1.38	1.69	3.71	99.34
CF9815b	Volcanic Flow	59.10	14.41	0.15	4.40	4.38	2.77	0.61	0.31	1.32	1.63	3.02	98.93
CF988b	Feldspar Porphyry	59.03	14.66	0.13	3.65	3.69	4.11	0.60	0.29	1.28	1.57	2.92	99.98
CF9824b	Volcanic Flow	65.77	14.39	0.07	1.99	1.54	1.84	2.93	0.22	0.64	0.86	3.97	99.61
CF9825b	Volcanic Flow	53.80	12.82	0.23	6.78	6.52	1.42	0.29	0.08	0.69	0.77	5.49	99.21
CF9832Ab	Volcanic Flow	55.65	12.15	0.21	6.85	6.42	3.79	0.30	0.08	0.69	0.77	4.73	99.27
CF9844blind		64.87	14.17	0.10	2.01	3.17	3.77	0.88	0.26	0.81	1.07	2.25	99.24
CF9830b	Volcanic Flow	51.90	11.00	0.18	3.40	9.07	1.86	0.18	0.15	1.28	1.43	7.69	98.82
CF9817b	Breccia	63.60	13.37	0.10	2.24	3.13	4.73	0.30	0.30	1.06	1.36	2.98	98.93
CF987b	Volcanic Flow	59.99	14.06	0.12	4.92	3.83	4.65	0.08	0.23	0.96	1.19	2.72	99.08
CF986b	Volcanic Flow	57.76	15.72	0.12	4.37	1.65	3.77	1.04	0.27	1.04	1.31	4.57	98.98
CF9811b	Cherty Tuff	72.80	14.96	0.03	0.85	0.49	7.16	0.32	0.04	0.12	0.16	0.96	99.98
CF9812b	Gabbro Dyke	46.78	12.21	0.20	4.77	5.99	1.20	0.64	1.02	4.07	5.09	5.22	98.20
CF9813b	Gabbro Sill	49.20	14.89	0.19	7.63	9.45	2.05	0.29	0.07	0.79	0.86	2.91	99.01
CF98VR8	Vitric Tuff	61.60	15.28	0.08	1.60	3.67	2.48	2.17	0.29	0.83	1.12	4.75	99.67
CF98NR1	Volcanic Flow	54.90	13.23	0.20	6.62	11.10	1.59	0.26	0.09	0.75	0.84	0.65	99.20
CF98NR3	Volcanic Flow	69.63	13.64	0.10	0.73	2.63	3.01	2.25	0.23	0.64	0.87	1.60	99.38
CF98NR4	Quartz Feldspar Porphyry	70.89	13.53	0.07	0.86	3.14	3.36	1.74	0.22	0.62	0.84	0.99	99.23
CF98NR4(PULP DUP)		71.17	13.58	0.07	0.86	3.13	3.35	1.74	0.22	0.61	0.83	1.07	99.60

Lithogeochem (Research Package) Job #: 17457 **Report#: 17301**

Trace Element Values Are in Parts Per Million. Negative Values Equal Not Detected at That Lower Limit.

Sample ID:		V	Cr	Co	Ni	Cu	Zn	Ga	Ge	As	Rb	Sr	Y	Zr	Nb	Mo	Ag	In	Sn	Sb	Cs	Ba	La	Ce
CF982	Quartz Feldspar Porphyry	36	-20	6	-15	14	66	19	0.8	54	54	60	37	268	13	-2	-0.5	-0.1	3	2.7	1.4	594	42.2	85
CF9818	Quartz Feldspar Porphyry	86	-20	13	-15	16	59	21	0.9	6	29	81	28	243	12	-2	-0.5	-0.1	2	1.6	0.3	529	38.5	77
CF9814	Volcanic Flow	161	149	31	118	98	84	18	1.2	30	23	183	31	206	13	-2	-0.5	-0.1	2	2.8	0.2	131	25.8	57
CF9815	Volcanic Flow	159	95	30	70	56	139	18	0.9	37	19	161	32	196	12	-2	-0.5	-0.1	2	1.9	0.8	182	29.3	62
CF988	Feldspar Porphyry	150	85	27	44	42	95	19	1.1	60	22	180	34	226	13	-2	-0.5	-0.1	2	5.2	1.0	115	30.6	66
CF9824	Volcanic Flow	37	475	10	1,630	19	87	21	1.1	29	94	48	39	344	14	7	-0.5	-0.1	3	6.3	1.1	731	50.5	101
CF9825	Volcanic Flow	220	330	41	95	48	150	14	1.1	14	4	109	19	67	2.3	-2	-0.5	-0.1	1	2.9	0.2	78	5.51	13
CF9832A	Volcanic Flow	222	159	35	54	31	65	11	0.8	9	4	50	18	71	2.4	-2	-0.5	-0.1	-1	1.1	0.1	59	3.41	7.9
CF9832A REP	Volcanic Flow	210	146	33	52	30	75	10	0.7	11	3	50	17	67	2.2	-2	-0.5	-0.1	-1	1.2	-0.1	54	3.31	7.7
CF9844	Repeat	91	41	14	52	21	58	22	1.2	51	20	163	34	240	11	-2	-0.5	-0.1	2	4.5	0.2	305	40.7	83
CF9830	Volcanic Flow	337	26	35	40	107	141	20	0.9	39	4	146	33	116	4.4	-2	-0.5	-0.1	1	1.8	0.2	57	11.4	26
CF9817	Breccia	156	20	19	33	36	80	17	0.7	33	4	79	26	208	9.4	-2	-0.5	-0.1	2	2.9	-0.1	70	24.0	52
CF987	Volcanic Flow	163	178	27	145	64	76	16	0.9	33	-2	112	23	176	7.4	-2	-0.5	-0.1	1	4.5	-0.1	35	19.0	40
CF986	Volcanic Flow	167	30	20	25	51	114	21	0.9	31	38	107	31	236	11	-2	-0.5	-0.1	2	6.3	0.7	445	29.1	63
CF9811	Cherty Tuff	14	-20	3	-15	-10	-30	21	0.6	32	5	168	30	135	8.7	-2	-0.5	-0.1	4	2.2	-0.1	63	19.9	43
CF9812	Gabbro Dyke	279	71	43	44	46	148	22	0.9	45	23	93	59	304	24	-2	-0.5	-0.1	2	1.8	1.5	127	26.4	75
CF9813	Gabbro Sill	250	254	51	149	126	89	16	0.9	23	9	145	18	52	1.7	-2	-0.5	-0.1	-1	2.8	0.2	43	3.05	8.1
CF98VR8	Vitric Tuff	67	-20	13	-15	44	74	22	0.8	19	77	115	48	284	14	-2	-0.5	-0.1	3	1.3	1.0	464	48.0	95
CF98NR1	Volcanic Flow	245	380	52	100	27	88	15	0.9	-5	4	85	22	79	2.6	2	-0.5	-0.1	1	0.6	0.1	47	5.65	13
CF98NR3	Volcanic Flow	33	-20	8	-15	11	63	18	-0.5	-5	80	107	30	251	12	-2	-0.5	-0.1	3	0.4	0.9	484	33.8	71
CF98NR4	Quartz Feldspar Porphyry	34	29	7	23	-10	73	18	0.6	-5	69	167	33	290	13	-2	-0.5	-0.1	3	0.3	1.2	475	36.7	77
CF98NR4 (PULP DUP)		34	-20	7	-15	55	68	18	0.7	-5	69	172	33	271	13	-2	-0.5	-0.1	3	0.3	1.3	480	36.3	77

Sample ID:		Pr	Nd	Sm	Eu	Gd	Tb	Dy	Ho	Er	Tm	Yb	Lu	Hf	Ta	W	Tl	Pb	Bi	Th	U
CF982	Quartz Feldspar Porphyry	9.78	37.1	6.84	1.460	7.39	1.07	6.10	1.29	3.74	0.574	3.44	0.531	7.1	1.0	1.0	1.15	5	-0.06	18.0	6.07
CF9818	Quartz Feldspar Porphyry	8.94	35.1	6.60	1.611	6.51	0.90	5.08	1.03	2.91	0.459	3.06	0.476	6.4	0.9	1.6	0.39	-5	-0.06	13.8	2.54
CF9814	Volcanic Flow	7.06	28.1	5.60	1.565	5.88	0.89	5.18	1.09	3.20	0.459	2.94	0.471	5.1	0.8	0.9	0.27	-5	0.10	8.53	2.51
CF9815	Volcanic Flow	7.58	30.9	5.94	1.540	6.40	0.94	5.52	1.13	3.16	0.485	3.01	0.453	4.9	0.8	0.8	0.25	8	-0.06	8.14	2.29
CF988	Feldspar Porphyry	7.81	30.5	5.85	1.547	6.57	0.95	5.56	1.17	3.41	0.510	3.16	0.502	5.9	0.9	0.9	0.26	5	-0.06	10.7	3.04
CF9824	Volcanic Flow	11.8	46.6	9.05	1.784	8.85	1.16	6.43	1.31	3.67	0.569	3.55	0.527	7.7	1.1	1.9	0.66	-5	-0.06	19.3	6.10
CF9825	Volcanic Flow	1.62	7.09	1.86	0.681	2.43	0.46	3.03	0.71	2.07	0.318	2.07	0.336	2.0	0.2	0.8	0.22	-5	-0.06	2.20	0.39
CF9832A	Volcanic Flow	1.08	5.31	1.60	0.426	2.23	0.42	2.82	0.64	1.96	0.317	1.94	0.318	2.0	0.2	0.2	0.11	-5	-0.06	1.51	0.33
CF9832A REP	Volcanic Flow	1.05	5.08	1.51	0.423	2.10	0.40	2.85	0.64	1.89	0.305	1.96	0.304	1.9	0.2	-0.2	0.07	-5	-0.06	1.56	0.23
CF9844	Repeat	9.62	37.1	7.20	2.188	7.60	1.09	6.18	1.24	3.38	0.511	3.26	0.512	6.4	0.9	0.8	0.11	6	0.06	14.2	3.79
CF9830	Volcanic Flow	3.40	15.7	3.80	1.742	4.55	0.81	5.29	1.22	3.60	0.568	3.69	0.576	3.1	0.3	0.6	0.09	-5	-0.06	2.41	0.65
CF9817	Breccia	6.42	25.9	5.02	1.348	5.63	0.81	4.67	0.96	2.78	0.424	2.61	0.411	5.0	0.7	1.0	0.08	-5	-0.06	5.00	1.06
CF987	Volcanic Flow	4.89	19.3	3.84	1.084	4.30	0.64	3.78	0.81	2.29	0.339	2.24	0.355	4.4	0.5	0.5	0.05	-5	-0.06	4.60	1.01
CF986	Volcanic Flow	7.52	29.0	5.50	1.520	5.98	0.89	5.13	1.09	3.08	0.443	2.79	0.424	5.8	0.7	0.6	0.19	-5	-0.06	8.42	2.52
CF9811	Cherty Tuff	4.84	17.4	3.51	1.144	4.07	0.71	4.61	1.02	3.16	0.514	3.28	0.530	5.0	1.9	0.5	0.11	-5	-0.06	35.2	11.3
CF9812	Gabbro Dyke	11.5	56.3	13.2	4.217	14.1	2.02	11.4	2.24	5.82	0.796	4.83	0.686	7.7	1.3	0.5	0.26	-5	-0.06	2.69	0.39
CF9813	Gabbro Sill	1.25	6.17	1.89	0.753	2.40	0.44	2.84	0.65	1.93	0.299	1.85	0.309	1.4	0.1	-0.2	0.15	-5	-0.06	0.58	-0.05
CF98VR8	Vitric Tuff	11.2	42.6	7.79	1.812	8.38	1.21	7.06	1.52	4.65	0.695	4.33	0.698	7.1	1.0	1.0	0.42	-5	0.06	16.1	4.57
CF98NR1	Volcanic Flow	1.76	7.92	2.21	0.717	2.98	0.54	3.56	0.80	2.34	0.357	2.29	0.359	2.2	0.2	0.8	0.17	-5	-0.06	2.31	0.36
CF98NR3	Volcanic Flow	8.11	31.8	5.82	1.316	6.20	0.88	5.02	1.06	3.08	0.490	3.01	0.461	6.6	1.0	0.8	0.38	5	-0.06	17.0	5.37
CF98NR4	Quartz Feldspar Porphyry	8.98	34.1	6.30	1.439	6.73	0.95	5.44	1.15	3.28	0.510	3.13	0.490	7.6	1.1	0.8	0.48	10	0.11	17.8	5.08
CF98NR4 (PULP DUP)		8.96	33.7	6.17	1.439	6.68	0.93	5.37	1.14	3.27	0.495	3.14	0.496	6.9	1.0	0.7	0.49	8	0.16	17.8	4.72

98

TRACE ELEMENTS

Analyte		Ag	Al	Au	Ba	Be	Ca	Cd	Co	Cr	Cu	Fe	Ga	Li	Mg	Mn	Mo	Ni	Pb	Sb	Sc	Sn	Ti	Tl	V	W	Zn
Units		ppm	ppm	ppm	ppm	ppm	ppm	ppm	ppm	ppm	ppm	ppm	ppm	ppm	ppm	ppm	ppm	ppm	ppm	ppm	ppm	ppm	ppm	ppm	ppm	ppm	ppm
Detecti		0.05	100	0.05	5	2	100	0.5	1	1	2	5	1	1	20	0.1	1	5	0.1	0.5	0.5	3	1	0.05	1	0.05	5
CF9833	Quartz Feldspar	N.M.	75531	N.M.	123	N.D.	22031	N.D.	24.61	53	24.2	53044	15.82	27.9	14124	413.6	N.D.	19.4	5.29	5.26	13.5	N.D.	4288	0.20	77	1.16	115
CF98V	Gabbro Sill	N.M.	75076	N.M.	141	N.D.	52177	N.D.	35.74	189	4.3	107026	15.44	48.5	43075	1291.5	N.D.	73.5	3.57	16.69	36.8	N.D.	4895	0.19	285	0.71	102
CF98N	Gabbro Sill	N.M.	79535	N.M.	30	N.D.	71853	N.D.	59.45	258	154.9	98220	15.02	13.6	49674	1153.8	N.D.	166.3	1.49	N.D.	36.2	N.D.	3818	0.06	246	0.79	90
CF997	Quartz Feldspar	N.M.	76078	N.M.	571	N.D.	24913	N.D.	8.68	5	28.7	36778	20.06	22.6	7685	387.6	N.D.	N.D.	11.36	0.64	10.0	3.2	3232	0.26	32	0.79	60
CF999	Feldspar Porphyry	N.M.	79048	N.M.	182	N.D.	40424	N.D.	27.01	145	44.7	59517	15.44	11.0	26692	1119.2	N.D.	81.6	6.76	0.55	20.5	N.D.	4455	0.14	152	1.23	76
CF9910	Breccia	N.M.	70036	N.M.	26	N.D.	50336	N.D.	54.40	68	125.1	119209	19.40	21.9	36866	1667.0	N.D.	75.5	2.37	1.52	35.7	N.D.	7167	N.D.	319	0.40	113
CF9916	Quartz Feldspar	N.M.	71551	N.M.	437	N.D.	14752	N.D.	5.19	4	50.0	27771	16.86	8.4	7561	271.8	N.D.	N.D.	9.81	1.37	9.0	N.D.	2887	0.12	30	2.16	41
CF9922	Quartz Feldspar	N.M.	74471	N.M.	609	N.D.	25640	N.D.	17.42	19	19.8	30874	16.29	13.1	8001	574.2	N.D.	17.9	9.64	3.32	10.4	N.D.	3808	0.22	55	1.00	57
CF9925	Quartz Feldspar	N.M.	73785	N.M.	67	N.D.	20480	N.D.	16.24	29	3.0	45256	14.73	13.6	15027	366.6	N.D.	13.6	6.07	3.84	12.0	N.D.	4138	N.D.	70	0.34	21
CF9926	Volcanic Flow	N.M.	78949	N.M.	156	N.D.	29322	N.D.	38.87	194	8.5	77574	18.38	37.9	31871	829.1	N.D.	97.7	3.59	2.67	22.9	N.D.	5768	N.D.	184	0.44	114
CF9927	Quartz Feldspar	N.M.	55479	N.M.	156	N.D.	50580	N.D.	6.45	5	16.2	18776	10.94	7.9	8028	828.1	N.D.	N.D.	6.49	1.44	6.6	N.D.	1804	N.D.	25	0.42	26
CF9934	Feldspar Porphyry	N.M.	63459	N.M.	211	N.D.	10366	N.D.	55.07	65	15.3	76301	19.92	59.5	9472	283.6	N.D.	48.2	7.21	13.27	13.7	N.D.	6570	0.41	132	4.38	114
CF9935	Feldspar Porphyry	N.M.	74619	N.M.	44	N.D.	24366	N.D.	40.02	123	17.9	83524	16.12	33.8	32727	755.7	N.D.	81.6	14.74	2.28	23.5	N.D.	6924	N.D.	161	0.45	147
CF9937	Quartz Carbonate	N.M.	69226	N.M.	582	N.D.	39243	N.D.	7.60	54	8.3	34974	16.89	7.6	15101	503.8	N.D.	28.7	7.70	3.68	9.9	N.D.	2324	0.58	74	0.50	39
CF9942	Lapilli Tuff	N.M.	67558	N.M.	266	N.D.	26795	N.D.	9.37	3	11.4	36826	16.82	23.1	9266	271.0	N.D.	N.D.	4.85	3.11	8.4	N.D.	2711	0.28	35	0.51	49
CF9948	Quartz Feldspar	N.M.	62855	N.M.	45	N.D.	28204	N.D.	7.04	4	42.9	17382	9.84	6.2	6567	358.6	N.D.	5.2	4.19	0.74	5.4	N.D.	1471	N.D.	31	0.20	29
CF9949	Quartz Feldspar	N.M.	75432	N.M.	499	N.D.	32477	N.D.	11.26	8	23.5	46072	18.48	26.8	7382	472.6	1.5	6.0	15.71	N.D.	11.3	N.D.	3539	0.42	50	0.48	78
CF9950	Gabbro Sill	N.M.	76564	N.M.	51	N.D.	74285	N.D.	52.31	224	79.1	94550	14.31	17.4	45974	1065.7	N.D.	131.1	1.78	N.D.	33.5	N.D.	3619	0.08	220	0.21	78
CF9954	Feldspar Porphyry	N.M.	71654	N.M.	495	N.D.	31043	N.D.	22.36	54	56.0	63497	18.67	19.4	16281	570.9	N.D.	30.3	14.52	1.67	17.7	N.D.	5337	0.40	116	1.29	89
CF9955	Feldspar Porphyry	N.M.	75007	N.M.	182	N.D.	27025	N.D.	26.01	74	58.4	71891	19.30	42.5	20609	626.1	N.D.	36.6	5.37	4.32	19.0	N.D.	5960	0.09	126	2.35	95

Analyte		La	Ce	Pr	Nd	Sm	Eu	Gd	Tb	Dy	Ho	Er	Tm	Yb	Lu	Rb	Sr	Nb	Cs	Hf	Ta	Th	U	Y	Zr
Units		ppm	ppm	ppm	ppm	ppm	ppm	ppm	ppm	ppm	ppm	ppm	ppm	ppm	ppm	ppm	ppm	ppm	ppm	ppm	ppm	ppm	ppm	ppm	ppm
Detection Limit		0.01	0.01	0.01	0.01	0.01	0.01	0.01	0.01	0.01	0.01	0.01	0.01	0.01	0.01	0.01	0.2	0.02	0.01	0.01	0.01	0.02	0.02	0.5	1
CF9833	Quartz Feldspar Porphyry	36.90	72.20	8.56	32.43	6.46	1.50	5.57	0.78	5.18	1.05	3.02	0.38	2.92	0.46	16.67	56.9	11.63	1.04	5.66	0.98	12.40	3.66	30.77	192.80
CF98V R1	Gabbro Sill	1.35	3.40	0.53	2.71	1.17	0.59	2.33	0.41	3.30	0.71	2.20	0.28	2.26	0.36	21.80	99.5	2.80	1.70	1.85	0.28	0.45	0.15	21.48	57.29
CF98N R2	Gabbro Sill	2.66	6.83	1.09	5.44	1.78	0.65	2.16	0.34	2.67	0.56	1.76	0.20	1.84	0.29	4.92	122.0	2.06	0.22	1.34	0.22	0.33	0.09	17.35	40.49
CF997	Quartz Feldspar Porphyry	49.16	94.21	11.04	39.90	7.93	1.76	7.06	1.00	6.68	1.33	3.83	0.52	3.71	0.60	71.87	93.3	13.56	0.64	7.40	1.17	18.25	5.35	39.12	248.76
CF999	Feldspar Porphyry	21.24	41.66	5.00	19.47	4.00	0.99	3.75	0.54	3.77	0.75	2.19	0.25	2.16	0.34	18.36	153.9	7.68	0.19	4.34	0.64	5.06	1.31	22.60	153.22
CF9910	Breccia	6.66	16.26	2.50	12.34	3.72	1.27	4.45	0.68	4.91	1.04	3.01	0.40	2.99	0.48	2.02	123.1	4.84	0.08	2.73	0.41	0.78	0.18	29.96	81.00
CF9916	Quartz Feldspar Porphyry	45.50	87.54	10.22	37.37	7.18	1.41	6.07	0.86	5.61	1.13	3.34	0.43	3.20	0.50	15.54	105.0	12.45	0.68	7.10	1.13	17.73	5.11	34.09	239.95
CF9922	Quartz Feldspar Porphyry	39.90	77.12	9.10	33.74	6.54	1.44	5.42	0.74	4.87	0.96	2.89	0.36	2.83	0.44	37.21	195.7	12.69	1.14	6.48	1.06	15.07	4.40	28.44	218.05
CF9925	Quartz Feldspar Porphyry	33.61	68.61	8.49	32.12	6.96	1.82	6.74	1.01	6.41	1.30	3.73	0.48	3.56	0.56	2.20	133.5	13.00	0.22	6.57	1.05	14.73	4.20	39.97	225.32
CF9926	Volcanic Flow	18.92	38.91	4.89	19.40	4.16	1.18	3.86	0.53	3.68	0.73	2.17	0.26	2.23	0.35	4.66	95.3	8.74	0.27	4.06	0.65	3.88	1.04	21.08	143.84
CF9927	Quartz Feldspar Porphyry	36.42	71.25	8.32	30.05	5.75	1.44	4.79	0.64	4.32	0.81	2.43	0.30	2.46	0.37	3.91	161.5	8.90	0.23	5.77	0.87	16.74	4.62	24.00	193.81
CF9934	Feldspar Porphyry	18.14	38.40	4.87	18.90	4.06	0.97	3.94	0.54	3.88	0.79	2.44	0.31	2.51	0.40	46.15	43.8	14.78	2.30	6.22	1.06	6.45	3.10	23.87	214.85
CF9935	Feldspar Porphyry	27.24	57.72	7.23	28.31	6.02	1.56	5.60	0.83	5.52	1.08	3.09	0.39	3.02	0.46	1.42	150.3	12.70	0.51	4.96	0.88	7.41	2.15	31.31	171.73
CF9937	Quartz Carbonate Sericite Schist	54.78	100.77	11.59	40.70	6.14	1.70	3.84	0.39	2.53	0.38	1.19	0.10	1.15	0.17	92.16	62.6	6.00	2.99	4.06	0.56	15.08	2.84	13.12	138.15
CF9942	Lapilli Tuff	55.65	103.56	11.94	42.86	7.88	1.63	6.52	0.90	5.82	1.18	3.46	0.44	3.27	0.52	52.66	52.8	11.83	1.07	6.22	1.05	17.00	5.06	36.30	205.73
CF9948	Quartz Feldspar Porphyry	30.56	57.24	6.54	23.53	4.34	0.78	3.61	0.51	3.63	0.72	2.21	0.28	2.31	0.35	4.49	85.4	7.20	0.30	5.03	0.80	18.40	4.11	22.10	159.57
CF9949	Quartz Feldspar Porphyry	44.60	87.10	10.28	37.64	7.40	1.51	6.55	0.94	6.23	1.26	3.73	0.48	3.51	0.55	80.48	174.0	13.18	1.66	7.05	1.09	15.80	4.61	37.27	238.47
CF9950	Gabbro Sill	2.70	6.70	1.02	5.08	1.69	0.58	2.05	0.30	2.52	0.53	1.60	0.18	1.68	0.27	12.34	127.1	1.97	0.40	1.23	0.21	0.33	0.08	16.17	36.96
CF9954	Feldspar Porphyry	37.21	73.05	8.97	34.02	6.99	1.76	6.36	0.89	5.88	1.19	3.37	0.44	3.26	0.53	61.77	182.7	12.92	2.21	5.87	0.99	11.14	3.28	35.10	202.18
CF9955	Feldspar Porphyry	31.99	63.28	7.56	28.11	5.60	1.32	5.21	0.80	5.62	1.15	3.30	0.43	3.20	0.50	13.19	153.7	13.22	0.35	5.61	0.99	10.79	3.10	33.85	195.88

APPENDIX B

MINERAL CHEMISTRY

Amphibole Chemistry
Basis Of 28 Oxygens

	1	2	3	4	5	6	8	9	10
SiO2	44.53	50.26	48.58	48.32	43.58	42.69	51.79	54.13	52.46
TiO2	0.32	0.13	0.29	0.58	1.78	2.15	0.02	0.01	0.82
Al2O3	11.78	5.65	7.32	4.35	8.08	8.67	3.96	2.03	2.83
Cr2O3	0.24	0.02	0.02	0.03	0.01	0.00	0.01	0.00	0.03
FeO	17.64	15.49	16.81	22.99	25.39	25.50	14.67	12.88	13.61
MnO	0.21	0.31	0.32	0.46	0.38	0.31	0.28	0.31	0.28
MgO	9.37	13.18	12.30	8.30	5.89	6.06	13.58	14.82	13.74
CaO	12.24	10.72	10.76	11.39	10.34	10.32	12.30	12.51	13.08
Na2O	0.94	0.53	0.71	0.74	1.29	1.30	0.36	0.19	0.30
K2O	0.33	0.11	0.10	0.25	0.21	0.26	0.16	0.08	0.09
Total	97.61	96.40	97.21	97.41	96.95	97.26	97.12	96.96	97.24
FeO	14.90	13.85	13.49	21.00	21.72	20.63	13.38	12.88	13.61
Fe2O3	3.04	1.83	3.69	2.21	4.08	5.41	1.44	0.00	0.00
Total	97.91	96.58	97.58	97.63	97.36	97.80	97.27	96.96	97.24
Si	6.6101	7.3937	7.1221	7.3534	6.7517	6.5865	7.5613	7.8485	7.6531
Al IV	1.3899	0.6063	0.8779	0.6466	1.2483	1.4135	0.4387	0.1515	0.3469
Ti	0.0362	0.0144	0.0318	0.0660	0.2074	0.2499	0.0022	0.0015	0.0896
Al VI	0.6717	0.3735	0.3873	0.1339	0.2275	0.1635	0.2429	0.1953	0.1406
Cr	0.0283	0.0021	0.0018	0.0039	0.0014	0.0000	0.0014	0.0000	0.0032
Fe3+	0.3397	0.2013	0.4045	0.2517	0.4709	0.6232	0.1573	0.0000	0.0000
Fe 2+	1.8502	1.7044	1.6566	2.6744	2.8189	2.6671	1.6339	1.5618	1.6605
Mn	0.0259	0.0387	0.0398	0.0596	0.0499	0.0409	0.0344	0.0382	0.0345
Mg	2.0729	2.8896	2.6874	1.8825	1.3600	1.3934	2.9548	3.2024	2.9873
Ca	1.9468	1.6898	1.6903	1.8573	1.7165	1.7061	1.9242	1.9436	2.0446
Na M4	0.0282	0.0861	0.1005	0.0765	0.1506	0.1559	0.0500	0.0531	0.0397
Na A	0.2434	0.0662	0.1019	0.1420	0.2370	0.2326	0.0510	0.0000	0.0464
K	0.0626	0.0203	0.0192	0.0482	0.0412	0.0504	0.0292	0.0144	0.0172
Total	######	######	######	######	######	######	######	######	######
T	8.0000	8.0000	8.0000	8.0000	8.0000	8.0000	8.0000	8.0000	8.0000
M 1-3	5.0000	5.0000	5.0000	5.0000	5.0000	5.0000	5.0000	4.9993	5.0000
M 4	2.0000	2.0000	2.0000	2.0057	2.0030	2.0000	2.0013	1.9960	2.0000
A	0.3059	0.0865	0.1211	0.1902	0.2781	0.2830	0.0802	0.0144	0.0636

1 cf9950c1amp1 Gabbro Sill
2 cf9950c1amp2 Gabbro Sill
3 cf9950c1amp3 Gabbro Sill
4 cf9810c1amp1 Gabbro Sill
5 cf9810c1amp2 Gabbro Sill
6 cf9810c1amp3 Gabbro Sill
8 cf9813c1amp1 Gabbro Sill
9 cf9813c1amp2 Gabbro Sill
10 cf9813c1amp3 Gabbro Sill

	1	2	3
SiO2	49.93	52.73	50.37
TiO2	0.69	0.01	0.08
Al2O3	5.07	2.67	5.58
Cr2O3	0.08	0.02	0.02
FeO	15.37	14.22	16.61
MnO	0.25	0.25	0.28
MgO	12.62	14.25	11.94
CaO	12.69	13.09	12.69
Na2O	0.46	0.29	0.43
K2O	0.15	0.09	0.24
Total	97.31	97.62	98.23
Si	7.3627	7.6793	7.3868
Al IV	0.6373	0.3207	0.6132
Ti	0.0770	0.0013	0.0088
Al	0.2441	0.1382	0.3515
Cr	0.0089	0.0018	0.0023
Fe	1.8955	1.7320	2.0372
Mn	0.0316	0.0313	0.0348
Mg	2.7734	3.0928	2.6096
Ca	2.0051	2.0427	1.9941
Na	0.1302	0.0806	0.1209
K	0.0288	0.0175	0.0442
Tot(cat)	15.1947	15.1381	15.2034

1 987amp Volcanic Flow
2 987amp2 Volcanic Flow
3 987amp3 Volcanic Flow

	1	2	3
SiO2	37.62	46.18	44.60
TiO2	0.07	0.31	0.37
Al2O3	25.19	9.41	11.72
Cr2O3	0.00	0.01	0.06
FeO	9.32	16.35	16.79
MnO	0.04	0.30	0.26
MgO	0.00	10.61	9.36
CaO	23.86	12.07	11.90
Na2O	0.00	0.78	1.14
K2O	0.00	0.17	0.24
Total	96.11	96.19	96.45
Si	5.6444	6.9413	6.7143
Al IV	2.3556	1.0587	1.2857
Ti	0.0084	0.0350	0.0420
Al	2.1001	0.6088	0.7944
Cr	0.0000	0.0011	0.0069
Fe	1.1695	2.0553	2.1139
Mn	0.0055	0.0378	0.0337
Mg	0.0002	2.3768	2.1000
Ca	3.8359	1.9440	1.9196
Na	0.0000	0.2286	0.3320
K	0.0000	0.0327	0.0469
Tot(cat)	15.1194	15.3200	15.3896

1	cf9911clamp1	Breccia
2	cf9911clamp1 repeat	Breccia
3	cf9911clamp2	Breccia

Mica Chemistry
Basis of 22 oxygens

	1	2	3	4	5	
SiO2	35.33	35.52	35.92	35.39	35.98	SiO2
TiO2	1.73	1.62	1.81	1.69	1.83	TiO2
Al2O3	16.22	16.10	16.01	16.24	16.66	Al2O3
Cr2O3	0.02	0.00	0.01	0.02	0.00	Cr2O3
FeO	22.18	22.13	22.97	22.83	21.85	FeO
MnO	0.23	0.25	0.25	0.20	0.22	MnO
MgO	8.79	8.63	9.12	9.09	9.29	MgO
CaO	0.05	0.06	0.03	0.02	0.00	CaO
BaO	0.17	0.29	0.25	0.14	0.09	BaO
Na2O	0.01	0.02	0.02	0.05	0.05	Na2O
K2O	9.49	9.34	9.34	9.08	9.13	K2O
Total	94.23	93.97	95.72	94.76	95.09	Total
Si	5.5516	5.5939	5.5651	5.5297	5.5593	Si
Al IV	2.4484	2.4061	2.4349	2.4703	2.4407	Al IV
Ti	0.2049	0.1923	0.2109	0.1983	0.2128	Ti
Al	0.5564	0.5831	0.4894	0.5213	0.5940	Al
Cr	0.0029	0.0000	0.0016	0.0029	0.0000	Cr
Fe	2.9148	2.9147	2.9763	2.9833	2.8235	Fe
Mn	0.0300	0.0337	0.0325	0.0269	0.0284	Mn
Mg	2.0585	2.0255	2.1058	2.1167	2.1392	Mg
Ca	0.0084	0.0104	0.0043	0.0039	0.0006	Ca
Ba	0.0107	0.0178	0.0150	0.0084	0.0051	Ba
Na	0.0033	0.0067	0.0046	0.0159	0.0143	Na
K	1.9025	1.8766	1.8461	1.8100	1.7997	K
Tot(cat)	15.6925	15.6608	15.6865	15.6877	15.6176	**Tot(cat)**

1 9954c1biot Feldspar Porphyry
2 9954c1biot Feldspar Porphyry
3 9954c1biot Feldspar Porphyry
4 9954c1biot Feldspar Porphyry
5 988c1biot Feldspar Porphyry

1	2	3	4	5	6	7	8	9	10
35.15	35.15	34.19	34.80	35.00	34.54	33.71	34.08	34.01	25.93
2.02	2.44	2.02	2.12	1.17	2.17	2.02	1.75	1.88	0.19
17.21	16.85	17.16	17.37	17.67	17.03	17.62	17.83	17.81	17.94
0.10	0.03	0.02	0.06	0.01	0.02	0.07	0.00	0.04	0.03
24.60	25.13	25.10	25.17	24.05	26.08	25.37	25.02	24.19	32.89
0.34	0.33	0.28	0.27	0.31	0.31	0.25	0.24	0.25	0.36
6.32	5.90	6.24	6.15	6.89	6.13	6.33	6.33	6.24	9.91
0.05	0.05	0.02	0.00	0.05	0.01	0.00	0.01	0.00	0.00
0.11	0.09	0.11	0.08	0.01	0.06	0.09	0.02	0.09	0.00
0.04	0.04	0.01	0.06	0.07	0.02	0.05	0.02	0.02	0.00
9.52	9.69	8.93	9.63	9.62	9.06	9.09	9.56	9.62	0.14
95.47	95.70	94.08	95.70	94.86	95.43	94.61	94.86	94.15	87.40
5.5085	5.5155	5.4470	5.4590	5.5026	5.4461	5.3564	5.3932	5.4091	4.5065
2.4915	2.4845	2.5530	2.5410	2.4974	2.5539	2.6436	2.6068	2.5909	3.4935
0.2384	0.2878	0.2416	0.2496	0.1379	0.2571	0.2419	0.2082	0.2251	0.0252
0.6881	0.6326	0.6701	0.6713	0.7777	0.6117	0.6570	0.7197	0.7484	0.1823
0.0119	0.0033	0.0029	0.0068	0.0018	0.0029	0.0091	0.0000	0.0050	0.0045
3.2241	3.2978	3.3443	3.3021	3.1622	3.4391	3.3714	3.3114	3.2176	4.7806
0.0458	0.0443	0.0383	0.0358	0.0416	0.0411	0.0342	0.0322	0.0342	0.0524
1.4761	1.3797	1.4816	1.4378	1.6144	1.4405	1.4990	1.4929	1.4790	2.5668
0.0086	0.0090	0.0031	0.0006	0.0092	0.0019	0.0000	0.0012	0.0000	0.0005
0.0070	0.0053	0.0067	0.0047	0.0004	0.0039	0.0056	0.0010	0.0055	0.0000
0.0114	0.0134	0.0045	0.0193	0.0220	0.0065	0.0145	0.0074	0.0053	0.0000
1.9034	1.9398	1.8151	1.9273	1.9296	1.8225	1.8427	1.9301	1.9520	0.0316
15.6147	15.6131	15.6082	15.6552	15.6968	15.6270	15.6754	15.7041	15.6722	15.6439

1 cf9949c2micQuartz Feldspar Porphyry
2 cf9949c2micQuartz Feldspar Porphyry
3 cf9949c2micQuartz Feldspar Porphyry
4 cf9949c2micQuartz Feldspar Porphyry
5 cf9949c3micQuartz Feldspar Porphyry
6 cf9949c3micQuartz Feldspar Porphyry
7 cf997c3micaQuartz Feldspar Porphyry
8 cf997c3micaQuartz Feldspar Porphyry
9 cf997c3micaQuartz Feldspar Porphyry
10 cf997c1micaQuartz Feldspar Porphyry

Chlorite Chemistry
Basis of 28 oxygens

	1	2	3	4	5	6	7	8	9	10	11
SiO2	24.14	24.45	24.67	25.25	25.05	24.97	24.96	24.53	24.00	24.11	27.10
TiO2	0.10	0.06	0.05	0.09	0.12	0.06	0.07	0.08	0.06	0.03	0.04
Al2O3	21.23	23.30	22.20	21.04	20.30	20.63	20.93	20.96	22.04	21.88	17.48
Cr2O3	0.00	0.03	0.37	0.00	0.01	0.11	0.02	0.11	0.00	0.02	0.55
FeO	23.08	26.23	25.97	26.61	28.14	28.33	29.24	29.26	31.64	31.44	28.44
MnO	0.05	0.09	0.11	0.38	0.44	0.36	0.10	0.14	0.17	0.11	0.36
MgO	12.11	12.58	13.56	13.17	13.04	12.79	12.63	12.60	11.05	11.19	14.96
CaO	4.07	0.06	0.01	0.00	0.03	0.04	0.01	0.01	0.00	0.11	0.03
Na2O	0.19	0.04	0.02	0.01	0.00	0.00	0.00	0.00	0.00	0.00	0.00
K2O	0.00	0.00	0.00	0.06	0.02	0.04	0.00	0.02	0.00	0.00	0.00
Total	84.98	86.84	86.95	86.62	87.14	87.33	87.97	87.70	88.96	88.89	88.96
Si	5.2838	5.2220	5.2670	5.4341	5.4135	5.3874	5.3580	5.2932	5.1640	5.1862	5.7381
Al IV	2.7162	2.7780	2.7330	2.5659	2.5865	2.6126	2.6420	2.7068	2.8360	2.8138	2.2619
Ti	0.0169	0.0098	0.0077	0.0151	0.0194	0.0103	0.0108	0.0126	0.0090	0.0055	0.0060
Al	2.7620	3.0889	2.8547	2.7724	2.5855	2.6348	2.6548	2.6254	2.7548	2.7349	2.1015
Cr	0.0000	0.0054	0.0616	0.0000	0.0013	0.0187	0.0040	0.0180	0.0000	0.0035	0.0920
Fe	4.2249	4.6853	4.6370	4.7895	5.0860	5.1119	5.2494	5.2805	5.6936	5.6560	5.0362
Mn	0.0100	0.0160	0.0199	0.0695	0.0804	0.0654	0.0177	0.0258	0.0301	0.0195	0.0644
Mg	3.9503	4.0043	4.3145	4.2241	4.1998	4.1126	4.0406	4.0521	3.5434	3.5873	4.7207
Ca	0.9545	0.0142	0.0012	0.0010	0.0058	0.0101	0.0030	0.0026	0.0000	0.0243	0.0076
Na	0.0819	0.0166	0.0073	0.0046	0.0000	0.0000	0.0000	0.0000	0.0005	0.0019	0.0000
K	0.0010	0.0000	0.0006	0.0154	0.0044	0.0109	0.0012	0.0044	0.0013	0.0005	0.0000
Tot(cat)	20.0017	19.8403	19.9046	19.8916	19.9826	19.9747	19.9814	20.0213	20.0326	20.0334	20.0283

1 9926c2chlor Volcanic Flow
2 9926c2chlor Volcanic Flow
3 9926c1chlor Volcanic Flow
4 9954c1chlor Feldspar Porphyry
5 9954c1chlor Feldspar Porphyry
6 9954c2chlor Feldspar Porphyry
7 9955c2chlor Feldspar Porphyry
8 9955c3chlor Feldspar Porphyry
9 9942c3chlor Quartz Feldspar Porphyry
10 9942c1chlor Quartz Feldspar Porphyry
11 987c2chlor Volcanic Flow
12 987c1chlor Volcanic Flow
13 9818c4chlor Quartz Feldspar Porphyry
14 9818c2chlor Quartz Feldspar Porphyry
15 982c2chlor Quartz Feldspar Porphyry
16 982c2chlor Quartz Feldspar Porphyry
17 9825cchlor Volcanic Flow
18 9825chlor2 Volcanic Flow
19 988c3chlor Feldspar Porphyry
20 988c3chlor Feldspar Porphyry
21 989chlor Quartz Feldspar Porphyry
22 989chlor rep Quartz Feldspar Porphyry
23 989chlor2 Quartz Feldspar Porphyry

12	13	14	15	16	17	18	19	20	21	22	23
25.72	26.51	25.98	25.62	24.89	26.06	25.32	25.63	25.20	63.08	24.40	23.77
0.04	0.08	0.18	0.06	0.14	0.09	0.06	0.07	0.07	0.02	0.03	0.05
20.85	16.88	17.38	22.90	20.03	20.34	21.18	20.91	21.58	22.68	20.91	22.07
0.10	0.00	0.00	0.00	0.00	0.07	0.08	0.01	0.01	0.00	0.00	0.00
26.05	33.44	33.39	33.07	34.12	24.75	25.05	28.23	28.93	2.11	34.30	31.61
0.31	0.42	0.32	0.18	0.23	0.39	0.41	0.49	0.39	0.00	0.23	0.11
15.28	11.15	11.09	9.84	9.56	15.61	15.28	13.31	13.02	0.99	9.83	9.98
0.03	0.06	0.07	0.07	0.10	0.04	0.06	0.08	0.03	0.23	0.07	0.06
0.01	0.03	0.01	0.15	0.02	0.01	0.03	0.00	0.00	10.64	0.01	0.04
0.01	0.11	0.11	0.03	0.08	0.01	0.00	0.09	0.00	0.11	0.03	0.00
88.40	88.67	88.53	91.92	89.16	87.36	87.47	88.82	89.24	99.86	89.81	87.69
5.4003	5.7954	5.6901	5.3317	5.4211	5.5009	5.3532	5.4219	5.3196	9.8034	5.2775	5.1936
2.5997	2.2046	2.3099	2.6683	2.5789	2.4991	2.6468	2.5781	2.6804	0.0000	2.7225	2.8064
0.0061	0.0125	0.0289	0.0099	0.0226	0.0148	0.0092	0.0112	0.0106	0.0029	0.0042	0.0081
2.5613	2.1458	2.1777	2.9500	2.5643	2.5625	2.6324	2.6368	2.6901	4.1554	2.6094	2.8785
0.0165	0.0000	0.0007	0.0000	0.0000	0.0113	0.0133	0.0020	0.0020	0.0000	0.0000	0.0003
4.5743	6.1138	6.1161	5.7557	6.2151	4.3692	4.4293	4.9945	5.1074	0.2739	6.2045	5.7761
0.0557	0.0775	0.0593	0.0312	0.0415	0.0688	0.0738	0.0874	0.0701	0.0003	0.0423	0.0203
4.7813	3.6327	3.6199	3.0518	3.1032	4.9107	4.8146	4.1963	4.0961	0.2283	3.1687	3.2497
0.0071	0.0131	0.0157	0.0158	0.0238	0.0083	0.0130	0.0179	0.0068	0.0384	0.0164	0.0134
0.0031	0.0115	0.0055	0.0615	0.0065	0.0022	0.0103	0.0014	0.0000	3.2062	0.0045	0.0183
0.0018	0.0316	0.0318	0.0079	0.0216	0.0020	0.0008	0.0232	0.0013	0.0210	0.0092	0.0000
20.0073	20.0385	20.0555	19.8839	19.9987	19.9499	19.9968	19.9707	19.9842	17.7297	20.0592	19.9649

Chlorite Chemistry
Basis of 28 oxygens

	1	2	3	4	5	6	7	8
SiO2	26.03	25.80	26.09	26.17	25.61	25.00	26.08	25.79
TiO2	0.04	0.09	0.08	0.09	0.12	0.27	0.16	0.26
Al2O3	20.99	21.42	20.50	20.24	18.11	19.48	17.67	17.68
Cr2O3	0.09	0.21	0.07	0.05	0.06	0.09	0.05	0.09
FeO	23.53	23.90	23.81	23.85	34.56	32.82	33.71	33.92
MnO	0.21	0.30	0.26	0.26	0.41	0.49	0.40	0.39
MgO	16.27	16.35	16.62	16.76	8.99	9.28	10.28	9.90
CaO	0.02	0.02	0.04	0.04	0.07	0.02	0.03	0.05
Na2O	0.00	0.00	0.00	0.00	0.00	0.00	0.03	0.00
K2O	0.01	0.00	0.04	0.00	0.07	0.19	0.03	0.03
Total	87.19	88.08	87.50	87.46	88.01	87.64	88.44	88.11
Si	5.4604	5.3716	5.4680	5.4886	5.6787	5.5205	5.7210	5.6919
Al IV	2.5396	2.6284	2.5320	2.5114	2.3213	2.4795	2.2790	2.3081
Ti	0.0064	0.0133	0.0123	0.0137	0.0207	0.0447	0.0270	0.0425
Al	2.6514	2.6293	2.5331	2.4931	2.4128	2.5918	2.2907	2.2921
Cr	0.0150	0.0345	0.0119	0.0076	0.0101	0.0164	0.0091	0.0158
Fe	4.1281	4.1616	4.1734	4.1833	6.4089	6.0611	6.1844	6.2609
Mn	0.0375	0.0523	0.0457	0.0469	0.0779	0.0909	0.0745	0.0729
Mg	5.0865	5.0732	5.1912	5.2386	2.9708	3.0540	3.3608	3.2563
Ca	0.0036	0.0048	0.0089	0.0084	0.0174	0.0053	0.0060	0.0125
Na	0.0000	0.0000	0.0000	0.0000	0.0000	0.0000	0.0125	0.0007
K	0.0038	0.0000	0.0098	0.0003	0.0199	0.0535	0.0075	0.0083
Tot(cat)	19.9322	19.9690	19.9861	19.9919	19.9385	19.9177	19.9726	19.9621

1	cf9911c2chlor1	Breccia
2	cf9911c2chlor2	Breccia
3	cf9911c1chlor3	Breccia
4	cf9911c1chlor4	Breccia
5	cf997c1chlor1	Quartz Feldspar Porphyry
6	cf997c1chlor2	Quartz Feldspar Porphyry
7	cf999c1chlor3	Feldspar Porphyry
8	cf999c3chlor2	Feldspar Porphyry

	1	2	3	4	5	6	7	8	9	10	11	12	13
SiO2	27.74	25.84	27.08	24.71	24.07	25.08	24.49	22.42	23.08	22.44	26.10	25.70	25.54
TiO2	0.07	0.07	0.09	0.07	0.06	0.23	0.07	0.00	0.01	0.01	0.03	0.02	0.03
Al2O3	17.72	20.47	17.73	21.05	21.69	20.37	21.45	25.02	23.85	24.41	20.42	20.42	21.03
Cr2O3	0.02	0.10	0.00	0.02	0.01	0.01	0.01	0.03	0.03	0.05	0.06	0.02	0.04
FeO	26.38	25.05	30.27	31.34	30.52	30.21	30.45	32.77	31.98	32.34	24.47	24.73	24.55
MnO	0.31	0.34	0.35	0.09	0.13	0.28	0.23	0.14	0.14	0.12	0.33	0.44	0.28
MgO	15.81	15.84	13.24	11.00	10.81	11.58	10.87	8.77	9.20	8.84	16.11	16.08	15.91
CaO	0.06	0.02	0.04	0.00	0.00	0.03	0.02	0.01	0.00	0.00	0.15	0.02	0.02
Na2O	0.00	0.00	0.00	0.00	0.00	0.00	0.01	0.00	0.00	0.01	0.00	0.00	0.00
K2O	0.05	0.02	0.03	0.03	0.03	0.02	0.18	0.01	0.00	0.01	0.01	0.00	0.00
Total	88.17	87.76	88.82	88.31	87.32	87.80	87.78	89.17	88.28	88.23	87.69	87.44	87.40
Si	5.8428	5.4405	5.7861	5.3439	5.2507	5.4297	5.3144	4.8391	5.0114	4.8911	5.4802	5.4262	5.3824
Al IV	2.1572	2.5595	2.2139	2.6561	2.7493	2.5703	2.6856	3.1609	2.9886	3.1089	2.5198	2.5738	2.6176
Ti	0.0110	0.0115	0.0137	0.0109	0.0092	0.0367	0.0120	0.0000	0.0010	0.0023	0.0048	0.0037	0.0046
Al	2.2429	2.5215	2.2522	2.7108	2.8288	2.6288	2.8020	3.2055	3.1166	3.1635	2.5350	2.5091	2.6074
Cr	0.0036	0.0165	0.0000	0.0036	0.0018	0.0013	0.0009	0.0043	0.0045	0.0083	0.0097	0.0040	0.0059
Fe	4.6469	4.4109	5.4091	5.6684	5.5680	5.4698	5.5262	5.9153	5.8073	5.8952	4.2970	4.3668	4.3270
Mn	0.0553	0.0612	0.0629	0.0169	0.0237	0.0510	0.0414	0.0265	0.0253	0.0220	0.0594	0.0787	0.0508
Mg	4.9628	4.9703	4.2161	3.5454	3.5144	3.7363	3.5154	2.8210	2.9771	2.8715	5.0412	5.0598	4.9970
Ca	0.0145	0.0049	0.0091	0.0002	0.0000	0.0063	0.0037	0.0018	0.0009	0.0004	0.0342	0.0044	0.0043
Na	0.0000	0.0000	0.0000	0.0000	0.0000	0.0000	0.0046	0.0000	0.0000	0.0035	0.0000	0.0000	0.0004
K	0.0146	0.0050	0.0082	0.0073	0.0087	0.0062	0.0511	0.0022	0.0000	0.0027	0.0027	0.0000	0.0009
Tot(cat)	19.9516	20.0017	19.9713	19.9636	19.9545	19.9365	19.9572	19.9767	19.9327	19.9694	19.9840	20.0266	19.9983

1	cf9815gmchlor1	Volcanic Flow
2	cf9815gmchlor2	Volcanic Flow
3	cf9815gmchlor3	Volcanic Flow
4	cf9916gmchlor1	Volcanic Flow
5	cf9916gmchlor2	Volcanic Flow
6	cf9922gmchlor1	Quartz Feldspar Porphyry
7	cf9922gmchlor2	Quartz Feldspar Porphyry
8	cf9934c2chlor1	Feldspar Porphyry
9	cf9934c3chlor1	Feldspar Porphyry
10	cf9934c3chlor2	Feldspar Porphyry
11	cf9935c1chlor1	Feldspar Porphyry
12	cf9935c1chlor2	Feldspar Porphyry
13	cf9935c2chlor1	Feldspar Porphyry

Chlorite Chemistry

Basis of 28 oxygens

	1	2	3	4	5	6
SiO2	27.66	26.53	25.81	24.91	25.57	26.60
TiO2	0.10	0.01	0.06	0.03	0.01	0.03
Al2O3	19.22	20.73	20.21	20.58	21.37	20.45
Cr2O3	0.00	0.06	0.02	0.12	0.00	0.02
FeO	21.82	22.98	26.42	28.68	21.73	21.86
MnO	0.11	0.14	0.29	0.30	0.27	0.23
MgO	17.21	16.95	14.65	12.66	17.23	17.66
CaO	0.08	0.09	0.05	0.07	0.02	0.00
Na2O	0.00	0.00	0.00	0.00	0.00	0.00
K2O	0.23	0.01	0.02	0.02	0.00	0.00
Total	86.42	87.50	87.52	87.38	86.20	86.85
Si	5.7940	5.5226	5.4872	5.3815	5.3814	5.5486
Al IV	2.2060	2.4774	2.5128	2.6185	2.6186	2.4514
Ti	0.0150	0.0023	0.0098	0.0054	0.0008	0.0043
Al	2.5405	2.6100	2.5526	2.6232	2.6836	2.5776
Cr	0.0000	0.0096	0.0029	0.0203	0.0000	0.0039
Fe	3.8226	4.0007	4.6975	5.1819	3.8247	3.8135
Mn	0.0195	0.0243	0.0513	0.0545	0.0486	0.0413
Mg	5.3727	5.2585	4.6417	4.0761	5.4042	5.4900
Ca	0.0169	0.0198	0.0107	0.0172	0.0041	0.0000
Na	0.0000	0.0000	0.0000	0.0014	0.0000	0.0000
K	0.0608	0.0025	0.0045	0.0053	0.0011	0.0000
Tot(cat)	19.8481	19.9278	19.9711	19.9854	19.9672	19.9307

1 cf9950c1chlor1Gabbro Sill
2 cf9950c1chlor2Gabbro Sill
3 cf9810c1chlor1Gabbro Sill
4 cf9810c1chlor2Gabbro Sill
5 cf9836c1chlor1Gabbro Sill
6 cf9836c1chlor2Gabbro Sill
7 cf9813c1chlor1Gabbro Sill
8 cf9813c1chlor2Gabbro Sill

7	8
25.92	25.82
0.01	0.04
20.97	20.86
0.00	0.00
23.85	24.04
0.26	0.25
15.94	15.77
0.12	0.07
0.00	0.00
0.01	0.01
87.08	86.86
5.4573	5.4568
2.5427	2.5432
0.0008	0.0064
2.6623	2.6542
0.0000	0.0000
4.1996	4.2491
0.0466	0.0442
5.0016	4.9670
0.0266	0.0156
0.0000	0.0000
0.0036	0.0032
19.9412	19.9397

Feldspar Mineral Chemistry

Basis of 8 oxygens

	1	2	3	4	5	6	7
SiO2	67.60	67.18	68.09	68.08	67.92	67.61	68.43
Al2O3	19.51	20.19	19.70	19.92	19.72	19.58	19.56
Fe2O3	0.00	0.01	0.14	0.07	0.06	0.00	0.00
CaO	0.27	0.48	0.18	0.15	0.04	0.12	0.04
Na2O	11.26	11.33	11.69	11.47	11.62	11.72	11.86
K2O	0.05	0.13	0.04	0.06	0.05	0.05	0.04
Total	98.69	99.33	99.83	99.74	99.40	99.07	99.94
Si	2.9889	2.9584	2.9812	2.9799	2.9836	2.9823	2.9911
Al	1.0170	1.0482	1.0169	1.0279	1.0213	1.0182	1.0079
Fe	0.0001	0.0005	0.0045	0.0021	0.0019	0.0000	0.0001
Ca	0.0127	0.0226	0.0082	0.0068	0.0017	0.0055	0.0021
Na	0.9653	0.9674	0.9924	0.9734	0.9897	1.0024	1.0051
K	0.0025	0.0075	0.0021	0.0031	0.0028	0.0026	0.0023
Tot(cat)	4.9865	5.0047	5.0053	4.9934	5.0011	5.0111	5.0086
An	0.0129	0.0227	0.0082	0.0069	0.0017	0.0054	0.0021
Ab	0.9845	0.9698	0.9897	0.9899	0.9954	0.9920	0.9957
Or	0.0026	0.0075	0.0021	0.0032	0.0028	0.0026	0.0023

1	cf9922c3plag1	Quartz Feldspar Porphyry
2	cf9922c3plag2	Quartz Feldspar Porphyry
3	cf9922c2plag3	Quartz Feldspar Porphyry
4	cf9922c2plag4	Quartz Feldspar Porphyry
5	cf9916c1plag1	Quartz Feldspar Porphyry
6	cf9916c3plag1	Quartz Feldspar Porphyry
7	cf9916c3plag2	Quartz Feldspar Porphyry
8	cf989c2plag1	Quartz Feldspar Porphyry
9	cf989c2plag2	Quartz Feldspar Porphyry
10	cf989c1plag1	Quartz Feldspar Porphyry
11	cf989c1plag2	Quartz Feldspar Porphyry
12	cf9935c2plag1	Feldspar Porphyry
13	cf9935c2plag1	Feldspar Porphyry
14	cf9935c2plag2	Feldspar Porphyry
15	cf9935c3plag2	Feldspar Porphyry
16	cf9935c3plag1	Feldspar Porphyry

8	9	10	11	12	13	14	15	16
67.35	67.48	67.39	67.40	67.11	67.11	67.25	67.58	67.90
19.78	19.97	19.81	19.82	19.76	19.76	20.10	20.12	20.06
0.00	0.08	0.05	0.00	0.16	0.16	0.13	0.11	0.12
0.45	0.37	0.17	0.46	0.40	0.40	0.61	0.55	0.47
11.56	11.33	11.78	11.24	11.29	11.29	11.39	11.13	11.42
0.06	0.11	0.07	0.04	0.04	0.04	0.03	0.03	0.05
99.20	99.34	99.27	98.96	98.75	98.75	99.51	99.51	100.02
2.9702	2.9692	2.9700	2.9747	2.9705	2.9705	2.9575	2.9664	2.9680
1.0284	1.0359	1.0293	1.0313	1.0311	1.0311	1.0421	1.0412	1.0337
0.0000	0.0028	0.0017	0.0000	0.0052	0.0052	0.0042	0.0036	0.0039
0.0212	0.0173	0.0082	0.0218	0.0189	0.0189	0.0289	0.0257	0.0222
0.9885	0.9666	1.0066	0.9619	0.9690	0.9690	0.9712	0.9473	0.9679
0.0031	0.0060	0.0039	0.0021	0.0022	0.0022	0.0018	0.0015	0.0026
5.0114	4.9978	5.0197	4.9917	4.9969	4.9969	5.0058	4.9856	4.9984
0.0209	0.0175	0.0081	0.0221	0.0191	0.0191	0.0289	0.0263	0.0224
0.9760	0.9764	0.9881	0.9757	0.9787	0.9787	0.9693	0.9721	0.9750
0.0031	0.0061	0.0038	0.0022	0.0022	0.0022	0.0018	0.0016	0.0026

Feldspar Mineral Chemistry
Basis Of 8 Oxygens

17	18	19	20	21	22	23	24
67.34	66.81	67.14	66.79	66.40	67.03	61.85	57.67
20.58	20.68	20.82	21.14	21.47	20.99	23.81	27.55
0.35	0.32	0.12	0.11	0.09	0.09	0.16	0.21
1.30	1.45	1.40	1.90	2.26	1.73	4.27	9.39
0.00	0.04	0.05	0.02	0.00	0.02	0.00	0.06
10.85	10.73	10.93	10.66	10.57	10.70	7.86	6.25
0.05	0.07	0.07	0.05	0.05	0.07	1.07	0.15
100.47	100.10	100.53	100.67	100.84	100.63	99.02	101.29
2.9372	2.9275	2.9286	2.9119	2.8937	2.9213	2.7664	2.5553
1.0583	1.0683	1.0707	1.0866	1.1031	1.0785	1.2555	1.4391
0.0115	0.0106	0.0039	0.0035	0.0029	0.0029	0.0053	0.0071
0.0607	0.0680	0.0655	0.0886	0.1057	0.0807	0.2046	0.4458
0.0000	0.0010	0.0012	0.0005	0.0000	0.0005	0.0000	0.0016
0.9176	0.9116	0.9244	0.9011	0.8932	0.9042	0.6817	0.5369
0.0029	0.0037	0.0039	0.0031	0.0028	0.0041	0.0610	0.0085
4.9882	4.9907	4.9982	4.9952	5.0013	4.9921	4.9745	4.9944
0.0618	0.0692	0.0659	0.0892	0.1055	0.0816	0.2160	0.4497
0.9352	0.9271	0.9302	0.9077	0.8917	0.9143	0.7196	0.5417
0.0030	0.0038	0.0039	0.0031	0.0028	0.0042	0.0644	0.0086

17	CF98-8 C2 grndms #3	Feldspar Porphyry
18	CF98-8 C2 grndms #4	Feldspar Porphyry
19	CF98-8 C3 pheno brtpat #5	Feldspar Porphyry
20	CF98-8 C3 pheno brtpat #6	Feldspar Porphyry
21	CF98-16 C1 grndms #1	Volcanic Flows
22	CF98-16 C1 grndms #2	Volcanic Flows
23	CF98-16 C2 grndms #3	Volcanic Flows
24	CF98-14 C1 patpheno #1	Volcanic Flows
25	CF98-14 C2 patpheno #2	Volcanic Flows
26	CF98-14 C3 grndms #3	Volcanic Flows
27	CF98-14 C3 grndms #3 (repeat)	Volcanic Flows
28	CF98-14 C3 grndms #4	Volcanic Flows
29	CF98-2 C1 pheno #1	Quartz Feldspar Porphyry
30	CF98-2 C1 pheno #1 (repeat)	Quartz Feldspar Porphyry
31	CF98-2 C2 pheno #2	Quartz Feldspar Porphyry
32	CF98-2 c3 pheno #3	Quartz Feldspar Porphyry

25	26	27	28	29	30	31	32
68.34	51.29	59.46	54.82	33.51	68.53	68.17	68.38
20.08	22.78	25.94	28.09	12.10	19.77	19.98	19.73
0.12	0.25	0.36	0.91	0.05	0.04	0.08	0.06
0.79	7.02	7.03	9.81	0.20	0.25	0.47	0.34
0.00	0.06	0.04	0.08	0.00	0.06	0.00	0.00
10.96	6.45	7.36	5.63	10.38	11.24	11.13	11.04
0.10	0.10	0.34	0.53	0.07	0.09	0.09	0.07
100.39	87.95	100.53	99.87	56.31	99.98	99.92	99.62
2.9736	2.6131	2.6412	2.4820	2.7135	2.9907	2.9782	2.9920
1.0300	1.3683	1.3584	1.4993	1.1551	1.0171	1.0291	1.0178
0.0040	0.0097	0.0119	0.0310	0.0029	0.0012	0.0026	0.0019
0.0368	0.3832	0.3346	0.4759	0.0172	0.0116	0.0222	0.0162
0.0000	0.0019	0.0010	0.0022	0.0000	0.0016	0.0000	0.0000
0.9247	0.6372	0.6339	0.4942	1.6297	0.9511	0.9428	0.9366
0.0054	0.0063	0.0193	0.0307	0.0077	0.0049	0.0051	0.0040
4.9745	5.0196	5.0003	5.0153	5.5262	4.9782	4.9799	4.9685
0.0380	0.3733	0.3387	0.4755	0.0104	0.0120	0.0229	0.0169
0.9564	0.6206	0.6417	0.4938	0.9850	0.9829	0.9719	0.9789
0.0056	0.0061	0.0195	0.0307	0.0046	0.0051	0.0052	0.0042

Feldspar Mineral Chemistry
Basis of 8 oxygens

		2	3	4	5	6	7	8	9
SiO2	59.77	57.77	69.30	68.57	98.93	68.61	58.07	58.10	60.36
Al2O3	25.96	27.06	19.87	19.89	2.29	19.80	26.50	26.52	25.15
Fe2O3	0.09	0.09	0.03	0.01	0.11	0.04	0.07	0.14	0.07
CaO	7.36	8.69	0.25	0.47	0.03	0.37	8.37	8.31	6.54
Na2O	7.42	6.65	11.54	11.47	1.33	11.46	6.89	6.67	7.61
K2O	0.13	0.11	0.07	0.05	0.01	0.06	0.11	0.15	0.07
Total	100.72	100.36	101.06	100.47	102.71	100.33	100.01	99.88	99.80
Si	2.6461	2.5773	2.9924	2.9815	3.8915	2.9860	2.5982	2.6008	2.6871
Al	1.3549	1.4233	1.0115	1.0196	0.1063	1.0159	1.3978	1.3995	1.3200
Fe	0.0029	0.0029	0.0011	0.0005	0.0033	0.0012	0.0024	0.0046	0.0023
Ca	0.3491	0.4154	0.0115	0.0220	0.0014	0.0173	0.4013	0.3986	0.3120
Na	0.6369	0.5753	0.9662	0.9670	0.1018	0.9671	0.5977	0.5789	0.6569
K	0.0071	0.0060	0.0036	0.0028	0.0003	0.0032	0.0062	0.0084	0.0039
Tot(cat)	4.9970	5.0002	4.9862	4.9934	4.1047	4.9906	5.0037	4.9908	4.9821
An	0.3515	0.4168	0.0117	0.0221	0.0137	0.0175	0.3992	0.4043	0.3207
Ab	0.6413	0.5771	0.9846	0.9750	0.9832	0.9792	0.5946	0.5872	0.6753
Or	0.0072	0.0061	0.0037	0.0028	0.0032	0.0032	0.0062	0.0085	0.0040

1	cf997c4 plag1	Volcanic Flow
2	cf997c2plag2	Volcanic Flow
3	cf999c2 plag1	Feldspar Porphyry
4	cf999c2 plag2	Feldspar Porphyry
5	cf999c1 plag3	Feldspar Porphyry
6	cf999c1 plag3 repeat	Feldspar Porphyry
7	cf9949c1plag1	Quartz Feldspar Porphyry
8	cf9949c1plag2	Quartz Feldspar Porphyry
9	cf9949c3plag1	Quartz Feldspar Porphyry

	1	2	3	4	5	6	7	8	9	10	11	12
SiO2	54.75	53.79	52.51	67.31	67.24	67.14	61.89	67.76	59.93	54.99	59.55	61.31
Al2O3	27.81	28.50	29.75	20.00	19.73	19.92	23.35	19.90	24.74	28.40	25.84	24.04
Fe2O3	0.74	1.16	1.29	0.37	0.26	0.26	0.31	0.13	0.13	0.24	0.25	0.28
CaO	10.31	8.18	11.93	0.60	0.58	0.52	4.59	0.38	6.63	10.60	5.54	5.41
Na2O	5.72	4.73	4.71	11.41	11.46	11.48	9.21	11.58	7.80	5.75	7.48	8.47
K2O	0.06	2.16	0.08	0.01	0.00	0.00	0.07	0.04	0.06	0.08	1.27	0.08
Total	99.39	98.52	100.27	99.70	99.27	99.32	99.42	99.79	99.30	100.07	99.93	99.59
Si	2.4866	2.4729	2.3802	2.9568	2.9655	2.9595	2.7613	2.9701	2.6864	2.4789	2.6603	2.7324
Al	1.4890	1.5447	1.5898	1.0357	1.0258	1.0352	1.2282	1.0283	1.3074	1.5093	1.3609	1.2631
Fe	0.0252	0.0401	0.0440	0.0124	0.0085	0.0086	0.0103	0.0043	0.0045	0.0083	0.0085	0.0094
Ca	0.5017	0.4029	0.5794	0.0280	0.0276	0.0247	0.2194	0.0179	0.3185	0.5120	0.2652	0.2583
Na	0.5037	0.4216	0.4140	0.9718	0.9800	0.9812	0.7967	0.9842	0.6779	0.5026	0.6479	0.7319
K	0.0038	0.1266	0.0048	0.0008	0.0001	0.0000	0.0040	0.0020	0.0036	0.0048	0.0722	0.0044
Tot(cat)	5.0100	5.0088	5.0123	5.0055	5.0074	5.0092	5.0199	5.0067	4.9984	5.0160	5.0150	4.9996

1	cf9813c3plag1	Gabbro Sill
2	cf9813c1plag1	Gabbro Sill
3	cf9813c1plag2	Gabbro Sill
4	cf9836c1plag1	Gabbro Sill
5	cf9836c1plag2	Gabbro Sill
6	cf9836c1plag3	Gabbro Sill
7	cf9810c1plag1	Gabbro Sill
8	cf9810c1plag2	Gabbro Sill
9	cf9810c1plag3	Gabbro Sill
10	cf9950c1plag1	Gabbro Sill
11	cf9950c1plag2	Gabbro Sill
12	cf9950c1plag3	Gabbro Sill

Feldspar Mineral Chemistry

Basis of 8 oxygens

	1	2	3	4	5	6	7
SiO2	67.64	67.21	67.09	67.02	68.74	67.93	68.80
Al2O3	20.03	20.51	20.25	20.36	19.91	20.60	19.87
Fe2O3	0.26	0.31	0.10	0.09	0.18	0.03	0.07
CaO	0.24	0.48	0.90	0.91	0.30	1.10	0.18
Na2O	11.63	11.38	11.57	11.48	11.42	11.13	11.84
K2O	0.13	0.22	0.08	0.06	0.04	0.05	0.03
Total	99.93	100.11	99.99	99.92	100.59	100.83	100.79
Si	2.9633	2.9426	2.9436	2.9413	2.9836	2.9484	2.9831
Al	1.0345	1.0586	1.0474	1.0534	1.0188	1.0541	1.0157
Fe	0.0087	0.0102	0.0033	0.0029	0.0060	0.0008	0.0024
Ca	0.0112	0.0225	0.0425	0.0427	0.0141	0.0510	0.0083
Na	0.9879	0.9661	0.9843	0.9769	0.9611	0.9367	0.9954
K	0.0070	0.0120	0.0043	0.0033	0.0021	0.0028	0.0015
Tot(cat)	5.0126	5.0120	5.0253	5.0206	4.9856	4.9939	5.0063
An	0.0111	0.0225	0.0412	0.0417	0.0144	0.0515	0.0082
Ab	0.9820	0.9655	0.9546	0.9550	0.9835	0.9456	0.9903
Or	0.0069	0.0120	0.0042	0.0032	0.0021	0.0028	0.0015

1 9926c3plag Volcanic Flow
2 9926c3plag Volcanic Flow
3 9954c2plag Feldspar Porphyry
4 9954c1plag Feldspar Porphyry
5 9955c1plag Feldspar Porphyry
6 9955c4plag Feldspar Porphyry
7 9942c3plag Quartz Feldspar Porphyry
8 9942c2plag Quartz Feldspar Porphyry
9 9818c3plag Quartz Feldspar Porphyry
10 9818c2plag Quartz Feldspar Porphyry
11 987c3plag Volcanic Flow
12 987c2plag Volcanic Flow
13 987c1chlor Volcanic Flow
14 987c1chlor Volcanic Flow

8	9	10	11	12	13	14
68.75	67.67	67.79	67.91	67.43	26.34	25.28
19.75	20.44	20.46	20.51	20.95	17.24	19.37
0.04	0.07	0.08	0.19	0.13	29.30	27.94
0.19	1.04	0.93	1.02	1.45	0.01	0.01
11.76	11.28	11.10	11.09	10.98	0.00	0.00
0.05	0.06	0.13	0.07	0.05	0.00	0.00
100.54	100.56	100.50	100.79	100.99	72.89	72.60
2.9874	2.9477	2.9522	2.9494	2.9273	1.8125	1.7380
1.0118	1.0497	1.0505	1.0502	1.0722	1.3986	1.5699
0.0013	0.0022	0.0027	0.0063	0.0041	1.5173	1.4455
0.0091	0.0486	0.0435	0.0476	0.0674	0.0010	0.0010
0.9908	0.9527	0.9373	0.9339	0.9242	0.0000	0.0000
0.0025	0.0036	0.0075	0.0039	0.0029	0.0001	0.0000
5.0028	5.0045	4.9936	4.9912	4.9981	4.7296	4.7543
0.0090	0.0484	0.0440	0.0483	0.0678	0.8894	1.0000
0.9885	0.9480	0.9484	0.9478	0.9293	0.0000	0.0000
0.0025	0.0036	0.0076	0.0039	0.0029	0.1106	0.0000

Feldspar Mineral Chemistry

Basis of 8 oxygens

	1	2	3	4	5	6	7	8
SiO2	68.04	68.34	67.47	67.99	67.60	67.66	67.33	61.76
Al2O3	20.32	20.42	20.18	20.37	20.13	20.33	20.65	23.97
Fe2O3	0.06	0.05	0.06	0.04	0.13	0.17	0.32	0.35
CaO	0.84	0.91	0.94	0.77	0.88	0.99	1.07	5.91
SrO	0.06	0.03	0.12	0.13	0.06	0.10	0.09	0.04
Na2O	11.32	11.26	11.29	11.30	11.41	11.21	11.22	8.12
K2O	0.07	0.07	0.07	0.07	0.13	0.06	0.06	0.08
Total	100.70	101.08	100.13	100.67	100.35	100.53	100.75	100.23
Si	2.9578	2.9584	2.9533	2.9570	2.9540	2.9499	2.9328	2.7360
Al	1.0414	1.0421	1.0414	1.0444	1.0371	1.0450	1.0604	1.2519
Fe	0.0018	0.0017	0.0020	0.0012	0.0044	0.0056	0.0105	0.0118
Ca	0.0391	0.0421	0.0443	0.0360	0.0411	0.0461	0.0501	0.2805
Sr	0.0015	0.0008	0.0030	0.0033	0.0016	0.0026	0.0024	0.0010
Na	0.9542	0.9451	0.9582	0.9529	0.9668	0.9476	0.9476	0.6975
K	0.0038	0.0039	0.0038	0.0038	0.0074	0.0034	0.0034	0.0044
Tot(cat)	4.9996	4.9942	5.0060	4.9986	5.0123	5.0003	5.0072	4.9831
An	0.0392	0.0425	0.0440	0.0362	0.0404	0.0463	0.0501	0.2856
Ab	0.9570	0.9536	0.9522	0.9600	0.9522	0.9503	0.9466	0.7100
Or	0.0038	0.0039	0.0038	0.0038	0.0073	0.0034	0.0034	0.0044

1	CF98-24 C1 phenocx #1	Quartz Feldspar Porphyry
2	CF98-24 C2 phenocx #2	Quartz Feldspar Porphyry
3	CF98-24 C2 phenocx #3	Quartz Feldspar Porphyry
4	CF98-24 C3 phenocx #4	Quartz Feldspar Porphyry
5	CF98-24 C3 phenocx #5	Quartz Feldspar Porphyry
6	CF98-24 C3 grndms #6	Quartz Feldspar Porphyry
7	CF98-24 C3 grndms #7	Quartz Feldspar Porphyry
8	CF98-25 C1 variole #1	Volcanic Flows
9	CF98-25 C2 variole #2	Volcanic Flows
10	CF98-15 C1 grndms #1	Volcanic Flows
11	CF98-15 C1 grndms #2	Volcanic Flows
12	CF98-15 C2 pheno brtpat #3	Volcanic Flows
13	CF98-15 C2 pheno brtpat #4	Volcanic Flows
14	CF98-15 C2 pheno drkpat #5	Volcanic Flows
15	CF98-8 C1 pheno #1	Feldspar Porphyry
16	CF98-8 C1 pheno #2	Feldspar Porphyry

9	10	11	12	13	14	15	16
59.19	59.69	59.92	61.09	59.78	68.56	65.20	66.88
25.49	24.89	24.63	25.13	25.19	19.95	20.30	20.81
0.53	0.19	0.30	0.10	0.29	0.04	0.12	0.14
5.93	7.11	6.61	6.46	7.24	0.58	3.15	1.54
0.01	0.06	0.06	0.03	0.04	0.00	0.05	0.10
6.97	7.74	7.85	8.13	7.68	11.46	10.68	10.89
1.29	0.06	0.51	0.09	0.05	0.05	0.09	0.08
99.41	99.74	99.88	101.04	100.28	100.64	99.59	100.45
2.6603	2.6706	2.6812	2.6909	2.6614	2.9775	2.8938	2.9229
1.3506	1.3129	1.2993	1.3050	1.3221	1.0214	1.0622	1.0722
0.0178	0.0064	0.0100	0.0034	0.0098	0.0013	0.0040	0.0047
0.2856	0.3409	0.3169	0.3049	0.3454	0.0270	0.1498	0.0723
0.0004	0.0017	0.0016	0.0008	0.0011	0.0000	0.0014	0.0026
0.6074	0.6714	0.6811	0.6944	0.6629	0.9650	0.9191	0.9228
0.0741	0.0034	0.0289	0.0051	0.0030	0.0028	0.0049	0.0046
4.9962	5.0072	5.0191	5.0046	5.0056	4.9950	5.0351	5.0023
0.2953	0.3356	0.3086	0.3036	0.3415	0.0271	0.1395	0.0724
0.6281	0.6611	0.6632	0.6913	0.6555	0.9701	0.8559	0.9231
0.0766	0.0034	0.0282	0.0051	0.0030	0.0028	0.0046	0.0046

APPENDIX C

SAMPLE LOCATIONS

Niven Lake Lenticle

Sample List

Cf997	Quartz Feldspar Porphyry
Cf998	Feldspar Porphyry
Cf999	Feldspar Porphyry
Cf9910	Hydrothermal Breccia
Cf9911	Hydrothermal Breccia
Cf9912	Hydrothermal Breccia
Cf9913	Quartz Feldspar Porphyry
Cf9950	Gabbro Sill
Cf9951	Feldspar Porphyry
Cf98NR1	Volcani Flow
Cf98NR2	Gabbro Sill
Cf98NR3	Volcanic Flow
Cf98NR4	Quartz Feldspar Porphyry

Niven Lake Lenticle Samples

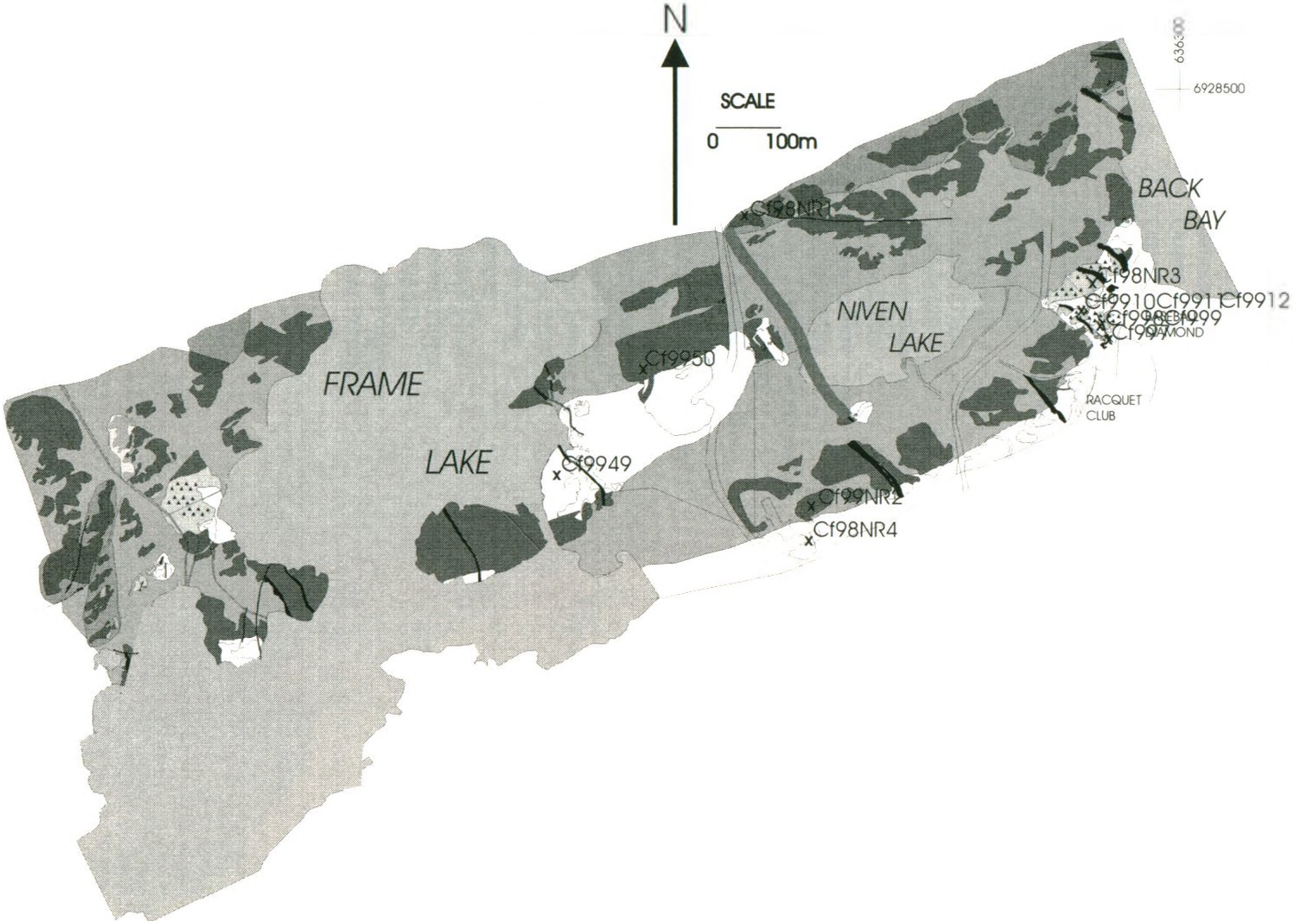

Brock Lenticle

Sample List

Cf981	Cherty Tuff
Cf982	Quartz Feldspar Porphyry
Cf983	Lamprophyre
Cf984	Quartz Feldspar Porphyry
Cf985	Quartz Feldspar Porphyry
Cf986	Volcanic Flow
Cf987	Volcanic Flow
Cf988	Feldspar Porphyry
Cf989	Quartz Feldspar Porphyry
Cf9810	Gabbro Sill
Cf9811	Cherty Tuff
Cf9812	Gabbro Dyke
Cf9813	Gabbro Sill
Cf9814	Volcanic Flow
Cf9815	Volcanic Flow
Cf9816	Volcanic Flow
Cf9817	Volcanic Flow
Cf9818	Quartz Feldspar Porphyry
Cf9819	Feldspar Porphyry
Cf9820	Quartz Feldspar Porphyry
Cf9821	Feldspar Porphyry
Cf9822	Quartz Feldspar Porphyry
Cf9823	Quartz Feldspar Porphyry
Cf9824	Quartz Feldspar Porphyry
Cf9825	Volcanic Flows
Cf9826	Volcanic Flow
Cf9827	Volcanic Flow
Cf9828	Gabbro Dyke
Cf9829	Diabase
Cf9830	Volcanic Flows
Cf9831	Volcanic Flows
Cf9832	Gabbro Sill
Cf9953	Feldspar Porphyry
Cf9954	Feldspar Porphyry

Brock Lenticle Samples

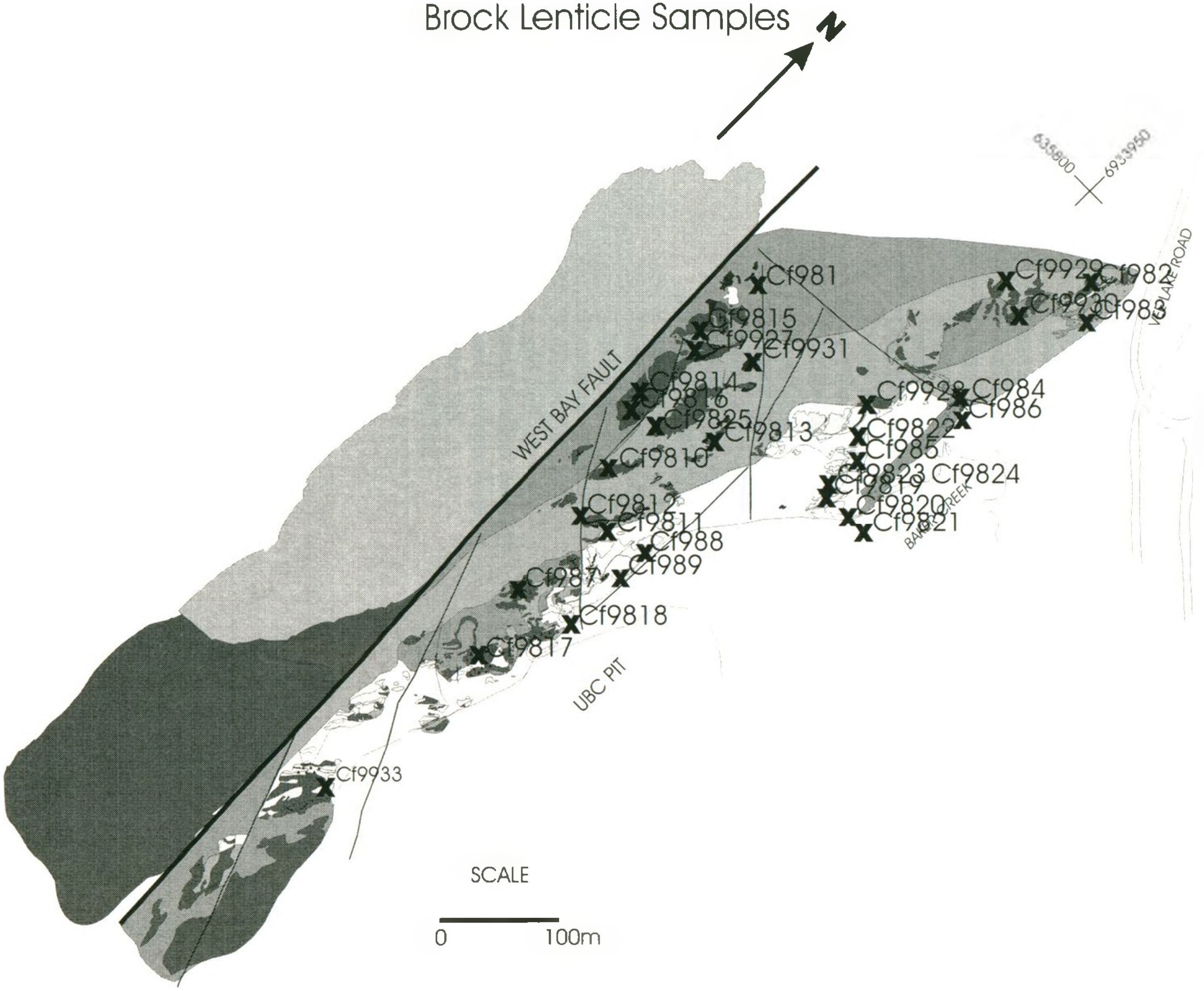

Vee Lake Lenticle

Sample List

Cf996	Quartz Feldspar Porphyry
Cf9914	Lapilli Tuff
Cf9915	Quartz Crystal Tuff
Cf9916	Quartz Feldspar Porphyry
Cf9917	Lapilli Tuff
Cf9918	Agglomerate
Cf9919	Lapilli Tuff
Cf9921	Lapilli Tuff
Cf9922	Quartz Feldspar
Cf9923	Lapilli Tuff
Cf9924	Quartz Feldspar Porphyry
Cf9925	Quartz Feldspar Porphyry
Cf9926	Volcanic Flow
Cf9927	Quartz Feldspars Porphyry
Cf9928	Lapilli Tuff
Cf9929	Ash Flow Tuff
Cf9930	Ash Flow Tuff
Cf9931	Quartz Crystal Tuff
Cf9932	Volcanic Sandstone
Cf9933	Lapilli Tuff
Cf9934	Feldspar Porphyry
Cf9935	Feldspar Porphyry
Cf9936	Felsic Dyke
Cf9937	Quartz Carbonate Sericite Schist
Cf9938	Lapill Tuff
Cf9939	Pyroclastic Breccia
Cf9940	Ash Flow Tuff
Cf9941	Lapill Tuff
Cf9942	Quartz Feldspar Porphyry
Cf9948	Quartz Feldspar Porphyry
Cf98VR1	Gabbro Sill
Cf98VR8	Vitric Ash Tuff


Vee Lake Lenticle Samples
N
SCALE
0
100m
JACKSON
LAKE
Cf9935
Cf9932
Cf9936
Cf9934
Cf9937
Cf98VR8
Cf9926
Cf9928
Cf98VR1
638000
694000
WALSH
LAKE
Cf9925
Cf9917
Cf9916
Cf9915
Cf9918
Cf9923
Cf9924
Cf9921
Cf9922
Cf9930
Cf9931
VEE
LAKE
Cf9914
Cf9942
GOLD
LAKE